

Electronic Thesis and Dissertation Repository

9-28-2022 1:00 PM

The Role of IL-12 and IL-27 in Modulating CD39 Expression on CD8⁺ T-cells and Their Effector Function

Lara E. Gerhardt, *The University of Western Ontario*

Supervisor: Maleki, Saman, *The University of Western Ontario*

A thesis submitted in partial fulfillment of the requirements for the Master of Science degree in Pathology and Laboratory Medicine

© Lara E. Gerhardt 2022

Follow this and additional works at: <https://ir.lib.uwo.ca/etd>



Part of the [Laboratory and Basic Science Research Commons](#)

Recommended Citation

Gerhardt, Lara E., "The Role of IL-12 and IL-27 in Modulating CD39 Expression on CD8⁺ T-cells and Their Effector Function" (2022). *Electronic Thesis and Dissertation Repository*. 9006.
<https://ir.lib.uwo.ca/etd/9006>

This Dissertation/Thesis is brought to you for free and open access by Scholarship@Western. It has been accepted for inclusion in Electronic Thesis and Dissertation Repository by an authorized administrator of Scholarship@Western. For more information, please contact wlsadmin@uwo.ca.

Abstract

CD8⁺ T-cells play a critical role in anti-tumour immunity, and cytokines IL-12 and IL-27 can modulate their phenotype and function. Tumour-specific CD8⁺ tumour-infiltrating lymphocytes (TILs) can be identified based on the surface expression of CD39, while CD8⁺ TILs that recognize cancer unrelated antigens do not. It is currently unclear how and why tumour-specific CD8⁺ T-cells uniquely express CD39. We hypothesize that IL-12 and IL-27 upregulate CD39 expression on CD8⁺ T-cells and improve effector activity of CD39⁺CD8⁺ T-cells, compared to their CD39⁻ counterparts. Using *in vitro* stimulation assays, we identified that CD8⁺ T-cells upregulate CD39 in the presence of IL-12 and IL-27. Moreover, CD39⁺CD8⁺ T-cells produced higher levels of effector molecules, such as IFN- γ , than CD39⁻ counterparts. Inhibiting IL-12 activity, *in vivo*, reduced CD39⁺CD8⁺ TIL frequency compared to controls, without changing the overall CD8⁺ TIL frequency. Our findings shed light on some underlying mechanisms of CD39 upregulation by CD8⁺ T-cells.

Keywords

Cancer, CD8⁺ T-cell, CD39, IL-12, IL-27, anti-tumour immunity

Abstract for Lay Audience

Strong immune responses are capable of mediating tumour regression. Immunotherapy is a modern form of cancer treatment that makes use of a patient's own immune system to kill cancerous cells. However, many cancer patients do not benefit from immunotherapy. To improve these therapies, further research is required to understand how immune responses can be altered. Most of the current immunotherapies work by boosting the action of killer T-cells that can specifically recognize cancerous cells. Tumour-specific killer T-cells are important because they can target and destroy cancerous cells while leaving healthy cells alone. Scientists can identify tumour-specific killer T-cells by a certain molecule found on the cell surface called CD39. More research is needed to understand why and how CD39 ends up on the surface of these cells, since this could be used to improve immunotherapies. We hypothesized that two other molecules, called IL-12 and IL-27, make killer T-cell express CD39. This is because IL-12 and IL-27 are known to boost anti-tumour immune responses and improve the function of killer T-cells. In this study, we activated killer T-cells in test tubes with or without IL-12 and IL-27. In the presence of IL-12 or IL-27, T-cells had more CD39 on their surface than the control conditions. In addition, the presence of both IL-12 and IL-27 in the test tube caused the highest amount of CD39. Next, we blocked IL-12 activity in animals that had tumours and found less CD39⁺ killer T-cells within those tumours. This supported our previous findings. Finally, we compared the function of CD39⁻ and CD39⁺ killer T-cells. We found that CD39⁺ killer T-cells had stronger immunological activities than CD39⁻ cells. These results help us better understand what factors influence tumour-specific killer T-cells. Our study shows that IL-12 and IL-27 can increase the level of CD39 on the surface of killer T-cells. Also, CD39⁺ killer T-cells can produce strong immune responses in test tubes. This research will contribute to the growing knowledge of tumour-specific killer T-cells and may help inform scientists when designing future immunotherapies.

Co-Authorship Statement

The following individuals contributed to this thesis.

Saman Maleki Vareki	Study design, data interpretation, grant funding, biosafety, ethics approvals, and supervision
Rene Figueredo	Generation of cell lines, animal care, and biosafety protocol
Megan Hong	Aided in neuro-2a lysate preparation and tissue processing at endpoint of <i>in vivo</i> experiments
Yeganeh Yousefi	Aided in neuro-2a lysate preparation and tissue processing at endpoint of <i>in vivo</i> experiments

Acknowledgements

During the completion of my master's degree, I have received an incredible amount of support, for which I am truly grateful. To my supervisor, Dr. Saman Maleki Vareki, thank you for your time and efforts throughout these last two (plus) years. I am thankful for the opportunity to delve into the field of immuno-oncology. I appreciate your continued guidance and encouragement, and I will carry the knowledge and skills I've gained, scientific and otherwise, throughout my life.

To all the past and current members of the Maleki lab, thank you for your advice, support, and friendship. In particular, to Megan Hong, thank you for all the thought-provoking discussions, technical assistance and motivation. To Dr. Pete Ferguson and Rene Figueredo Pupo, you have taught me invaluable lessons on the importance of patience, kindness, and attention to detail. To the members of my advisory committee, Dr. Joe Mymryk, Dr. Lisa Cameron, and Dr. John Lenehan, thank you for your advice and perspectives, which helped me to improve the quality of my research and writing. I would also like to thank Accessible Education and the Department of Pathology and Laboratory Medicine for creating a supportive educational environment. To Dr. Zia Khan, thank you for your efforts and dedication, participating in your classes helped me to develop a more curious, analytical mindset. To Dr. Kristin Chadwick, thank you for facilitating my flow cytometry education and trouble shooting skills; you have helped me more than you know.

I would also like to acknowledge our funding sources, including the Western University Graduate Scholarship, Departmental awards, and LHSC Catalyst Grants for providing me the opportunity to do this research.

To my family, thank you for your unconditional love and selfless efforts over the last two years (and beyond). Thank you to Josée and my friends, new and old, for your understanding, positivity and support. To my loving partner, Colin, thank you for always believing in me and inspiring me every day.

It is difficult to put into words the gratitude I have to everyone (including those unnamed), as I could not have accomplished much of what I have without their support. This thesis is dedicated to my friends and family that lost their lives to cancer, those in remission, and those that continue on having lost a loved one. May we never forget why we are doing this research in the first place.

Table of Contents

Abstract.....	ii
Keywords.....	ii
Abstract for Lay Audience.....	iii
Co-Authorship Statement.....	iv
Acknowledgements.....	v
Table of Contents.....	vi
List of Tables.....	ix
List of Figures.....	x
List of Abbreviations.....	xii
Chapter 1 – Introduction.....	1
1.1 Anti-tumour immunity against solid tumours.....	1
1.2 CD8 ⁺ T-cells.....	2
1.2.1 Tumour-specific CD8 ⁺ T-cell priming and cytotoxicity.....	3
1.2.2 CD8 ⁺ T-cell regulation by IL-12 and IL-27.....	5
1.2.3 Characterizing tumour-infiltrating CD8 ⁺ T-cells.....	7
1.3 Purinergic signalling in the TME and the canonical function of CD39.....	10
1.4 Anti-tumour activity and prognostic role of CD39 ⁺ CD8 ⁺ T-cells.....	12
1.5 Immunotherapy for cancer treatment.....	13
1.6 MMR pathway and inducing MMR deficiency in neuroblastoma.....	15
1.7 Rationale, Hypothesis, and Aims.....	18
1.7.1 Hypothesis.....	18
1.7.2 Aims.....	18
Chapter 2 – Methods.....	19
2.1 Cell lines.....	19

2.2 Animal models	19
2.3 Tissue processing.....	20
2.4 Tumour lysate preparation	21
2.5 Immune cell stimulation assays	21
2.5.1 Stimulation assays using CD8 ⁺ T-cells.....	21
2.5.2 Stimulation assays using bulk splenocytes for intracellular cytokine staining.....	23
2.6 Extracellular protein staining.....	24
2.7 Intracellular cytokine staining	24
2.8 Flow cytometry	25
2.9 Statistical analysis.....	26
Chapter 3 – Results	27
3.1 MLH1 KO neuro-2a tumours contain a higher frequency of tumour-specific CD39 ⁺ CD8 ⁺ T-cells than control neuro-2a tumours, which correlates with reduced tumour burden.....	27
3.2 The effects of IL-12 and IL-27 on the expression of CD39 on CD8 ⁺ T-cells from neuro-2a antigen-naïve and -experienced mice	33
3.2.1 IL-12 and IL-27 induce CD39 expression on CD8 ⁺ T-cells from naïve mice	35
3.2.2 IL-12 and IL-27 induce CD39 expression on CD8 ⁺ T-cells from control and immunogenic neuro-2a vaccinated mice.....	40
3.3 The effect of IL-12 neutralization on CD39 ⁺ CD8 ⁺ T-cell populations from neuro-2a tumour-bearing mice	46
3.3.1 IL-12 neutralization has no effect on the frequency of CD39 ⁺ CD8 ⁺ TILs in control neuro-2a tumours.....	52
3.3.2 Immunogenic neuro-2a tumours show a reduced frequency of CD39 ⁺ CD8 ⁺ TILs upon IL-12 neutralization.....	54

3.3.3 In vitro stimulation with IL-12 results in the greatest frequency of CD39 ⁺ CD8 ⁺ T-cells expressing inhibitory receptors.....	56
3.4 The effector functionality of CD39 ⁺ -CD8 ⁺ T-cells after stimulation with IL-12 and/or IL-27	61
3.4.1 CD39 expression positively correlates with effector molecule production when stimulated with α CD3/CD28 and IL-2.....	66
3.4.2 The presence of IL-12 and IL-27 differentially affects CD39 ⁺ CD8 ⁺ T-cells effector molecule production	73
Chapter 4 – Discussion	76
References.....	83
Curriculum Vitae	103

List of Tables

Table 1. Summary of antibodies used for flow cytometry staining.....	26
--	----

List of Figures

Figure 1. Naïve CD8 ⁺ T-cells require three signals for optimal priming and activation....	4
Figure 2. Characterization of IL-12 and IL-27.	6
Figure 3. CD39 identifies tumour-specific CD8 ⁺ TILs.	9
Figure 4. Ectonucleotidases CD39 and CD73 convert ATP to adenosine.....	11
Figure 5. Turning immunologically cold tumours hot by inducing MMR deficiency.	17
Figure 6. Simplified method comparing the immune characteristics of control and <i>MLH1</i> KO neuro-2a tumours.	28
Figure 7. Tumour burden of control and <i>MLH1</i> KO neuro-2a tumours.	30
Figure 8. Frequency of CD39 ⁺ CD8 ⁺ T-cells from tumours and spleens of neuro-2a tumour-bearing mice.....	32
Figure 9. Frequency of naïve, stem cell-like memory, effector, and central memory CD39 ⁺ CD8 ⁺ T-cells from spleens and tumours of immunogenic neuro-2a tumour-bearing mice.....	34
Figure 10. Simplified stimulation assay method with CD8 ⁺ T-cells from neuro-2a antigen naïve mice.	36
Figure 11. Frequency of CD39 ^{high} CD8 ⁺ T-cells from naïve mice after <i>in vitro</i> stimulation with IL-12 or IL-27.....	38
Figure 12. MFI of CD39 from CD39 ⁺ CD8 ⁺ T-cells from naïve mice after <i>in vitro</i> stimulation with IL-12 or IL-27.....	39
Figure 13. Simplified stimulation assay methodology with CD8 ⁺ T-cells from neuro-2a antigen-experienced mice.	41
Figure 14. Frequency of CD39 ^{high} CD8 ⁺ T-cells from neuro-2a primed mice after <i>in vitro</i> stimulation with IL-12 and/or IL-27.	44
Figure 15. MFI of CD39 from CD39 ⁺ CD8 ⁺ T-cells from neuro-2a primed mice after <i>in vitro</i> stimulation with IL-12 and/or IL-27.	45
Figure 16. Simplified method for comparing T-cell characteristics from control or immunogenic neuro-2a tumour-bearing mice treated with αIL-12 or isotype control.	47
Figure 17. Tumour burden of neuro-2a tumour-bearing mice treated with αIL-12 or isotype control.	49

Figure 18. Frequency of naïve and effector CD8 ⁺ TILs from tumours of immunogenic neuro-2a tumour-bearing mice after αIL-12 treatment.	51
Figure 19. Frequency of CD38 ⁺ or CD39 ⁺ CD8 ⁺ T-cells from tumours and spleens of control neuro-2a tumour-bearing mice after αIL-12 treatment.	53
Figure 20. Frequency of CD39 ⁺ CD8 ⁺ T-cells and other phenotypes from tumours and spleens of immunogenic neuro-2a tumour-bearing mice after αIL-12 treatment.	55
Figure 21. Inhibitory receptor expression on CD39 ⁺ CD8 ⁺ T-cells from immunogenic neuro-2a primed mice after <i>in vitro</i> stimulation with IL-12 and/or IL-27.	59
Figure 22. Frequency of TIM-3 ⁺ PD-1 ⁺ LAG-3 ⁺ CD39 ⁺ CD8 ⁺ T-cells from immunogenic neuro-2a primed mice after <i>in vitro</i> stimulation with IL-12 and/or IL-27.	60
Figure 23. Simplified stimulation assay methodology with bulk splenocytes from neuro-2a antigen-experienced mice for ICS.	62
Figure 24. Frequency of CD39 ⁺ CD8 ⁺ T-cells from immunogenic neuro-2a primed mice after <i>in vitro</i> stimulation in bulk splenocyte culture with IL-12 and/or IL-27.	64
Figure 25. MFI of CD39 from CD39 ⁺ CD8 ⁺ T-cells from immunogenic neuro-2a primed mice after <i>in vitro</i> stimulation in bulk splenocyte culture with IL-12 and/or IL-27.	65
Figure 26. Effector molecule expression of CD39 ⁺ and CD39 ⁻ CD8 ⁺ T-cells after <i>in vitro</i> stimulation with αCD3/CD28 and IL-2.	68
Figure 27. Effector molecule expression of CD39 ⁺ and CD39 ⁻ CD8 ⁺ T-cells after <i>in vitro</i> stimulation with PMA, ionomycin, and IL-2.	70
Figure 28. MFI of IFNγ from IFNγ ⁺ CD39 ⁺ and CD39 ⁻ CD8 ⁺ T-cells after <i>in vitro</i> stimulation with αCD3/CD28 and IL-2.	72
Figure 29. Effector molecule expression of CD39 ⁺ CD8 ⁺ T-cells after <i>in vitro</i> stimulation with IL-12 and/or IL-27.	75

List of Abbreviations

ACK	Ammonium-Chloride-Potassium
ACT	Adoptive cell therapy
ADA	Adenosine deaminase
ADP	Adenosine 5'-diphosphate
AMP	Adenosine monophosphate
APC	Antigen presenting cell
ATCC	American Type Culture Collection
ATP	Adenosine 5'-triphosphate
BFA	Brefeldin A
BSA	Bovine serum albumin
BV	Brilliant violet
Cas9	CRISPR associated protein 9
CRISPR	Clustered regularly interspaced short palindromic repeats
CTLA-4	Cytotoxic T-lymphocyte-associated protein-4
DC	Dendritic cell
eATP	Extracellular ATP
EDTA	Ethylenediaminetetraacetic acid
EBI3	Epstein-Barr virus-induced gene 3
FACS buffer	Fluorescence-activated cell sorting flow cytometry staining buffer
FBS	Fetal bovine serum
FMO	Fluorescence minus one
H.I.	Heat inactivated
HNSCC	Head and neck squamous cell carcinoma

ICI	Immune checkpoint inhibitor
IFN γ	Interferon- γ
IL	Interleukin
i.p.	Intraperitoneal
JAK	Janus kinase
KO	Knockout
LAG-3	Lymphocyte-activation gene 3
LAMP	Lysosomal-associated membrane glycoprotein
mAb	Monoclonal antibody
MHC I	Major histocompatibility complex class I
MLH1	MutL homologue 1
MMR	Mismatch repair
MSH2	MutS homologue 2
MSH6	MutS homologue 6
MSI-h	High microsatellite instability
NK	Natural killer
ns	Not significant
NSCLC	Non-small cell lung cancer
PBS	Phosphate buffered saline
PCNA	Proliferating cell nuclear antigen
PD-1	Programmed cell death protein-1
PD-L1	Programmed cell death ligand-1
PD-L2	Programmed cell death ligand-2
PGE ₂	Prostaglandin E ₂
PMA	Phorbol 12-myristate 13-acetate

PMS2	Post-meiotic segregation increase 2
RPA	Replication protein A
RT	Room temperature
RUNX3	Runt-related transcription factor 3
s.c.	Subcutaneous
SD	Standard deviation
SEM	Standard error of the mean
STAT	Signal transducer and activator of transcription
TAM	Tumour-associated macrophage
TCR	T-cell receptor
TGF- β	Transforming growth factor- β
TIL	Tumour-infiltrating lymphocyte
TIM-3	T-cell immunoglobulin and mucin domain-3
TMB	Tumour mutational burden
TME	Tumour microenvironment
TNF α	Tumour necrosis factor- α
TP	Triple positive
Treg	Regulatory T-cell
VEGF	Vascular endothelial growth factor

Chapter 1 – Introduction

1.1 Anti-tumour immunity against solid tumours

Solid tumours are comprised of the tumour cells (i.e., malignant neoplastic cells) and the stroma. Broadly, non-malignant cells, connective tissue elements, adhesion molecules, and immune cells belong to the stromal compartment. These cells collectively make up the tumour microenvironment (TME), and the interplay between cellular and molecular compartments of the TME influences the fate of a tumour^{1,2}.

Though long overlooked, the immune system is now recognized for its fundamental role in developing and controlling tumours; such that immune evasion is considered a hallmark of cancer³. The cancer immunoediting hypothesis describes this phenomenon in three phases; elimination, equilibrium, and escape⁴. During elimination, the innate and adaptive arms of the immune system identify and destroy developing tumours. The term ‘anti-tumour immunity’ refers to the innate and adaptive immune responses that facilitate tumour control.

The tumour cells that survive the elimination phase may enter the equilibrium phase, where anti-tumour immunity maintains tumour dormancy. There is an equilibrium between tumour cell proliferation and cell death, in which the immune system maintains the sum total of tumour cells. However, selective pressure can occur through processes known as immunoselection and immunosubversion⁵. Immunoselection is described as the selection for non-immunogenic tumour cell variants, since tumour cells that elicit an immune response would be destroyed. Non-immunogenic tumour cell variants can escape immune recognition by loss of immunogenic antigens or deficiencies in processing and presenting the antigens⁴.

Immunosubversion is defined as the active suppression of the immune response. Tumour cells can produce molecules (e.g., transforming growth factor- β (TGF- β), vascular endothelial growth factor (VEGF), and prostaglandin E₂ (PGE₂)) which can directly hinder anti-tumour immune responses, as well as promote the activity of immunosuppressive cells, like tumour-associated macrophages (TAMs) and regulatory T- (Treg) cells. In addition, tumour cells can negatively regulate natural killer (NK) and T-cell responses by engaging their inhibitory receptors, inducing apoptosis or anergy⁵.

By acquiring the ability to evade immune recognition and induce immune suppression, tumours advance into the escape phase, in which they progressively grow into a clinically detectable mass^{4,6}. By nature, the cancer immunoediting process shapes the immunogenicity of the tumour.

A variety of preclinical data have highlighted the significance of T-cells in anti-tumour immune responses⁷⁻⁹. In accordance, clinical reports correlate the quantity, specificity, and spatial distribution of tumour-infiltrating lymphocytes (TILs) with patient survival in several cancer types, including melanoma, colorectal, bladder, and breast cancers¹⁰⁻¹³. Among TILs, CD8⁺ T-cells are cytotoxic effectors that can eliminate tumour cells and play a critical role in anti-tumour immunity. For example, tumours with high CD8⁺ T-cell infiltration are often considered ‘immunologically hot’, while those with low infiltration or exclusion of CD8⁺ T-cells are ‘immunologically cold’^{14,15}. Tumours with immunologically hot phenotypes are generally more responsive to immunotherapies using immune checkpoint inhibitors (ICIs)¹⁴⁻¹⁷, which will be described in detail in a separate section.

1.2 CD8⁺ T-cells

Cytotoxic CD8⁺ T-cells recognize non-self-antigenic peptide epitopes presented by major histocompatibility complex (MHC) class I (MHC I) molecules^{18,19}. Such antigens often arise from the translation of genes carrying somatic mutations, which form aberrant proteins that are degraded intracellularly. Immunogenic peptides are then loaded onto MHC molecules and translocated to the cell surface during antigen presentation^{20,21}. Generation of tumour-specific antigens, or neoantigens, may result from exposure to carcinogens, infections, and errors in the DNA mismatch repair (MMR) process^{21,22}.

Neoantigens can differentiate neoplastic cells from healthy ones because central immune tolerance disables thymic development of T-cells that recognize self-peptide epitopes²². Therefore, neoantigens facilitate CD8⁺ T-cell recognition of tumour cells as foreign. Herein, CD8⁺ T-cells that recognize neoantigens are referred to as tumour-specific CD8⁺ T-cells.

1.2.1 Tumour-specific CD8⁺ T-cell priming and cytotoxicity

Priming naïve tumour-specific CD8⁺ T-cells often requires tumour cells to produce and release neoantigens^{21,22}. Ideally, antigen-presenting cells (APCs), such as dendritic cells (DCs), will take up those neoantigens and cross-present them to T-cells within lymph nodes²³. T-cell receptor (TCR) activation via antigen presentation in the context of MHC I is one of three signals required to activate naïve CD8⁺ T-cells optimally (Figure 1). The second signal occurs through co-stimulatory receptors, mainly CD28 which binds to CD80 or CD86 on APCs. While these two signals trigger proliferation, they are insufficient for T-cells to acquire strong effector functions or support long-term persistence. In other words, antigen recognition and co-stimulation alone leads to T-cell anergy. Pro-inflammatory cytokines, such as IL-12, act as a third signal, which can stimulate T-cell proliferation, robust effector functionality, and the development of memory populations (Figure 1). The type of cytokine(s) will influence the phenotype of the newly primed CD8⁺ T-cells. Moreover, the cytokine and molecular milieu that primed CD8⁺ T-cells encounter will regulate their persistence and function^{24,25}.

In addition to APCs, CD4⁺ T-cells provide necessary help for CD8⁺ T-cell priming²⁶; although this is only effective when both T-cells recognize their respective antigens on the same APC²⁷. Activated CD4⁺ T-cells upregulate the CD40 Ligand, which engages CD40 on APCs. This ligation enhances antigen-presentation and promotes pro-inflammatory cytokine production by APCs. In addition, CD40 engagement upregulates co-stimulatory ligands CD80 and CD86 on APCs, which supports effective CD8⁺ T-cell priming^{26,28,29}. Activated CD4⁺ T-cells can directly influence CD8⁺ T-cell priming through the secretion of IL-2, providing further pro-inflammatory signals³⁰. Overall, CD4⁺ T-cells help APCs to drive the clonal expansion and differentiation of tumour-specific CD8⁺ T-cells capable of effective anti-tumour activity (Figure 1)²⁶.

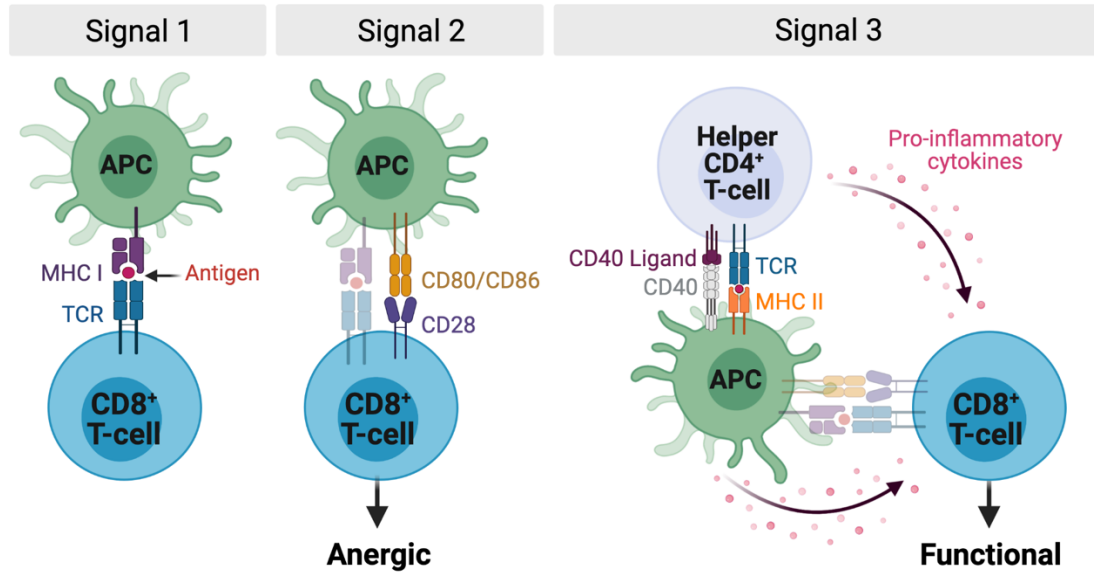


Figure 1. Naïve CD8⁺ T-cells require three signals for optimal priming and activation. TCR engagement (signal 1), co-stimulatory (e.g., CD28) activation (signal 2), and stimulation by pro-inflammatory cytokines (signal 3) are all required for CD8⁺ T-cells to develop optimal effector functionality.

The fully primed tumour-specific CD8⁺ T-cells can travel through the lymphatic system and bloodstream to the tumour and infiltrate into the tumour bed. Tumour-specific CD8⁺ TILs can recognize their cognate neoantigens on the surface of tumour cells in the context of MHC I, initiating clonal expansion and effector activity³¹. Neoantigen recognition stimulates the production of homeostatic and pro-inflammatory cytokines such as IL-2, interferon- γ (IFN γ), and tumour necrosis factor- α (TNF α)^{32–34}. In addition, CD8⁺ T-cells will release cytotoxins, such as perforin and granzymes, to induce tumour cell death. These cytotoxins are located within pre-formed lytic granules or lysosomes in the cytoplasm of T-cells. Degranulation is the process by which responding tumour-specific CD8⁺ T-cells release these granules toward the tumour cell. The lipid bilayer that encapsulates the granular core contains lysosomal-associated membrane glycoproteins (LAMPs), including CD107a (LAMP-1). Therefore, degranulating CD8⁺ T-cells can be identified by the presence of CD107a on the cell surface^{35–37}.

1.2.2 CD8⁺ T-cell regulation by IL-12 and IL-27

Cytokine signalling has the power to modulate CD8⁺ T-cell development and effector function, especially those mediated by the IL-12 family cytokines. Recent data have highlighted the role of IL-12 and IL-27 in cytotoxic IFN γ ⁺CD8⁺ T-cell development³⁸. IL-12 and IL-27 are produced by activated APCs. These cytokines share structural and functional similarities, though each has its own unique properties (Figure 2)³⁸. The IL-12 cytokine is a heterodimer (termed IL-12 p70) consisting of p40 and p35 subunits. IL-27 is composed of Epstein-Barr virus-induced gene 3 (EBI3) and p28 subunits, which resemble the p40 and p30 proteins, respectively. IL-12 and IL-27 bind their cognate receptors, which activates Janus kinase/signal transducer and activator of transcription (JAK/STAT) signalling pathways. IL-12 predominantly activates STAT4, and IL-27 activates STAT1 and STAT3. Phosphorylated STAT proteins dimerize and translocate to the nucleus to regulate the expression of their target genes^{39,40}. Notably, IL-12 and IL-27 receptors are not exclusively expressed by T-cells and have been identified on B-cells and NK cells³⁸.

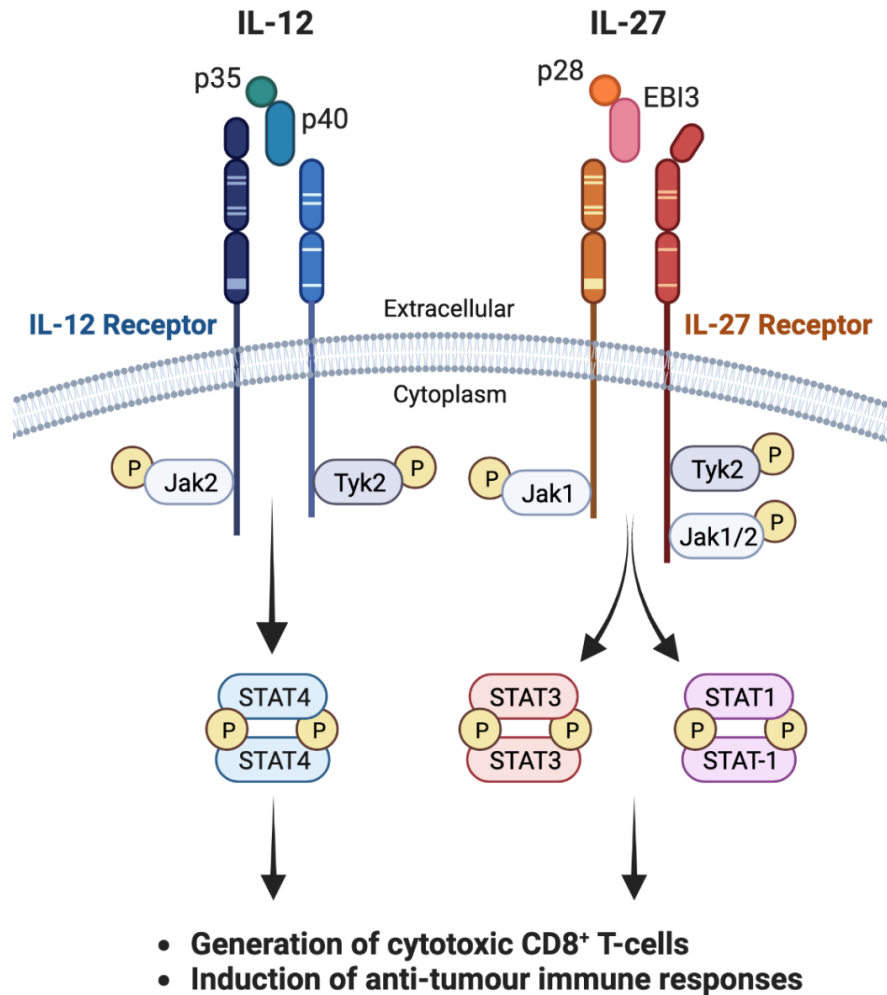


Figure 2. Characterization of IL-12 and IL-27.

IL-12 is a heterodimeric cytokine composed of p35 and p40 subunits. IL-12 activates STAT4 upon binding the IL-12 receptor. IL-27 is a heterodimeric cytokine composed of p28 and EBI3 subunits. IL-27 activates STAT1 and STAT3 after binding the IL-27 receptor. IL-12 and IL-27 signalling promotes the generation of cytotoxic CD8⁺ T-cells, supports effector function and induces anti-tumour immune responses; however, they signal through different pathways.

IL-12 has potent anti-tumour activity, most notably by stimulating the production of IFN γ ^{38,41}. IFN γ can upregulate MHC molecules, promoting the recognition of tumour cells by T-cells⁴². There is also a positive feedback mechanism by which IFN γ stimulates IL-12 production by APCs⁴³. In addition, IL-12 can limit the immunosuppressive capacity of CD4⁺ Tregs⁴⁴, which may liberate anti-tumour responses by effector T-cells. *In vitro* studies have demonstrated that recombinant IL-12 treatment reinvigorates anergic CD8⁺ T-cells⁴⁵. As such, IL-12 can prevent and revert CD8⁺ T-cell dysfunction. Unfortunately, the systemic administration of IL-12 causes severe toxicities in mice and humans, limiting its clinical use⁴⁶. Recently, a novel method was proposed in which IL-12 is tethered to the surface of CD8⁺ T-cells in order to regulate its activity. Adoptive transfer of IL-12-tethered tumour-specific CD8⁺ T-cells exhibited powerful anti-tumour efficacy across multiple preclinical and cell therapy models, without inducing overt toxicities⁴⁷. Overall, it is well established that IL-12 stimulates anti-tumour immune responses, and this cytokine has renewed potential for cancer immunotherapy.

IL-27 is newly recognized for its role in promoting CD8⁺ T-cell anti-tumour activity. Upon TCR stimulation, IL-27 can induce IFN γ production by CD8⁺ T-cells⁴⁸⁻⁵². Another study demonstrated that IL-27 synergizes with IL-12 to induce high levels of IFN γ ⁵³. IL-27 enhances the cytotoxicity of tumour-specific CD8⁺ T-cells, as demonstrated by increased expression of perforin and granzyme B, cytotoxicity assays, and *in vivo* models⁴⁹⁻⁵⁴. Additionally, there are reports that IL-27 upregulates MHC I on tumour cells^{50,55}. Together, it is clear that IL-12 and IL-27 can induce dynamic anti-tumour CD8⁺ T-cell responses.

1.2.3 Characterizing tumour-infiltrating CD8⁺ T-cells

Tumour-specific CD8⁺ TILs play a crucial role in tumour control and regression^{56,57}. While they have the ability to kill tumour cells, the TME poses a unique challenge for CD8⁺ T-cells^{19,58-60}. Exhaustion is a differentiation state acquired by T-cells exposed to persistent antigen stimulation within an immunosuppressive environment^{61,62}. Notably, CD8⁺ T-cell exhaustion was first identified during chronic viral infection, and such studies provided significant insight into its potential role in cancer⁶³.

In brief, exhausted T-cells can be characterized by the progressive loss of effector functions (i.e., cytokine production and degranulation), sustained expression of various inhibitory receptors (e.g., programmed cell death protein-1 (PD-1), lymphocyte-activation gene 3 (LAG-3), T-cell immunoglobulin and mucin domain-3 (TIM-3)), and distinct transcriptional, epigenetic and metabolic signatures^{62,64,65}. Loss of effector function in T-cells occurs in phases. Initially, IL-2 production is lost, followed by the inability of these cells to produce TNF α , and then partial or complete inability to produce IFN γ and degranulate⁶⁶. Analyzing these factors can provide a potential measure of the level of CD8⁺ T-cell exhaustion, while the expression of multiple inhibitory receptors can be used as a biomarker for exhaustion^{62,64,65}.

Logically, exhausted CD8⁺ TILs should be tumour-specific^{58,64,65}, but this is not always the case. Recent developments in CD8⁺ TIL phenotyping revealed that many CD8⁺ TILs do not recognize tumour antigens, despite expressing inhibitory receptors⁶⁷. Instead, these cells recognize various epitopes unrelated to cancer, and have been termed ‘bystander’ CD8⁺ TILs. One study compared the phenotype of CD8⁺ TILs and showed that tumour-specific CD8⁺ T-cells expressed the transmembrane ectonucleotidase CD39, while bystander CD8⁺ T-cells did not (Figure 3)⁶⁷. Additional studies have corroborated that CD39 expression primarily identifies tumour-specific CD8⁺ TILs in both humans^{68–70} and mice^{71,72}. Prior to this finding, CD39 was recognized as an exhaustion marker for CD8⁺ T-cells^{73,74}. The knowledge that CD39 can be used to identify tumour-specific CD8⁺ TILs is substantial given the significance of these cells in anti-tumour immunity. Although, it raises many questions, because the enzymatic function of CD39 is considered immunosuppressive^{75,76}.

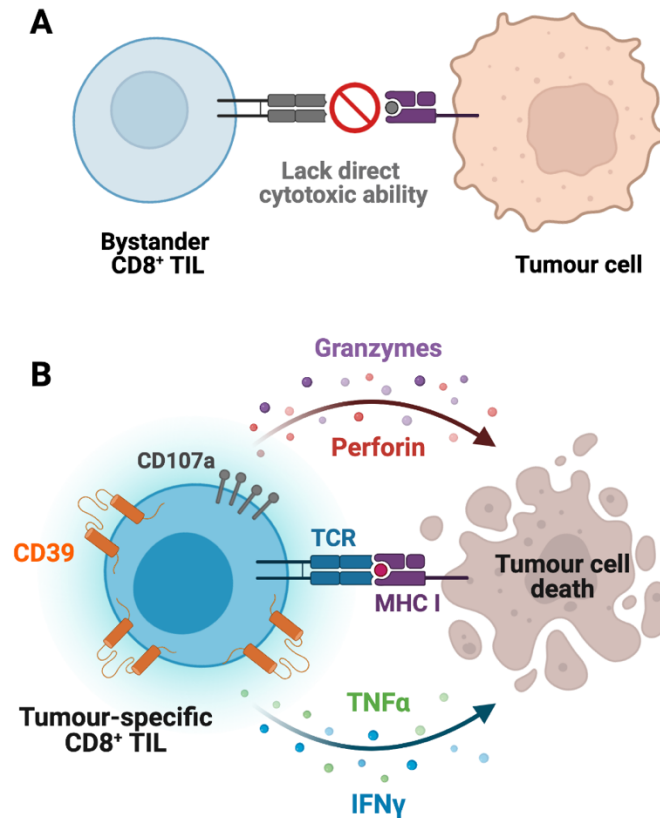


Figure 3. CD39 identifies tumour-specific CD8⁺ TILs.

CD8⁺ T-cells within the tumour (TILs) are not all tumour-specific, there are bystander CD8⁺ TILs that recognize cancer-unrelated antigens (A). These cells cannot recognize or directly induce tumour cell death. Tumour-specific CD8⁺ TILs express CD39 (B), while bystander CD8⁺ TILs do not. Upon neoantigen recognition, tumour-specific CD8⁺ TILs produce effector molecules like TNFα and IFNγ, and cytotoxic molecules like granzyme B and perforin.

1.3 Purinergic signalling in the TME and the canonical function of CD39

Ectonucleotidases catalyze the hydrolysis of nucleotides (tri-, di-, and monophosphate nucleosides) into their respective metabolites, ultimately leading to the generation of nucleosides⁷⁷. Nearly all mammalian cells express transmembrane ectonucleotidases, each in their own distinct pattern and arrangement, in order to regulate their local extracellular environment. The canonical function of CD39 is to hydrolyze extracellular adenosine 5'-triphosphate (ATP, eATP) to adenosine 5'-diphosphate (ADP) and then to adenosine monophosphate (AMP) (Figure 4). Ecto-5'-nucleotidase, CD73, subsequently catalyzes the conversion of AMP to adenosine^{75,76}. In this cascade, CD39 is the rate-limiting enzyme⁷⁸.

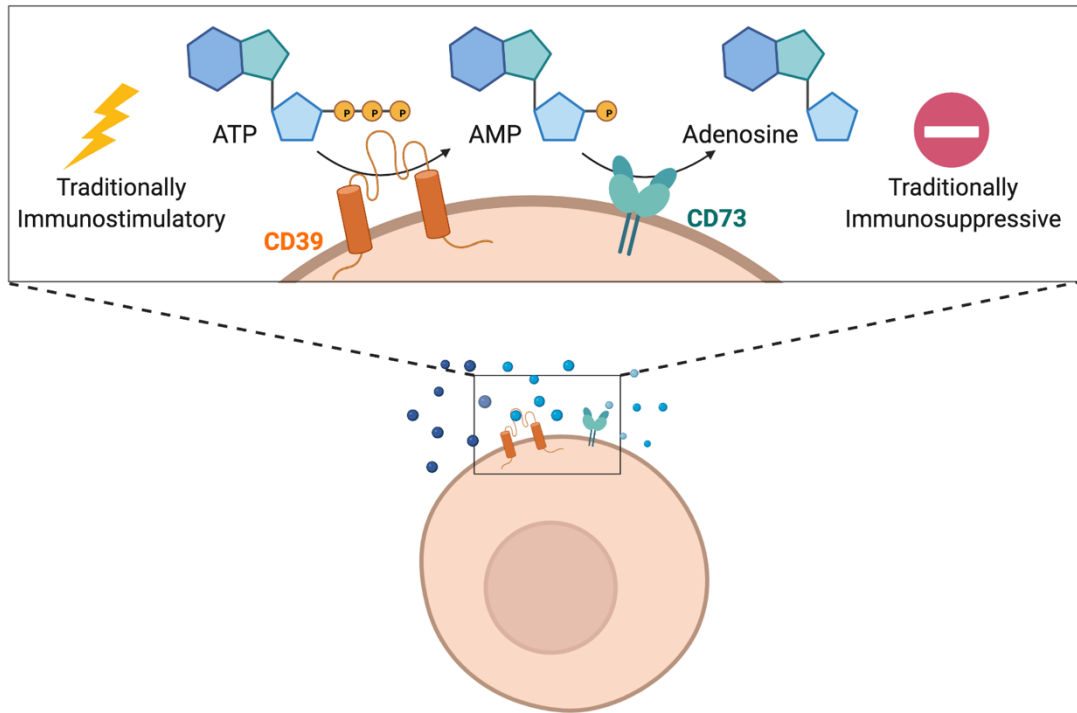


Figure 4. Ectonucleotidases CD39 and CD73 convert ATP to adenosine.

Extracellular ATP is a pro-inflammatory molecule. CD39 functions to hydrolyze ATP to ADP and then AMP. CD73 can then convert AMP to adenosine, which is an immunosuppressive molecule.

Purinergic signalling mediated by ATP and adenosine tightly regulates the functional response of immune cells, among other cellular processes. ATP is a potent immunostimulatory signal, while its metabolite, adenosine, acts as an immunosuppressive signal. These extracellular molecules are present in negligible amounts in healthy tissue, but they can become highly concentrated in the TME⁷⁹.

The accumulation of eATP can result from a broad spectrum of activities. Cells can employ active mechanisms to secrete ATP, to potentiate autocrine and paracrine signalling. For example, T-cells release ATP to the immunological synapse through pannexin I channels upon TCR cross-linking⁸⁰⁻⁸². ATP can bind ATP-gated ion channels, called P2X receptors, thereby inducing Ca²⁺ influx and facilitating autocrine T-cell activation and proliferation^{80,83}. Paracrine signalling can result from ATP released from stressed, damaged, or dying cells. Apoptotic and necrotic cells release ATP, which acts as a ‘find-me signal for immune cells^{75,84}. The rapid degradation of eATP, by CD39 and other ectonucleotidases, restricts P2 receptor activation, limiting receptor sensitization and mitigating ATP-induced cell death^{76,85,86}.

The accumulation of extracellular adenosine primarily comes from the proteolysis of extracellular ATP by ectonucleotidases⁸⁷. Generally, adenosine protects cells and tissues from stress-induced damage, such as inflammatory or hypoxic conditions^{88,89}. Fibroblasts, tumour cells, and some regulatory immune cells within the TME take advantage of ectonucleotidase activity and adenosine production to suppress effector immune cell activity^{78,88,90}. In the context of activated T-cells, adenosine binds stimulatory G protein-coupled receptors, A_{2A} and A_{2B}, which upregulates intracellular cAMP and inhibits T-cell activation, proliferation, and cytokine production⁹¹⁻⁹⁵. CD73 and ecto-enzyme adenosine deaminase (ADA) can regulate the bioavailability of local extracellular adenosine, because ADA irreversibly catalyzes the deamination of adenosine to inosine; restricting adenosine-mediated immunosuppressive signals^{96,97}.

1.4 Anti-tumour activity and prognostic role of CD39⁺CD8⁺ T-cells

The immunosuppressive function of CD39 has, understandably, driven investigations into its purpose and functional consequence on tumour-specific CD8⁺ T-cells. The current literature contains conflicting evidence of the effects of CD39

expression. Depending on the study, CD39 expression is associated with reduced or improved effector function of T-cells. For example, some studies demonstrate that CD39 expression by CD8⁺ T-cells is associated with diminished IFN γ and TNF α production, and reduced cytotoxic abilities^{73,74,98,99}. Concurrently, other studies have shown CD39⁺CD8⁺ T-cells have more potent cytotoxic abilities than their CD39⁻ counterparts, with high granzyme B and IFN γ production^{68,100–104}. Data from various clinical studies demonstrate that a high frequency of CD39⁺CD8⁺ TILs correlates with improved survival^{104–106}. Notably, these cohorts ranged across tumour types, including head and neck squamous cell carcinoma (HNSCC), breast and ovarian cancer. CD39⁺CD8⁺ TILs have also been positively associated with response to treatment with ICIs in cohorts of patients with non-small cell lung cancer (NSCLC) and melanoma^{107,108}. In contrast, a different cohort of melanoma patients showed that CD39 expression on CD8⁺ TILs was associated with lack of response to ICI therapy¹⁰⁹. Currently, there is no definitive answer as to the anti-tumour potential CD39⁺CD8⁺ TILs. Additional studies are required to determine their baseline capabilities and the factors contributing to their function.

1.5 Immunotherapy for cancer treatment

The term ‘immunotherapy’ encompasses treatment approaches that harness the immune system to fight cancer. Currently, T-cells are the backbone of immunotherapies such as ICIs and adoptive cell therapy (ACT). Inhibitory receptors (also known as immune checkpoints) are expressed by various immune cells, including CD8⁺ T-cells, in order to control their activity and prevent excessive inflammatory immune responses. PD-1, TIM-3, LAG-3, and cytotoxic T-lymphocyte-associated protein-4 (CTLA-4) are all examples of inhibitory receptors; however, CTLA-4 acts in a distinct way. CTLA-4 signals are most effective during naïve T-cell priming, while PD-1, TIM-3 and LAG-3 act during the effector phase. Inhibitory receptors function to prevent overactivation and negatively regulate conventional T-cell responses. However, tumour cells and other immunosuppressive cells within the TME can exploit inhibitory receptor pathways to restrain CD8⁺ T-cell function. ICIs are antagonistic monoclonal antibodies (mAb) with strong affinities, designed to block inhibitory receptors and limit their suppressive effects^{19,110}.

CTLA-4 is bound by the same ligands (CD80/CD86) as co-stimulatory receptor CD28, but with a much higher affinity. Since CD28 engagement is required for proper T-cell activation (signal two), CTLA-4 can outcompete CD28 for CD80 and CD86, which impedes T-cell activation. CD4⁺ T-cells express higher levels of CTLA-4 compared to CD8⁺ cells, indicating that anti-CTLA-4 therapies primarily activate CD4⁺ T-cells¹¹¹. Nevertheless, preclinical studies have demonstrated that anti-CTLA-4 treatment during CD8⁺ T-cell priming enhances their cytotoxic function and promotes memory formation^{112,113}. These findings suggest that the success of anti-CTLA-4 therapy could be mediated, in part, by CD8⁺ T-cells. The first FDA-approved ICI was an anti-CTLA-4 mAb named ipilimumab, approved for metastatic melanoma. In addition, ipilimumab in combination with the anti-PD-1 antibody, nivolumab, has been approved for a wide range of cancers¹⁹.

PD-1 is an inhibitory receptor that effectively inhibits CD8⁺ T-cell function after priming, during the effector phase. This occurs through binding by programmed death ligand-1 (PD-L1) or -2 (PD-L2) expressed by tumour cells or APCs¹¹⁴. Specifically, downstream signalling from PD-1 engagement limits cytokine production, alters metabolism, and eventually induces cell cycle arrest^{115,116}. Therefore, anti-PD-1 therapy using nivolumab or pembrolizumab can liberate tumour-specific CD8⁺ T-cells to destroy tumour cells and control tumour growth¹⁹. As such, tumour-specific CD8⁺ T-cells are essential for the efficacy of ICIs.

Immunologically hot tumours can be characterized by high CD3⁺ and CD8⁺ T-cell infiltration, demonstrating that these tumours have pre-existing anti-tumour immunity. This phenotype is associated with a positive response to ICIs, as tumour-specific TILs mediate this therapeutic response¹⁴⁻¹⁷. As previously discussed, immunologically hot tumours are typically more immunogenic because their immunogenic properties can facilitate tumour cell recognition^{21,22}. Tumours with high tumour mutational burden (TMB), i.e., high frequency of genetic mutations, are more likely to generate immunogenic neoantigens¹⁶.

MMR deficiency and genomic instability are factors that affect TMB^{16,21,22,117}. Impairments in the DNA MMR system result in MMR deficiency, which facilitates the accumulation of insertion, deletions, and frameshift mutations at coding microsatellites

(regions of repetitive sequences); thereby increasing genomic instability. For example, colorectal adenocarcinomas with high microsatellite instability (MSI-h) have high TMB and are more immunogenic¹¹⁷. In accordance, these tumours are immunologically hot and patients generally show favourable responses to ICIs¹¹⁷. Tumours with low TMB, such as neuroblastoma, are typically less immunogenic and ICIs have little clinical benefit^{16,118}. Overall, these characteristics highlight a relationship between the genomic instability of tumour cells and the phenotype of a tumour, which influence the efficacy of ICIs.

1.6 MMR pathway and inducing MMR deficiency in neuroblastoma

Neuroblastomas are solid tumours that develop from neural crest cells that normally give rise to cells of the peripheral nervous system. Most commonly, these tumours are found in the adrenal glands or sympathetic ganglia^{118,119}. Neuroblastoma is considered a rare childhood cancer; however, it is the primary cause of death from paediatric cancers for children aged 1-5 years old. Patients diagnosed after the age of 18 months often present with unresectable tumours and metastatic disease¹¹⁸⁻¹²⁰.

Neuroblastomas are considered immunologically cold, meaning there is minimal CD8⁺ T-cell infiltration¹⁶. This is partly due to the low TMB and therefore, low immunogenicity of neuroblastoma tumours^{118,121-123}. As previously discussed, tumours with these characteristics are more capable of evading anti-tumour immunity and they are less susceptible to immunotherapy with ICIs. To put simply, T-cells cannot benefit from ICIs if there are no immunogenic neoantigens to elicit an anti-tumour immune response in the first place.

Given that MMR deficiency promotes the translation of unique tumour-specific neoantigens, it makes tumour cells more likely to be recognized by the immune system¹¹⁷. As such, it is possible that inducing MMR deficiency in an immunologically cold tumour, like neuroblastoma, could increase the immunogenicity of the tumour, promote anti-tumour immunity, and boost the efficacy of ICIs.

In order to induce MMR deficiency, an understanding of the MMR pathway is required. There are four crucial protein-encoding genes that make up the MMR system; including MutL homologue (*MLH1*), MutS homologue (*MSH2*), MutS homologue 6 (*MSH6*) and post-meiotic segregation increase 2 (*PMS2*). MSH2 and MSH6 proteins form

heterodimers (MutS) which identify and bind the initial DNA base mismatch. MutS recruits replication factor C, proliferating cell nuclear antigen (PCNA), and MLH1 and PMS2 protein heterodimers (MutL). PCNA-activated MutL creates an incision at the mismatch site, facilitating the removal of mismatched bases by exonuclease 1. Replication protein A (RPA) displaces the mismatched bases and protects the single stranded DNA gap, until DNA polymerase and ligase synthesize and integrate the correct DNA bases^{124,125}.

MMR deficiency can arise from mutations in MMR pathway genes (*MLH1*, *MSH2*, *MSH6*, *PMS2*) or sporadic epigenetic abnormalities affecting expression of those genes^{125,126}. Our lab has generated an immunogenic murine neuro-2a (neuroblastoma) cell line through CRISPR/Cas9 (clustered regularly interspaced short palindromic repeats/CRISPR-associated protein 9) knockout (KO) of the *MLH1* gene. The MLH1 protein plays a crucial role in DNA MMR processing¹²⁶.

In summary, inducing MMR deficiency enables the accumulation of somatic mutations, increasing the likelihood of immune detection through neoantigen production (Figure 5)^{117,125}. This model allows us to study tumour-specific T-cells since the MLH1 protein plays a crucial role in DNA MMR processing¹²⁶. Thus, knocking out *MLH1* renders neuro-2a cells MMR-deficient and more immunogenic.

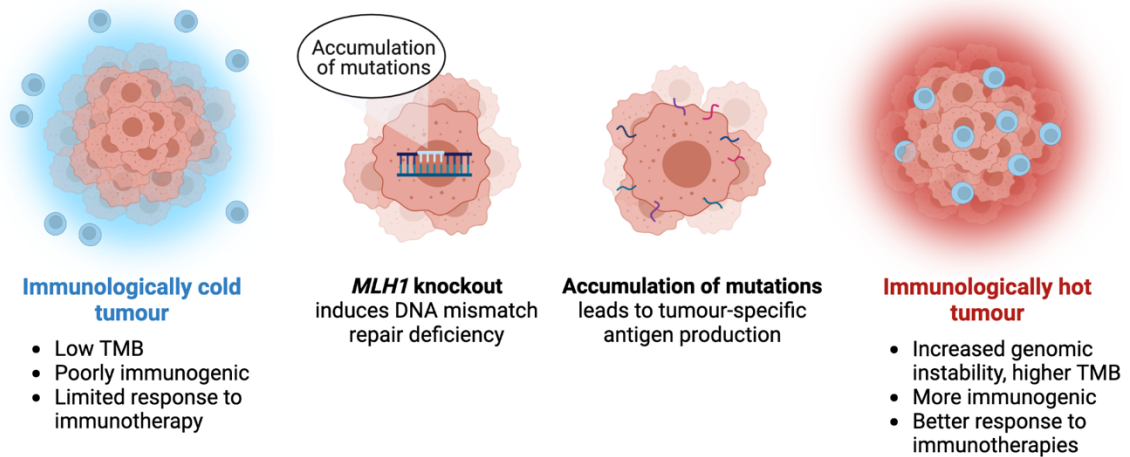


Figure 5. Turning immunologically cold tumours hot by inducing MMR deficiency.

Immunologically cold tumours are poorly immunogenic with low TMB and lack T-cell infiltration. Inducing DNA MMR deficiency by knocking out the *MLH1* gene will increase genomic instability, which facilitates the accumulation of mutations and increases TMB. This increases the likelihood of tumours to produce immunogenic neoantigens, which in turn, enables tumour-specific CD8⁺ T-cells to recognize tumour cells as foreign. Inducing MMR deficiency will convert the tumour to an immunologically hot phenotype, since tumour-specific CD8⁺ T-cells will be recruited to the more immunogenic tumour.

1.7 Rationale, Hypothesis, and Aims

Recently, CD39 has been described as a marker for tumour-specific CD8⁺ TILs, as bystander CD8⁺ TILs do not express this enzyme⁶⁷⁻⁷². CD39 has also been recognized as an exhaustion marker for CD8⁺ T-cells^{73,74}. Given that CD39 facilitates the production of immunosuppressive adenosine, it is commonly theorized that the expression of CD39 by CD8⁺ TILs contributes to their exhaustion. However, enzymes such as ADA can regulate the bioavailability of extracellular adenosine, highlighting that CD39 is not the only enzyme regulating local molecular milieu. Moreover, some studies have found that CD39⁺CD8⁺ TILs can exhibit meaningful anti-tumour activity^{68,100-104}.

IL-12 and IL-27 can modulate CD8⁺ T-cell differentiation and effector function. These cytokines share structural and functional similarities but can exert different effects on CD8⁺ T-cells³⁸. Upon neoantigen recognition, tumour-specific CD8⁺ T-cells acquire effector functionality, which is essential for anti-tumour activity³¹. Therefore, IL-12 and IL-27 can modulate the anti-tumour activity of tumour-specific CD8⁺ T-cells. Since IL-12 and IL-27 contribute to CD8⁺ T-cell effector function and tumour-specific cells express CD39, these cytokines could play a role in regulating CD39 expression. This notion is supported by studies demonstrating that IL-12 and IL-27 can induce CD39 expression on T-regulatory cells^{127,128}. Due to the significance of tumour-specific T-cells in anti-tumour immunity and response to immunotherapy, an investigation of the factors contributing to CD39 expression and their consequential effects on CD8⁺ T-cell function are required.

1.7.1 Hypothesis

IL-12 and IL-27 upregulate CD39 expression on CD8⁺ T-cells. CD39⁺CD8⁺ T-cells exhibit improved effector cell activity compared to CD39⁻CD8⁺ T-cells, and such functions will be differentially affected by IL-12 and IL-27.

1.7.2 Aims

1. Examine whether IL-12 and IL-27 induce CD39 expression on CD8⁺ T-cells and assess the effects of IL-12 and IL-27 on CD8⁺ T-cell phenotypes.
2. Determine whether CD39⁺CD8⁺ T-cells have improved effector function compared to CD39⁻CD8⁺ T-cells.

Chapter 2 – Methods

2.1 Cell lines

Neuro-2a cells were purchased from American Type Culture Collection (ATCC). Immunogenic (*MLH1* KO) neuro-2a cells were generated by our labs technician, through CRISPR/Cas9 knockout (plasmid from Santa Cruz Biotechnology) of the *MLH1* gene, and cells were expanded from a single clone¹²⁹. Control neuro-2a cells were expanded from a different clone, in which the transfection process was successful, but the knockout of the *MLH1* gene was not. Thus, the *MLH1* gene is intact in control neuro-2a cells. The control cells were used as the control, rather than the parental (wildtype) neuro-2a cells, to account for the transfection process. The *MLH1* KO and control neuro-2a cells had similar proliferation rates *in vitro*¹²⁹.

The day in which neuro-2a cells were transfected was considered day 0. Cells were cultured for 7 weeks after transfection, to allow for the accumulation of mutations, followed by cryopreservation at -80 °C. Cells were thawed and expanded for an additional 1-2 weeks (8-9 weeks total) for experimental use. This was to keep the mutational burden consistent across experiments, as the length of time in culture of MMR-deficient cells can affect tumour immunogenicity¹³⁰.

Cells were cultured in RPMI 1640 medium (Wisent Bio Products) supplemented with 10% heat-inactivated (H.I.) fetal bovine serum (FBS) (GIBCO, Life Technologies) at 37 °C and 5% CO₂. For relevant experiments, 7-week-cultured neuro-2a cells were grown for an additional 1-2 weeks until they reached 70-90% confluency. Cells were washed with phosphate-buffered saline (PBS) (Wisent Bio Products) before adding 1-3 ml of pre-warmed Trypsin (Wisent Bio Products) and incubated at room temperature (RT) until cells were visibly detached. Trypsin activity was inhibited with supplemented RPMI media. Cells were washed with PBS and counted with the Beckman Coulter Cell Counter (Beckman Coulter) for use in the methods described below.

2.2 Animal models

Female A/J mice were purchased from the Jackson Laboratory for use in a syngeneic mouse model. Mice were 6-10 weeks of age when acquired and housed in the

Victoria Research Laboratories Vivarium. Animal work was approved by the Animal Care Committee at Western University (London, ON, Canada), Animal Use Protocol 2021-102.

For tumour model experiments, 5×10^5 control or immunogenic (*MLH1* KO) 8-week-cultured neuro-2a cells (in PBS) were subcutaneously (s.c.) injected into the right flank of mice (day 0). The length and width of each tumour was determined by calliper measurement once tumours became palpable. Tumour volumes were calculated with the following formula: $\text{volume} = (\text{length} \times \text{width}^2)/2$. Tumour volumes were measured every 2-3 days. All mice were euthanized via CO₂ asphyxiation once the first tumour volumes reached approximately 1500 mm³.

For IL-12 neutralization experiments, tumours were palpable ~12 days post tumour inoculation. At such time, mice were injected intraperitoneally (i.p.) with 0.5 mg of *InVivo*MAb anti-mouse IL-12 p75 (α IL-12, clone R2-9A5, BioXCell) or Ultra-LEAF Purified Rat IgG2b, κ Isotype Ctrl antibody (isotype control, clone RTK4530, BioLegend) in PBS, every 3-4 days until endpoint^{131–133}.

2.3 Tissue processing

Throughout this protocol, cold reagents were used unless otherwise stated, and samples were kept on ice during wait periods. Mice were euthanized via CO₂ asphyxiation, after which the spleen and/or tumour were isolated from each mouse. The spleen was cut into multiple pieces and mechanically disrupted with the plunger of a 10 ml syringe. Splenocytes were filtered through a 70 μ m cell strainer with RPMI to remove stromal tissue. Each tumour was weighed, mechanically disrupted using a scalpel, and transferred to a gentleMACS C Tubes (Miltenyi Biotec). Cell suspensions of tumour tissue were generated using the Mouse Tumour Dissociation Kit and GentleMACS Dissociator (Miltenyi Biotec) according to the manufacturer's instructions; this included reducing the amount of Enzyme R to 20% of recommended volume in order to preserve TILs. Tumour cell suspensions were filtered through a 70 μ m cell strainer to remove stromal tissue.

Filtered cell suspensions were centrifugated at 300 rcf for 5 minutes at 4 °C. Splenocyte and tumour tissue cell pellets were resuspended in 1 and 3 ml of Ammonium-Chloride-Potassium (ACK) lysis buffer (deionized water, 150 mM NH₄Cl, 10 mM KHCO₃, 100 μ M EDTA, pH 7.1), respectively. Cell suspensions were incubated for 3 minutes at

RT to remove red blood cells. The ACK lysis reaction was inhibited with 30 ml of PBS and 2% H.I. FBS. Samples were washed with PBS and quantified using the Beckman Coulter Cell Counter. Splenocyte and tumour cell suspensions were diluted at 5×10^6 cells/ml for further analysis. Tumour samples from each group were pooled when yields were low, in order to provide sufficient quantities for flow cytometric analysis.

2.4 Tumour lysate preparation

For tumour lysate preparation, 8-9-week-cultured control or immunogenic (*MLH1* KO) neuro-2a cells were harvested and counted. Cell concentrations were adjusted to 5×10^7 cells/ml in PBS. Approximately 1 ml of cell suspensions were aliquoted into 1.5 Eppendorf tubes for lysate generation. Cell suspensions were frozen in a slurry of dry ice with 70% EtOH for 5 minutes and thawed in a 37 °C water bath for 5 minutes. The freeze-thaw cycles were repeated for a total of 5 times, to produce whole neuro-2a cell lysates. Cell viability was assessed with a haemocytometer or Countess 3 Automated Cell Counter (Thermo Fisher Scientific) using trypan blue. If the viability was greater than 1%, additional freeze-thaw cycles were completed until it was less than 1%. Aliquots were stored at -80 °C until further use.

2.5 Immune cell stimulation assays

Stock solutions of recombinant mouse IL-2, IL-12, and IL-27 (carrier-free, BioLegend) were prepared at 50 or 100 µg/ml in sterile 1% bovine serum albumin (BSA) and stored as aliquots at -80 °C. BSA was used as a carrier protein to improve the stability of recombinant cytokines¹³⁴. Cytokine supplemented lymphocyte media were prepared using lymphocyte medium (RPMI with 10% H.I. FBS, 1% penicillin/streptomycin, 2 mM L-glutamine, and 50 µM β-mercaptoethanol) with IL-2 (30 ng/ml), IL-12 (10 ng/ml), and/or IL-27 (50 ng/ml)^{50,135–138}. Throughout this protocol, cold reagents were used unless otherwise stated, and samples were kept on ice during wait periods. All centrifugation steps were completed at 300 rcf for 5 minutes at 4 °C.

2.5.1 Stimulation assays using CD8⁺ T-cells

For CD8⁺ T-cell priming experiments, each mouse received an i.p. injection of 100 µl of control or immunogenic (*MLH1* KO) neuro-2a lysate (equivalent of 5×10^6 cells) on

day 0 and day 7. On day 11, mice were euthanized, and spleens from each group were pooled for processing. Similarly, for naïve CD8⁺ T-cell experiments, naïve animals were euthanized, and spleens were pooled for processing (as described in the tissue processing section). The ACK lysis reaction was inhibited by adding 30 ml of 1X MojoSort buffer (BioLegend). Splenocytes were washed with MojoSort buffer once more. Samples were quantified with a haemocytometer or Countess 3 using trypan blue, and the cell suspension volumes were adjusted to a final concentration of 1×10^8 cells/ml in MojoSort buffer.

CD8⁺ T-cells were then isolated using the MojoSort Mouse CD8 T-cell Negative Selection Isolation Kit (BioLegend) according to the manufacturer's instructions. Upon completion, the CD8⁺ T-cell fractions were washed with lymphocyte medium and quantified using the Countess 3. Cell suspensions were separated into 3-4 tubes depending on the experimental conditions. Following centrifugation, CD8⁺ T-cells were resuspended at a concentration of 250,000 cells/ml in lymphocyte media containing IL-2 alone, IL-2 and IL-12, IL-2 and IL-27, or all three recombinant cytokines. Aliquots of 50,000 cells (200 μ l) were transferred to 96-well u-bottom plates containing an equivalent number of washed Dynabeads Mouse T-Activator CD3/CD28 (Thermo Fisher Scientific, prepared according to manufacturer's instructions). Samples were homogenized before incubation at 37 °C, 5% CO₂ (day 11). Each technical replicate was comprised of 10 wells, with three replicates per experimental condition.

After 24 hours (day 12), samples were resuspended. Dynabeads were magnetically separated by placing the plates on a DynaMag-96 Side Skirted magnet (Thermo Fisher Scientific) for 5 minutes. Cell suspensions were transferred to new 96-well u-bottom plates, while the Dynabeads remained in the original plates. This process was done twice to ensure the removal of any Dynabeads that were missed the first time. The remaining Dynabeads were thoroughly washed with 50 μ l of the appropriate, pre-warmed, cytokine-supplemented lymphocyte media to remove any Dynabead-bound cells. This process was followed by another magnetic separation. Cells were transferred to corresponding wells of the new plates and incubated at 37 °C and 5% CO₂. After 24 hours (day 13), cells were washed with PBS and then technical replicate wells were pooled (10 wells to 1 well). Samples were transferred to a 96-well v-bottom plate and washed with PBS prior to extracellular cytokine staining for flow cytometric analysis.

2.5.2 Stimulation assays using bulk splenocytes for intracellular cytokine staining

Mice received a s.c. injection of 100 μ l of immunogenic (*MLHI* KO) neuro-2a lysate (the equivalent of 5×10^5 cells) on day 0 and day 7. On day 11, cell culture T-75 flasks were prepared prior to splenocyte collection by coating them with 8 ml of α CD3 (1 μ g/ml) and α CD28 (1 μ g/ml) antibodies (Abs) in PBS. Flasks were incubated for at least 3 hours at 37 $^{\circ}$ C, to allow Abs to adhere to the bottom. Mice were euthanized and spleens were pooled for processing (as described in the tissue processing section). The ACK lysis reaction was inhibited with 30 ml of lymphocyte media (RPMI with 10% H.I. FBS, 1% penicillin/streptomycin, 2 mM L-glutamine and 50 μ M β -mercaptoethanol).

Cells were washed additionally with lymphocyte media and the sample was quantified with the Countess 3 using trypan blue. The sample was divided into four tubes and centrifuged. Cell pellets were resuspended at a concentration of 1×10^6 cells/ml in lymphocyte media containing IL-2 alone, IL-2 and IL-12, IL-2 and IL-27, or all three cytokines. Flasks with plate-bound α CD3 and α CD28 Abs were removed from the incubator, PBS was aspirated, and 20 ml of each cell suspension was added to a T-75 flask. The bulk splenocyte suspensions were incubated at 37 $^{\circ}$ C and 5% CO₂ for 48 hours.

After 48 hours, the cells were harvested. Flasks were washed with PBS before incubating with 5 ml of 0.5 mM ethylenediaminetetraacetic acid (EDTA) on ice for 10 minutes. EDTA was used in an attempt to remove cells that were still bound to the plate, as trypsin can affect the membrane protein structures and potentially destroy surface antigens¹³⁹. Cells were washed twice with the appropriate cytokine supplemented lymphocyte medium, and the cell concentration was adjusted to 1×10^6 cells/ml. Brefeldin A (5 μ g/ml, BioLegend), and CD107a-Brilliant Violet 510 Ab (1/200 dilution, BioLegend) were added, and samples were mixed thoroughly. To the positive control groups, a cell activation cocktail (BioLegend) was added, which was composed of phorbol 12-myristate 13-acetate (PMA, 81 nM) and ionomycin (1.34 μ M). To the experimental groups, aliquots of 250,000 cells (250 μ l) were transferred to 96-well u-bottom plates containing 50 ng/well of plate-bound α CD3 and α CD28. Plates were incubated at 37 $^{\circ}$ C, 5% CO₂ for 5 hours. After 5 hours, cells were washed with PBS and pooled (4 wells to 1 well). Samples were

transferred to a 96-well v-bottom plate and washed twice with PBS, prior to extracellular and intracellular cytokine staining for flow cytometric analysis.

2.6 Extracellular protein staining

Throughout this protocol, cold reagents were used unless otherwise stated. All incubation steps occurred in the dark. Tumour tissue, splenocyte, or CD8⁺ T-cell suspensions were generated as described above, in order to analyze cell CD8⁺ T-cell phenotypes. In a 96-well v-bottom plate, 1×10^6 cells were suspended in 50 μ l PBS with Zombie NIR, Red, or Green Viability Dye (1/1000, BioLegend) and incubated at RT for 20 minutes. Cells were washed twice with FACS buffer (Fluorescence-activated cell sorting flow cytometry staining buffer: 1x PBS with 5% HI FBS and 0.02% NaN₃). Cells were resuspended in 50 μ l of anti-mouse CD16/32 Ab (10 μ g/ml, Clone 93, BioLegend) and incubated on ice for 10 minutes to block Fc-receptors. Cells were washed once with FACS buffer and resuspended in 50 μ l of Ab stains (Table 1, all Abs were obtained from BioLegend). Cells were incubated on ice for 20 minutes. Samples that were only stained for extracellular markers were washed with FACS buffer twice and resuspended in 50 μ l of 2% paraformaldehyde (Fixation buffer, BioLegend, diluted 1:1 with PBS). Cells were incubated for 20 minutes at RT to fix cells. Samples were washed once and resuspended in FACS buffer for flow cytometric analysis.

2.7 Intracellular cytokine staining

The extracellular cytokine staining method in section 2.6 was followed until the extracellular Ab incubation stage. For intracellular cytokine staining, cells were washed with FACS buffer once, followed by a wash with 1X Cyto-Fast Perm Wash solution (BioLegend). Cells were resuspended in 100 μ l of Cyto-Fast Fix/Perm buffer (BioLegend) and incubated for 20 minutes at RT. Cells were washed twice with Cyto-Fast Perm Wash solution and resuspended in 100 μ l of [intracellular] Ab stains (Table 1.). Samples were incubated for 20 min at RT. Cells were washed with Cyto-Fast Perm Wash solution, then FACS buffer, then resuspended in FACS buffer for flow cytometric analysis.

2.8 Flow cytometry

For each independent experiment, single stains of splenocytes, tumour samples, and/or UltraComp eBeads (Thermo Fisher Scientific) were prepared for use as compensation controls. Data were acquired using the BD LSR II flow cytometer with BD FACS Diva software. FlowJo v10.8 software (BD Biosciences) was used to calculate compensation matrices and data analysis. Fluorescence minus one (FMO) samples were used as a control measure, in which a sample is stained with all Abs except one. These were used to distinguish where the positive cells should be gated on a flow plot because, for example, the CD39-Alexa Fluor 647 FMO should contain no CD39⁺ cells. The cut-off for a positive gate on an FMO is < 1%.

Table 1. Summary of antibodies used for flow cytometry staining

Location	Antibody Target	Fluorophore	Clone	Dilution
Surface	CD8a	PerCP	53-6.7	1:100
	CD3	Brilliant Violet 711	17A2	1:200
	CD39	Alexa Fluor 647	Duha59	1:100
	PD-1 (CD279)	Brilliant Violet 605	29F.1A12	1:200
	PD-1 (CD279)	PE	29F.1A12	1:200
	TIM-3 (CD366)	PE	B8.2C12	1:200
	LAG-3 (CD223)	PE/Cyanine7	C9B7W	1:200
	CD38	Alexa Fluor 488	90	1:400
	CD45	Pacific Blue	30-F11	1:200
	CD44	PE	IM7	1:800
	CD62L	Brilliant Violet 605	MEL-14	1:200
	Fas (CD95)	FITC	SA367H8	1:400
Surface/ intracellular	CD107a	Brilliant Violet 510	1D4B	1:200
Intracellular	IFN γ	PE	XMG1.2	1:400
	TNF α	Alexa Fluor 488	MP6-XT22	1:400
	IL-2	Brilliant Violet 421	JES6-5H4	1:200

2.9 Statistical analysis

Data are represented as mean \pm standard error of the mean (SEM). Data were analyzed using the unpaired t-test, one-way or two-way analysis of variance (ANOVA) with Tukey's multiple comparison test. Statistical analyses were performed using GraphPad Prism v9 software, and p values ≤ 0.05 were considered significant as indicated by an asterisk (*) and 'ns' means not significant.

Chapter 3 – Results

3.1 MLH1 KO neuro-2a tumours contain a higher frequency of tumour-specific CD39⁺CD8⁺ T-cells than control neuro-2a tumours, which correlates with reduced tumour burden

In general, neuroblastomas are immunologically cold. This can be attributed to the paucity of somatic mutations and the immunosuppressive TME^{118,121–123}. Previously, the lab established that the baseline tumour kinetics were analogous between the *MLH1* KO and control neuro-2a tumours when grown in immunodeficient SHO mice. Importantly, this was not the case for tumour-bearing immunocompetent A/J mice. The *MLH1* KO neuro-2a tumour-bearing mice showed significantly delayed tumour growth compared to those with control neuro-2a tumours¹²⁹. These results indicate that the elevated tumour control observed in *MLH1* KO neuro-2a tumour-bearing mice is immune-mediated. Thus, inducing mismatch repair deficiency (*MLH1* KO) enables stronger anti-tumour immunity.

To validate these findings, I repeated the experiment using immunocompetent mice. A/J mice were inoculated s.c. with control or *MLH1* KO neuro-2a cells on day 0. Tumour volumes were measured over an 18-day period. This experiment also allowed the investigation of CD39⁺CD8⁺ T-cell levels within tumours and spleens (as a systemic measure) of the animals using flow cytometry (Figure 6).

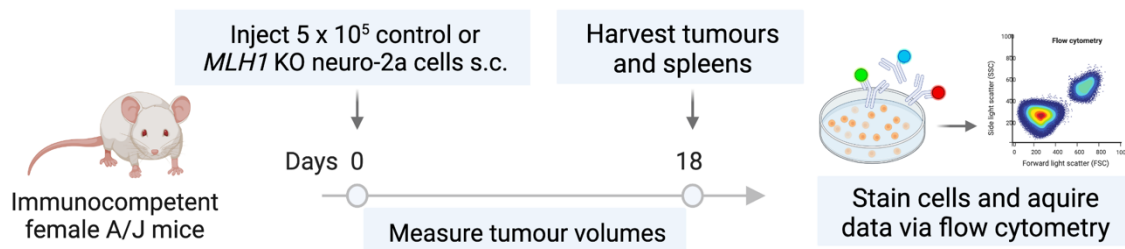


Figure 6. Simplified method comparing the immune characteristics of control and *MLH1* KO neuro-2a tumours.

Female A/J mice were inoculated s.c. with 5×10^5 control ($n = 14$) or *MLH1* KO ($n = 10$) neuro-2a cells. Tumour volumes were measured over time using callipers. On day 18, all mice were euthanized. Tumours from each group were pooled and processed, while spleens were processed individually. Samples were stained for flow cytometric analysis of CD39⁺CD8⁺ T-cell populations.

Tumour volume measurements were used to compare control or *MLHI* KO neuro-2a tumour burden over time. By day 14, reduced tumour burden was observed in mice-bearing *MLHI* KO neuro-2a tumours compared to those with control neuro-2a tumours (Figure 7 a). This difference was also statistically significant at the endpoint (day 18). As an additional measure of tumour burden, tumours were weighed immediately following excision. As expected, *MLHI* KO neuro-2a tumours had significantly less mass than the control neuro-2a tumours (Figure 7 b). These data demonstrate that inducing mismatch repair deficiency (*MLHI* KO) in neuro-2a tumours results in delayed tumour growth, as observed by reduced tumour burden. Together with previous data from immunodeficient mouse experiments, these results support the notion that *MLHI* KO neuro-2a tumours are more immunogenic than control neuro-2a tumours.

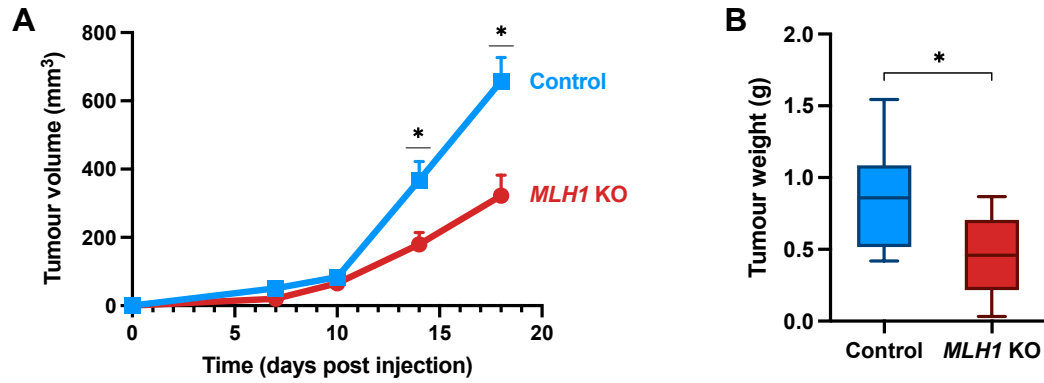


Figure 7. Tumour burden of control and *MLH1* KO neuro-2a tumours.

Mice were inoculated s.c. with 5×10^5 control ($n = 14$) or *MLH1* KO ($n = 10$) neuro-2a cells. **A)** Tumour volume of control and *MLH1* KO neuro-2a tumours plotted against time. Data represent mean \pm SEM of two pooled experiments. **B)** The weights of control and *MLH1* KO neuro-2a tumours at endpoint (day 18) depicted as box plots. Mean \pm standard deviation (SD) was calculated for statistical analysis. * $p \leq 0.05$ by unpaired t-test.

Previously, our lab investigated whether CD8⁺ TILs from control and *MLHI* KO neuro-2a tumours displayed different phenotypes. One of the phenotypic markers assessed was CD39, as it was previously shown to distinguish tumour-specific CD8⁺ TILs from bystander CD8⁺ TILs^{67,68,98}. The earlier flow cytometry data showed that *MLHI* KO neuro-2a tumours had a higher frequency of CD39⁺CD8⁺ TILs than control neuro-2a tumours¹²⁹. Those results suggested a relatively higher frequency of tumour-specific CD8⁺ TILs were present in *MLHI* KO neuro-2a tumours. Therefore, we sought to confirm these results.

Flow cytometry was used to examine the frequency of CD39⁺CD8⁺ T-cell levels from the tumours and spleens of mice. Splenocytes were used as a measure of systemic immunity, to see whether enhanced immunogenicity of neuro-2a tumours would affect the systemic immune landscape. Data analysis of TILs demonstrated that *MLHI* KO neuro-2a tumours contained a greater frequency of CD39⁺CD8⁺ TILs compared to control neuro-2a tumours, while the frequency of CD8⁺ TILs was not different (Figure 8 a-c). These results correspond with data from the past experiments completed in the lab¹²⁹. This also correlates with reduced tumour burden found in these mice relative to those with control neuro-2a tumours (Figure 7 a, b). Given the reduced tumour burden in the *MLHI* KO group and elevated frequency of CD39⁺CD8⁺ TILs, the *MLHI* KO neuro-2a cells will be referred to, herein, as immunogenic.

We found no differences in the frequencies of splenic CD8⁺ or CD39⁺CD8⁺ T-cells between groups (Figure 8 d, e). There is no quantitative difference in the systemic level of CD39⁺CD8⁺ T-cells between groups. As such, it is possible that the differences in tumour burden may be attributed to the CD8⁺ TIL anti-tumour activity within the TME. These results suggest that the primary CD8⁺ T-cell anti-tumour immune response is within the tumour.

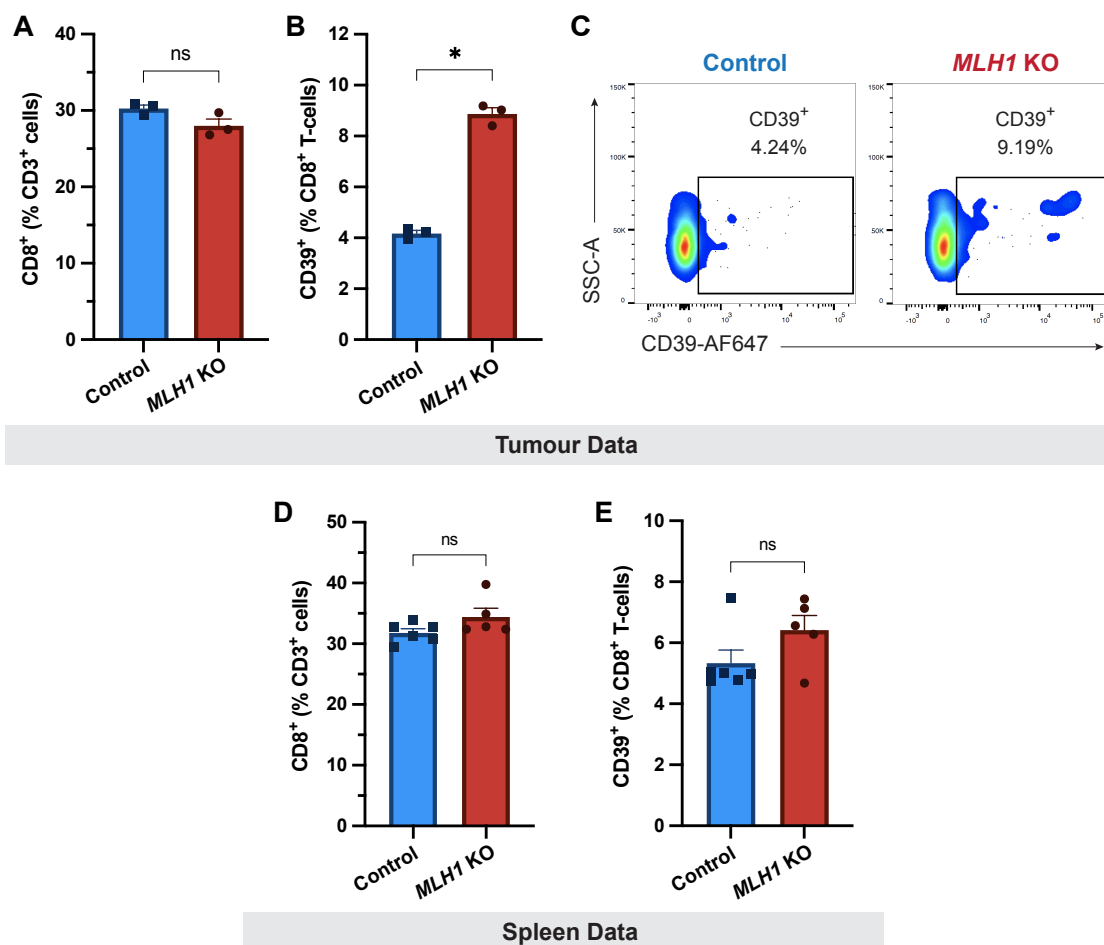


Figure 8. Frequency of CD39⁺CD8⁺ T-cells from tumours and spleens of neuro-2a tumour-bearing mice.

Tumours and spleens from control (n = 6) or *MLH1* KO (n = 5) were harvested 18 days after inoculation. Tumours from each group were pooled and processed, while spleens were processed individually. Samples were stained for flow cytometric analysis of CD8⁺ T-cell populations. **A-C)** Frequency of CD3⁺ TILs expressing CD8 (**A**) and CD8⁺ TILs expressing CD39 (**B**) from control or *MLH1* KO neuro-2a tumours. Data represent mean ± SEM of technical replicates. Representative dot plots depicting CD39⁺ expression, gated on CD8⁺CD3⁺ cells (**C**). **D-E)** Frequency of CD3⁺ T-cells expressing CD8 (**D**) and CD8⁺ T-cells expressing CD39 (**E**) from spleens of control or *MLH1* KO neuro-2a tumour-bearing mice. Data represent mean ± SEM of biological replicates. * p ≤ 0.05, ns = not significant by unpaired t-test.

3.2 The effects of IL-12 and IL-27 on the expression of CD39 on CD8⁺ T-cells from neuro-2a antigen-naïve and -experienced mice

Recent data have highlighted a role for IL-12 and IL-27 in cytotoxic CD8⁺ T-cell differentiation and effector function^{51,140}. Upon neoantigen recognition, tumour-specific CD8⁺ T-cells elicit effector activity^{21,22}. To confirm whether CD39 was expressed by effector CD8⁺ T-cells, the differentiation state of CD8⁺ T-cells from spleens and tumours of immunogenic neuro-2a tumour-bearing mice were phenotyped using flow cytometry. The surface expression pattern of CD44, CD62L and Fas was used to distinguish naïve ($T_{\text{naïve}} = \text{CD44}^{-}\text{CD62L}^{+}\text{Fas}^{-}$), stem cell-like memory ($T_{\text{SCM}} = \text{CD44}^{-}\text{CD62L}^{+}\text{Fas}^{+}$), memory ($T_{\text{CM}} = \text{CD44}^{+}\text{CD62L}^{+}$) or effector ($T_{\text{EFF}} = \text{CD44}^{+}\text{CD62L}^{-}$) CD8⁺ T-cells^{141,142}. CD44 is upregulated upon activation and facilitates cell adhesion and migration¹⁴³. In addition, Fas is considered an activation marker and functions as a cell death receptor¹⁴⁴. CD62L is a homing receptor that facilitates cell migration to and from peripheral lymph nodes and acts as a marker for naïve and memory T-cells¹⁴⁵.

We found CD39 was predominantly expressed by effector and central memory CD8⁺ T-cells, with little to no expression on naïve or stem cell-like memory cells, regardless of their tissue of origin (Figure 9 a, b). These results are in agreement with the literature, which show that CD39 is expressed by activated T-cells (those with effector capabilities)^{146–148}.

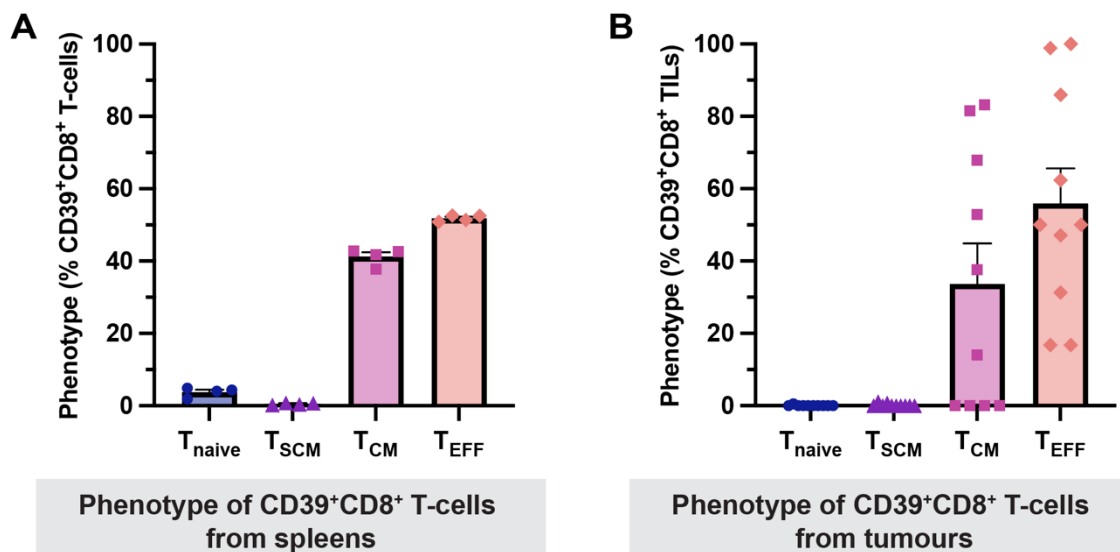


Figure 9. Frequency of naïve, stem cell-like memory, effector, and central memory CD39⁺CD8⁺ T-cells from spleens and tumours of immunogenic neuro-2a tumour-bearing mice.

Mice were inoculated s.c. with 5×10^5 immunogenic neuro-2a cells. After 21 days, tumours and spleens were processed individually and stained for flow cytometric analysis of CD39⁺CD8⁺ T-cell populations. **A-B**) Frequency of CD39⁺CD8⁺ T-cells from the tumour ($n = 9$) (**A**) or spleens ($n = 4$) (**B**) with a naïve ($T_{naive} = CD44^-CD62L^+Fas^-$), stem cell-like memory ($T_{SCM} = CD44^-CD62L^+Fas^+$), memory ($T_{CM} = CD44^+CD62L^+$) or effector ($T_{EFF} = CD44^+CD62L^-$) phenotype. Data represent the mean \pm SEM of biological replicates.

3.2.1 IL-12 and IL-27 induce CD39 expression on CD8⁺ T-cells from naïve mice

First, we sought to examine whether splenic CD8⁺ T-cells from tumour-antigen naïve mice (untreated) would differentially express CD39 when activated in the presence of IL-12 or IL-27. In this experiment, we were not concerned about the antigen specificity of the CD8⁺ T-cells, but rather the factors that could be contributing to CD39 expression. To do so, a stimulation assay was conducted¹³⁶ (Figure 10). For the control group, CD8⁺ T-cells were stimulated with α CD3/CD28 Dynabeads (signal 1 and 2) and recombinant IL-2 (signal 3). Experimental groups were stimulated as described, with the addition of recombinant cytokines IL-12 or IL-27. After 48 hours, cells were stained for flow cytometric analysis of CD39 expression. An acute activation period was used rather than chronic activation, as CD39 expression has been associated with exhaustion^{73,74}. Thus, acute stimulation (48 hours) was used to minimize this confounding variable.

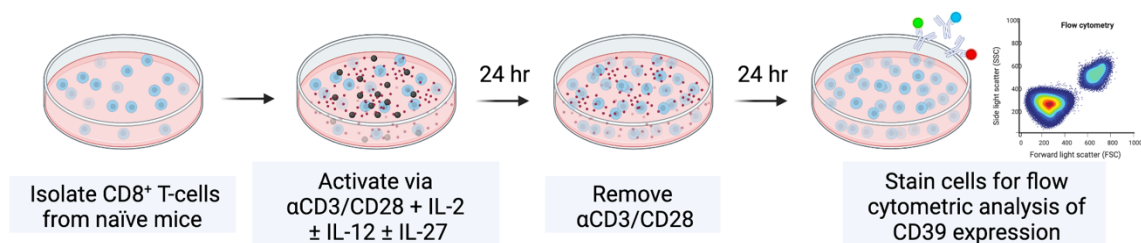


Figure 10. Simplified stimulation assay method with CD8⁺ T-cells from neuro-2a-antigen naïve mice.

Splenic CD8⁺ T-cells from untreated (naïve) mice were isolated via negative selection using a magnetic sorting kit. For the control group, CD8⁺ T-cells were stimulated at a 1:1 ratio with αCD3/CD28 Dynabeads and recombinant IL-2. Experimental groups were stimulated with additional recombinant cytokines, either IL-12 or IL-27. After 24 hours, αCD3/CD28 Dynabeads were magnetically removed, and cells remained in culture for an additional 24 hours with cytokines. Finally, cells were stained for flow cytometry analysis of CD39 expression.

Two sets of data were obtained by flow cytometry, the frequency of CD8⁺ T-cells which express CD39, and the level of CD39 expression. First, the frequency of CD39⁺CD8⁺ T-cells were analyzed using a low vs. high CD39 expression gating strategy philosophy, based on that of Canale et al. (2018)⁷⁴. When stimulated in the presence of IL-12 or IL-27, a greater frequency of CD8⁺ T-cells expressed high levels of CD39 (CD39^{high}) compared to the control group (Figure 11 a, b). Interestingly, the frequency of CD39^{high}CD8⁺ T-cells was significantly higher in the IL-12 treated group compared to the IL-27 treated group (Figure 11 a, b). Overall, these results indicate that IL-12 and IL-27 play a role in the induction of CD39 expression.

Second, the level of CD39 expression for each group was measured. This can be measured using the median fluorescence intensity (MFI), as the intensity of the fluorescent CD39-targetted Ab (CD39-AF647) can be used to signify the amount of CD39 on a per cell basis. Here, CD39 expression was quantified on all CD39⁺CD8⁺ T-cells, which was initially determined based on the CD39 FMO. The FMO is a control measure used in flow cytometry, in which a sample is stained with all Abs except one (CD39-AF647 in this case). Total CD39⁺CD8⁺ T-cells were analyzed rather than CD39^{high}CD8⁺ T-cells to minimize bias. Data showed that CD39⁺CD8⁺ T-cells from the IL-12 and IL-27 stimulated groups show significantly higher MFI of CD39 compared to the control conditions (Figure 12 a, b). Moreover, the highest expression of CD39 was found in the IL-27 treated group. These two data sets suggest that IL-12 and IL-27 signalling can upregulate CD39 expression on CD8⁺ T-cells, since CD39⁺CD8⁺ T-cells from the control group have relatively lower expression.

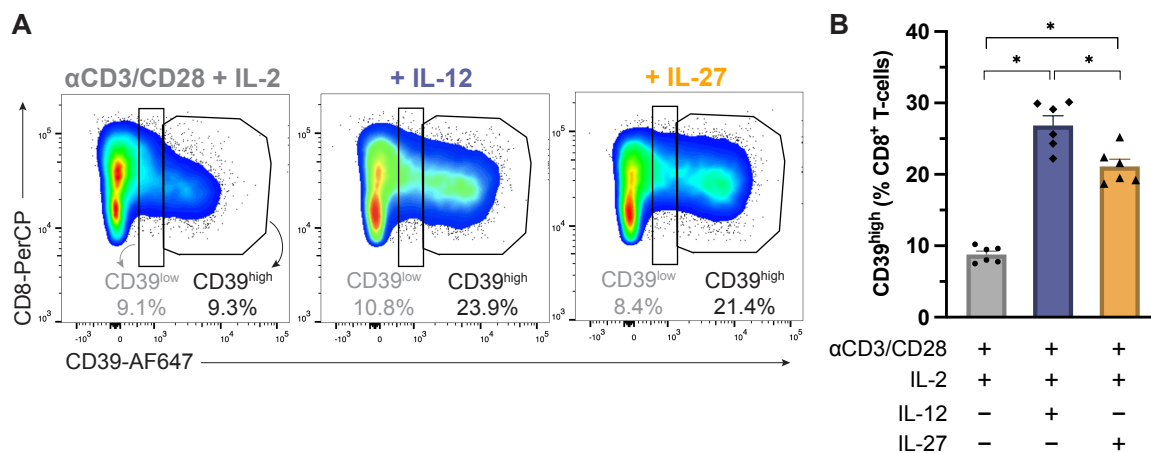


Figure 11. Frequency of CD39^{high}CD8⁺ T-cells from naïve mice after *in vitro* stimulation with IL-12 or IL-27.

Splenic CD8⁺ T-cells from naïve mice were stimulated with αCD3/CD28 Dynabeads and IL-2 (control), with or without IL-12 or IL-27. After 48 hours, samples were stained for flow cytometric analysis of CD39 expression. **A)** Representative dot plots depicting CD39^{high} expression, gated on CD8⁺CD3⁺ cells, corresponding to **B)** Frequency of CD8⁺ T-cells expressing high levels of CD39. Data are displayed as mean ± SEM of technical replicates from two separate experiments (n = 6). * p ≤ 0.05 by one-way ANOVA.

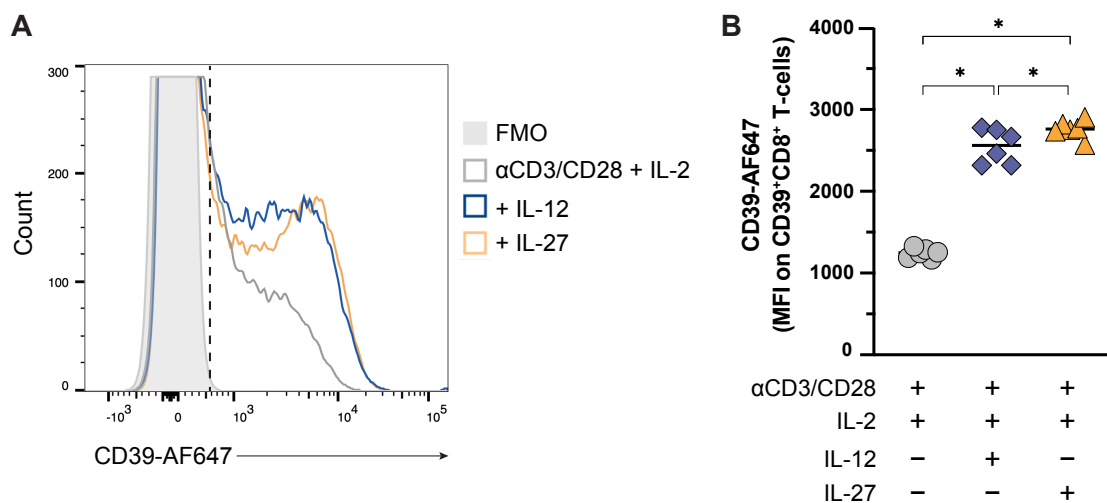


Figure 12. MFI of CD39 from CD39⁺CD8⁺ T-cells from naïve mice after *in vitro* stimulation with IL-12 or IL-27.

A) Representative histogram of CD39 expression, in which the dotted line separates CD39⁻ (left) and CD39⁺ (right) CD8⁺ T-cells. **B)** Quantification of median fluorescence intensity (MFI) of CD39-AF647 on CD39⁺CD8⁺ T-cells. Data are displayed as mean \pm SEM of technical replicates from two separate experiments (n = 6). * $p \leq 0.05$ by one-way ANOVA.

3.2.2 IL-12 and IL-27 induce CD39 expression on CD8⁺ T-cells from control and immunogenic neuro-2a vaccinated mice

In the context of cancer, tumour-specific T-cells can be exposed to their cognate antigens upon tumour infiltration. In the stimulation assay, we were curious whether *in vitro* CD8⁺ T-cell activation following two rounds of *in vivo* tumour-lysate vaccination would affect the ability of IL-12 or IL-27 to induce CD39 expression. This also provides a more physiologically relevant model as neoantigens are required for T-cell priming.

Vaccination using whole tumour lysate vaccination can be used to prime and activate T-cells. This allows the direct delivery of tumour proteins and antigens to the immune cells, overcoming immunosuppressive actions by the TME^{149,150}. Therefore, we analyzed the effects of IL-12 and IL-27 on CD39 expression on CD8⁺ T-cells from mice primed with neuro-2a cell lysates. Either the control or immunogenic neuro-2a cell lysates were used to observe whether the presence of neoantigens at the time of priming would affect cytokine-induced CD39 expression *in vitro*.

As such, stimulation assays were completed (Figure 13). Mice were vaccinated with whole neuro-2a lysates (control or immunogenic) via s.c. injection, both 10 and 3 days prior to starting the assay. Splenic CD8⁺ T-cells were stimulated as previously described (3.2.1 and Methods). An additional experimental group was included, in which CD8⁺ T-cells were stimulated with IL-12 and IL-27, to determine whether they would have a synergistic effect.

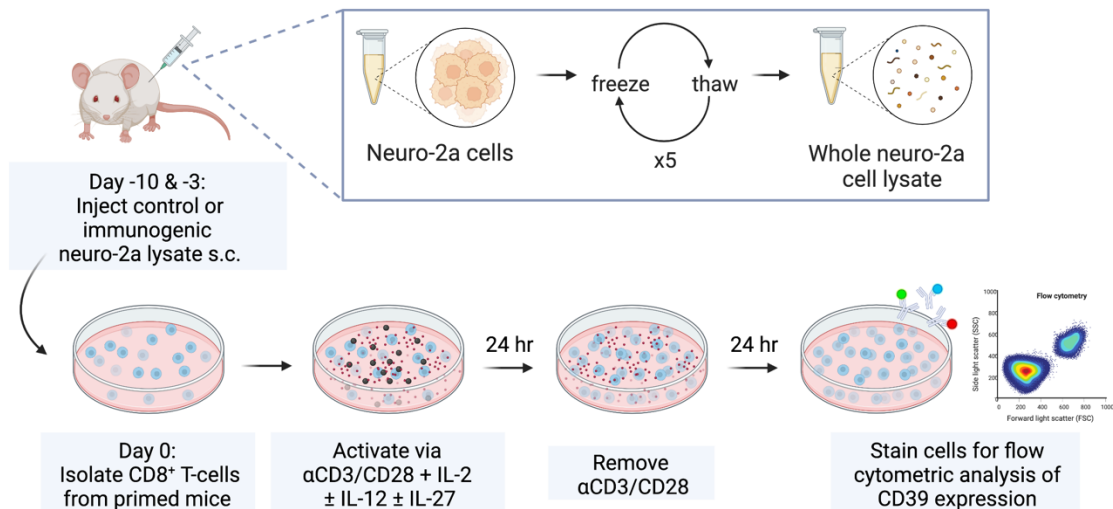


Figure 13. Simplified stimulation assay methodology with CD8⁺ T-cells from neuro-2a-antigen-experienced mice.

Control and immunogenic neuro-2a lysates were generated by repeated freeze-thaw cycles. Mice were s.c. vaccinated twice prior to beginning the assay. Splenic CD8⁺ T-cells were isolated via negative selection using a magnetic sorting kit. For the control group, CD8⁺ T-cells were stimulated at a 1:1 ratio with αCD3/CD28 Dynabeads and recombinant IL-2. Experimental groups were stimulated with additional recombinant IL-12 or IL-27, individually or in combination. After 24 hours, αCD3/CD28 Dynabeads were magnetically removed, and cells cultured for an additional 24 hours with cytokines before staining the cells for flow cytometry analysis of CD39 expression.

First, the frequency of CD39^{high}CD8⁺ T-cells were analyzed. Results demonstrated that CD8⁺ T-cells from control neuro-2a primed mice stimulated with both IL-12 and IL-27 showed significantly more CD39^{high} cells than all other conditions (Figure 14 a-i, b-i). However, stimulation with either cytokine alone did not significantly affect the frequency CD39^{high} cells. In contrast, data from immunogenic neuro-2a vaccinated mice showed a significantly greater frequency of CD39^{high}CD8⁺ T-cells when activated with IL-12 or IL-27, compared to the control (Figure 14). The frequency of CD39^{high}CD8⁺ T-cells was higher in the IL-12 treated group compared to the IL-27 treated group, as previously observed (Figure 11). The highest frequency of CD39^{high}CD8⁺ T-cells from immunogenic neuro-2a primed mice was achieved when stimulated with both IL-12 and IL-27 (Figure 14). Together, these results suggest that combining both cytokines can have an additive effect on inducing CD39 expression. There seems to be more pronounced effect in the cells from immunogenic neuro-2a primed mice compared to that of the control (Figure 14 c-f), although this was not statistically significant in the IL-27 stimulated group (Figure 14 e).

Next, the level of CD39 expression for each group was measured using MFI. CD8⁺ T-cells from control neuro-2a primed mice stimulated with IL-12 had no significant effect compared to the control (Figure 15 a-i, b-i). However, stimulation with IL-27 resulted in significantly higher MFI of CD39 compared to the control. For CD8⁺ T-cells from immunogenic neuro-2a primed mice, stimulation with either IL-12 or IL-27 resulted in significantly higher MFIs compared to the control (Figure 15 a-ii, b-ii). Regardless of the source of CD8⁺ T-cells, the highest MFI was observed after stimulation with both IL-12 and IL-27 (Figure 15 a, b), suggesting these cytokines can upregulate CD39 on CD8⁺ T-cells in an additive manner.

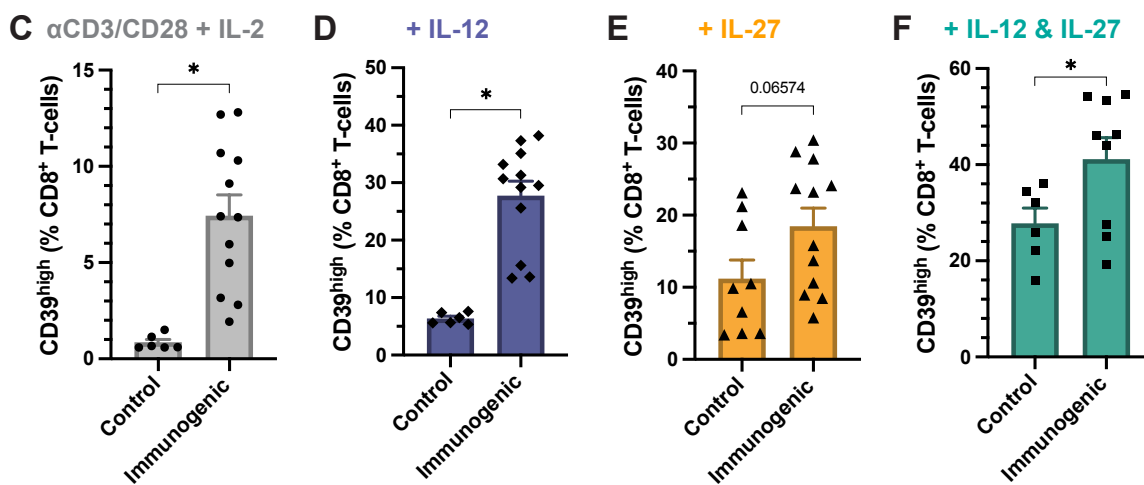
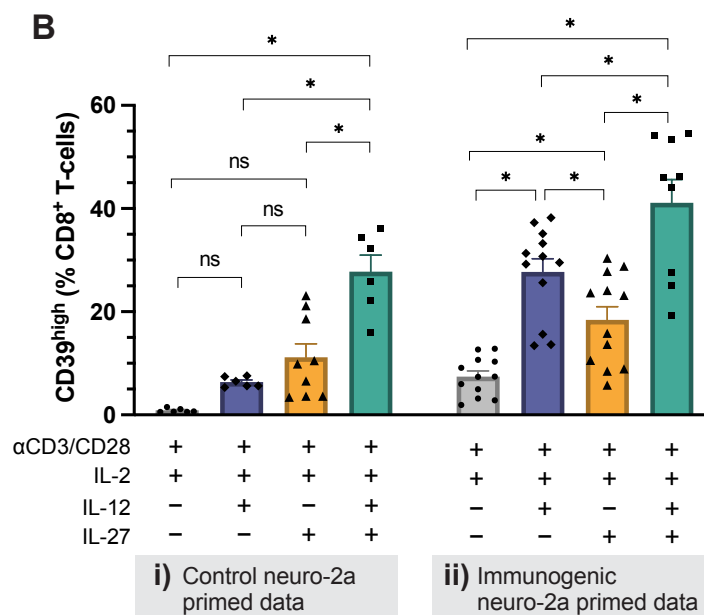
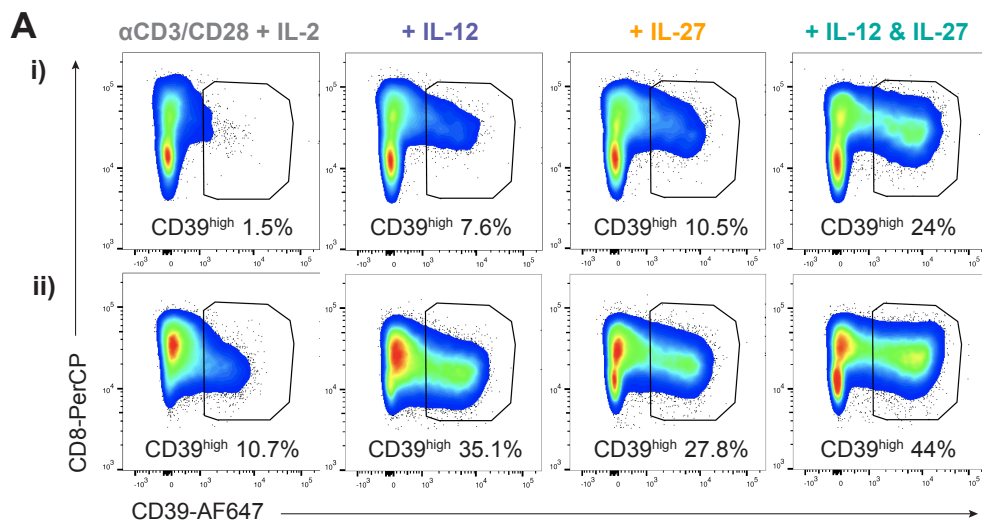


Figure 14. Frequency of CD39^{high}CD8⁺ T-cells from neuro-2a primed mice after *in vitro* stimulation with IL-12 and/or IL-27.

Splenic CD8⁺ T-cells from neuro-2a primed mice were stimulated with α CD3/CD28 Dynabeads and IL-2 (control conditions), with or without IL-12 or IL-27. After 48 hours, samples were stained for flow cytometric analysis of CD39 expression. **A)** Representative dot plots depicting CD39^{high} expression, gated on CD8⁺CD3⁺ cells, from mice primed with the control (**i**) or immunogenic (**ii**) neuro-2a lysate. **B)** Frequency of CD8⁺ T-cells expressing high levels of CD39 from control (**i**) or immunogenic (**ii**) neuro-2a primed mice. **C-F)** Comparing the frequency of CD39^{high}CD8⁺ T-cells from control vs. immunogenic neuro-2a primed mice stimulated with α CD3/CD28 and IL-2 (**C**), + IL-12 (**D**), + IL-27 (**E**), and + IL-12 & IL-27 (**F**). Data is displayed as mean \pm SEM of technical replicates from two to four experiments (n = 6-12). * $p \leq 0.05$, ns = not significant by two-way ANOVA (**B**) or unpaired t-tests (**C-F**).

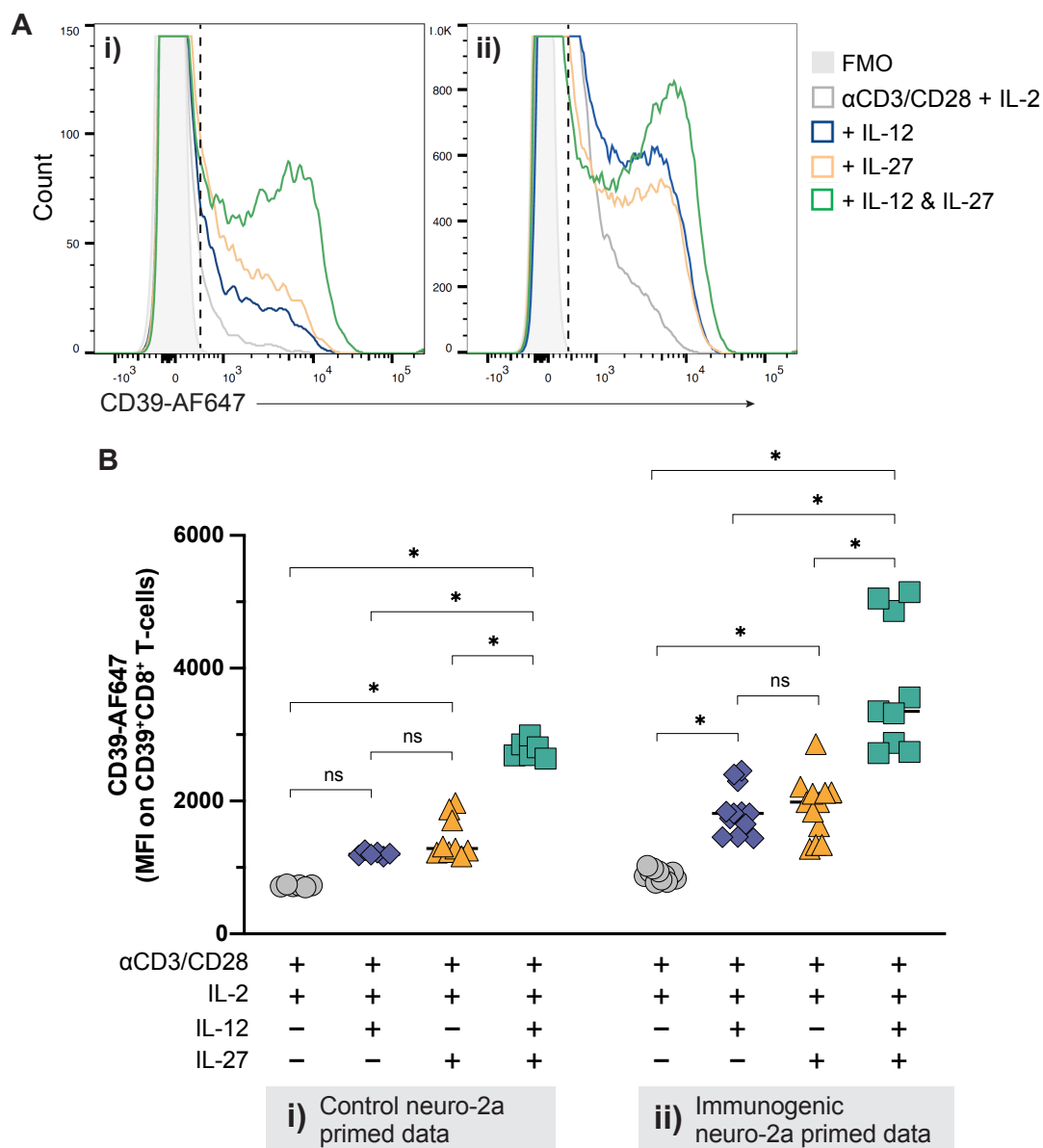


Figure 15. MFI of CD39 from CD39⁺CD8⁺ T-cells from neuro-2a primed mice after *in vitro* stimulation with IL-12 and/or IL-27.

A) Representative histograms of CD39 expression, in which the dotted line separates CD39⁻ (left) and CD39⁺ (right) CD8⁺ T-cells from mice primed with control (**i**) or immunogenic (**ii**) neuro-2a lysate. **B)** Quantification of MFI of CD39-AF647 on CD39⁺CD8⁺ T-cells from mice primed with control (**i**) or immunogenic (**ii**) neuro-2a lysate. Data is displayed as mean ± SEM of technical replicates from two to four experiments (n = 6-12). * p ≤ 0.05 by two-way ANOVA.

3.3 The effect of IL-12 neutralization on CD39⁺CD8⁺ T-cell populations from neuro-2a tumour-bearing mice

We next aimed to validate the effect of IL-12 on CD39 expression *in vivo*. IL-12 was chosen because CD8⁺ T-cells from antigen-naïve and immunogenic neuro-2a antigen-experienced mice showed a higher frequency of CD39^{high}CD8⁺ T-cells when stimulated with IL-12 than IL-27 (Figure 11 b and Figure 14 b-ii). In this *in vivo* experiment, an IL-12 neutralizing Ab or isotype control was i.p. injected into mice once neuro-2a tumours became palpable. Injections continued every 3-4 days until the endpoint (Figure 16). The α IL-12 Ab blocks the heterodimeric IL-12 from binding to its receptor, thereby neutralizing IL-12¹⁵¹.

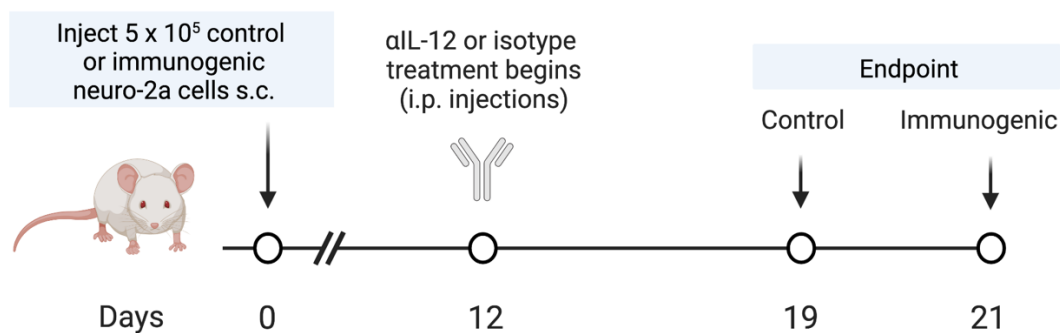


Figure 16. Simplified method for comparing T-cell characteristics from control and immunogenic neuro-2a tumour-bearing mice treated with α IL-12 or isotype control.

Female A/J mice were inoculated s.c. with 5×10^5 control or immunogenic neuro-2a cells. Tumour volumes were measured over time using callipers. Once tumours became palpable ~ day 12, mice of the same tumour type were randomized and injected with 0.5 mg of isotype control (IgG2b, k) or α IL-12 Abs every 3-4 days until endpoint. On days 19 or 21, mice bearing control or immunogenic neuro-2a tumours were euthanized, respectively. Tumours and spleens were processed individually and stained for flow cytometric analysis of CD8⁺ T-cell populations.

Tumours volumes were measured over time. We compared the tumour volumes between treatment groups, to determine whether IL-12 neutralization would affect tumour burden. At the respective endpoints, there was no difference in tumour volume between mice receiving isotype or α IL-12 treatment, regardless of their tumour type (Figure 17).

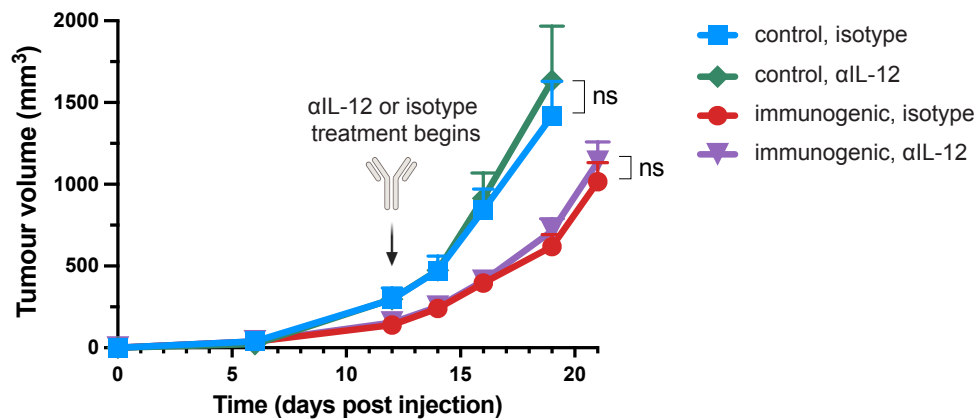


Figure 17. Tumour burden of neuro-2a tumour-bearing mice treated with α IL-12 or isotype control.

Female A/J mice were inoculated s.c. with 5×10^5 control or immunogenic neuro-2a cells. Tumour volumes were measured over time using callipers. Once tumours became palpable (day ~12), mice of the same tumour type were randomized and treated with either α IL-12 or isotype control (IgG2b, k). Thus, mice were grouped into control isotype control (n = 5), control α IL-12 (n = 5), immunogenic isotype control (n = 9) and immunogenic α IL-12 (n = 11). Data represents the mean \pm (SEM) of biological replicates. ns = not significant by unpaired t-test.

We wanted to confirm that α IL-12 was indeed neutralizing the biological activity of IL-12 *in vivo*. According to the manufacturer, the α IL-12 Ab should not deplete or change the concentration of IL-12; therefore, an ELISA or western blot could not be used to verify the IL-12 neutralizing activity of the antibody. Instead, considering that IL-12 plays a key role in effector T-cell differentiation and activation, we used the differentiation state of TILs as a surrogate. The expression patterns of CD44, CD62L and Fas were used to distinguish naïve and effector CD8⁺ T-cells (Figure 18 a, as described previously in section 3.2). We expected the ratio of naïve and effector TILs would be altered in mice treated with α IL-12 compared to isotype control.

Data from immunogenic neuro-2a tumour-bearing mice treated with isotype control showed a significant difference between the frequency of naïve and effector CD8⁺ TILs (Figure 18 b). This was not the case for α IL-12 treated group. This can be attributed to the reduced frequency of effector CD8⁺ TILs from the α IL-12 treated group relative to the isotype control treated group. The low frequency of naïve CD8⁺ TILs detected is consistent with data from the literature of human and murine tumours^{152–154}. No conclusions could be made from the flow cytometric analysis of control tumours, as the downstream phenotyping of the differentiation states was skewed by the limited frequency of CD8⁺ TILs.

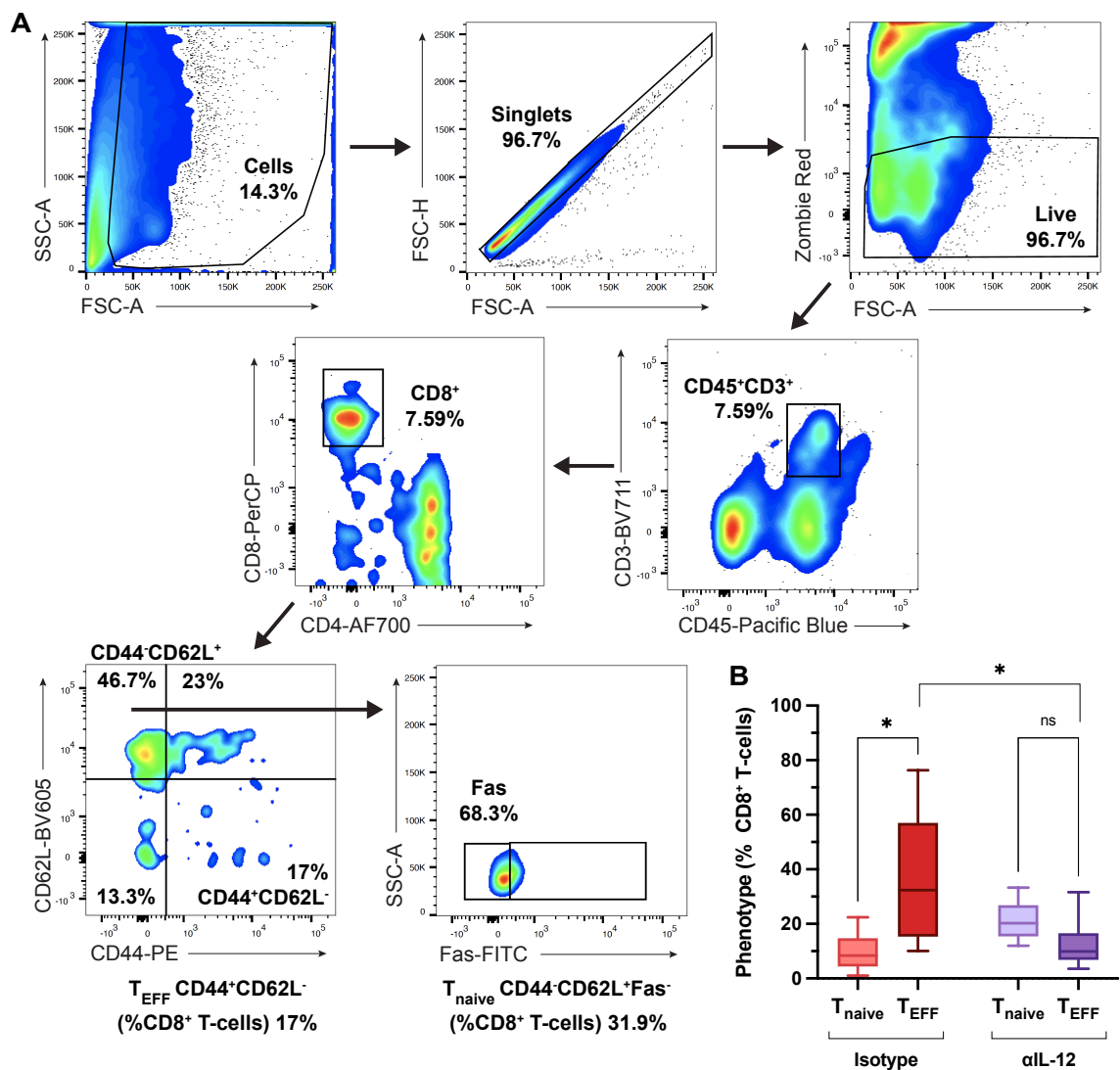


Figure 18. Frequency of naïve and effector CD8⁺ TILs from tumours of immunogenic neuro-2a tumour-bearing mice after αIL-12 treatment.

Mice were inoculated s.c. with 5×10^5 immunogenic neuro-2a cells. On day ~12, mice were treated with αIL-12 Ab or isotype control (IgG2b, k). At endpoint, tumours were processed individually and stained for flow cytometric analysis of CD8⁺ TIL populations. **A)** Gating strategy to identify naïve and effector CD8⁺ TILs. **B)** Frequency of CD8⁺ TILs with a naïve (T_{naive} = CD44⁻CD62L⁺Fas⁻) or effector (T_{EFF} = CD44⁺CD62L⁻) phenotype. Data are displayed as box plots and mean ± SD were calculated for statistical analysis, * p ≤ 0.05 and ns = not significant by two-way ANOVA.

3.3.1 IL-12 neutralization has no effect on the frequency of CD39⁺CD8⁺ TILs in control neuro-2a tumours

To study the effect of IL-12 on CD39 expression *in vivo*, we analyzed the effect of IL-12 neutralization on CD8⁺ TILs and T-cells from control or immunogenic neuro-2a tumour-bearing mice. Focusing on data from control neuro-2a tumour-bearing mice, IL-12 neutralization did not affect the frequency of CD8⁺ TILs or CD39⁺CD8⁺ TILs compared to the isotype control group (Figure 19 a-c). We were not expecting there to be a difference, as these tumours have poor immunogenicity. Analysis of CD38 showed that treatment with α IL-12 resulted in reduced frequency of activated CD8⁺ TILs (CD38⁺CD8⁺) relative to the control group (Figure 19 d). As IL-12 is involved in T-cell activation, this provided further evidence that IL-12 was neutralized in the α IL-12 treated mice.

As with previous experiments, splenocytes were used as a systemic measure. Similar to results from the tumour, there was no difference between the frequency of CD8⁺ T-cells or CD39⁺CD8⁺ T-cells between mice treated with α IL-12 or isotype control (Figure 19 e, f). This indicates that IL-12 neutralization did not affect CD39⁺CD8⁺ T-cells, from the tumours or systemically, in control neuro-2a tumour-bearing mice.

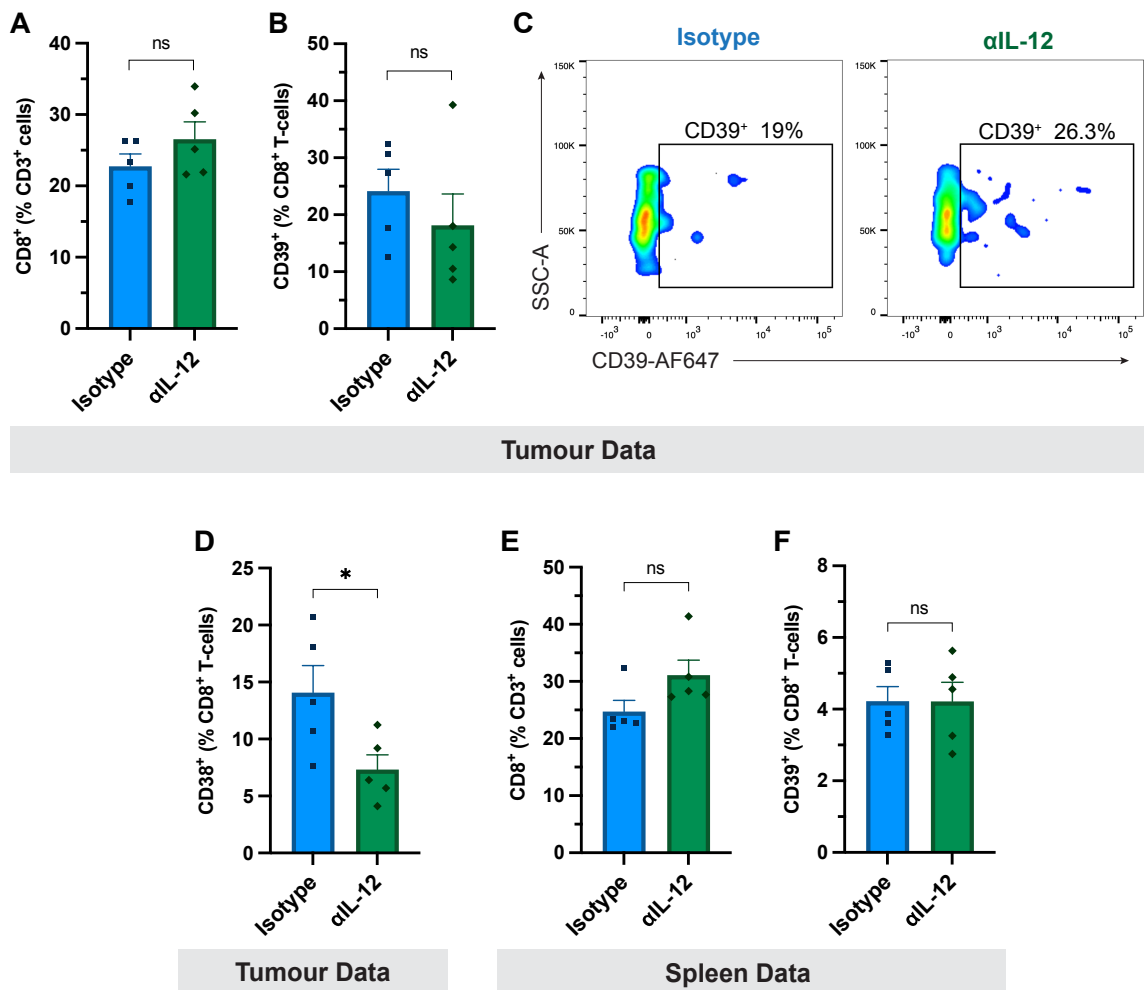


Figure 19. Frequency of CD38⁺ or CD39⁺CD8⁺ T-cells from tumours and spleens of control neuro-2a tumour-bearing mice after α IL-12 treatment.

Mice were inoculated s.c. with 5×10^5 control neuro-2a cells. Isotype control (IgG2b, k) or α IL-12 treatment (0.5 mg via i.p. injections) began on day ~12. At endpoint, tumours and spleens were processed individually and stained for flow cytometric analysis of CD8⁺ T-cell populations. **A-D**) Data depicts results from tumours. Frequency of CD3⁺ TILs expressing CD8 (**A**). Frequency of CD8⁺ TILs expressing CD39 (**B**) and corresponding representative dot plots with a gate depicting CD39⁺ cells (**C**). Frequency of CD8⁺ TILs expressing CD38 (**D**). **E-F**) Data depicts results from spleens. Frequency of CD3⁺ T-cells expressing CD8 (**E**) and frequency of CD8⁺ T-cells expressing CD39 (**F**). Data represents mean \pm SEM of biological replicates. * $p \leq 0.05$, ns = not significant by unpaired t-test.

3.3.2 Immunogenic neuro-2a tumours show a reduced frequency of CD39⁺CD8⁺ TILs upon IL-12 neutralization

Upon flow cytometric analysis of immunogenic neuro-2a tumours, we found that the frequency of CD8⁺ TILs remained the same, regardless of αIL-12 treatment (Figure 20 a). However, treatment with αIL-12 resulted in reduced frequency of CD39⁺CD8⁺ TILs relative to the control group (Figure 20 b, c). This data supports our hypothesis that IL-12 induces CD39 expression by CD8⁺ T-cells, as IL-12 neutralization correlates with reduced frequency of CD39⁺CD8⁺ TILs.

In addition, we found a significant decrease in the frequency of activated (CD38⁺), dysfunctional (PD-1⁺CD38⁺) and exhausted (PD-1⁺TIM-3⁺, PD-1⁺CD39⁺, TIM-3⁺CD39⁺, and LAG-3⁺CD39⁺) CD8⁺ TILs from mice treated with αIL-12, compared to isotype control (Figure 20 b). These results provide further evidence that IL-12 neutralization by αIL-12 treatment was effective.

Analysis of splenocytes showed no difference between the frequency of CD8⁺ T-cells or CD39⁺CD8⁺ T-cells between mice treated with αIL-12 or isotype control (Figure 20 d, e). This data, in combination with TIL analyses (Figure 20 b), indicate that IL-12 plays a role in modulating the CD8⁺ T-cell phenotype *in vivo*, and more specifically their CD39⁺ phenotype, within the tumour. However, this was not true for control neuro-2a tumours (Figure 19 b), suggesting that the immunogenicity of the tumour influences the effect of IL-12 on modulating CD8⁺ T-cell phenotypes.

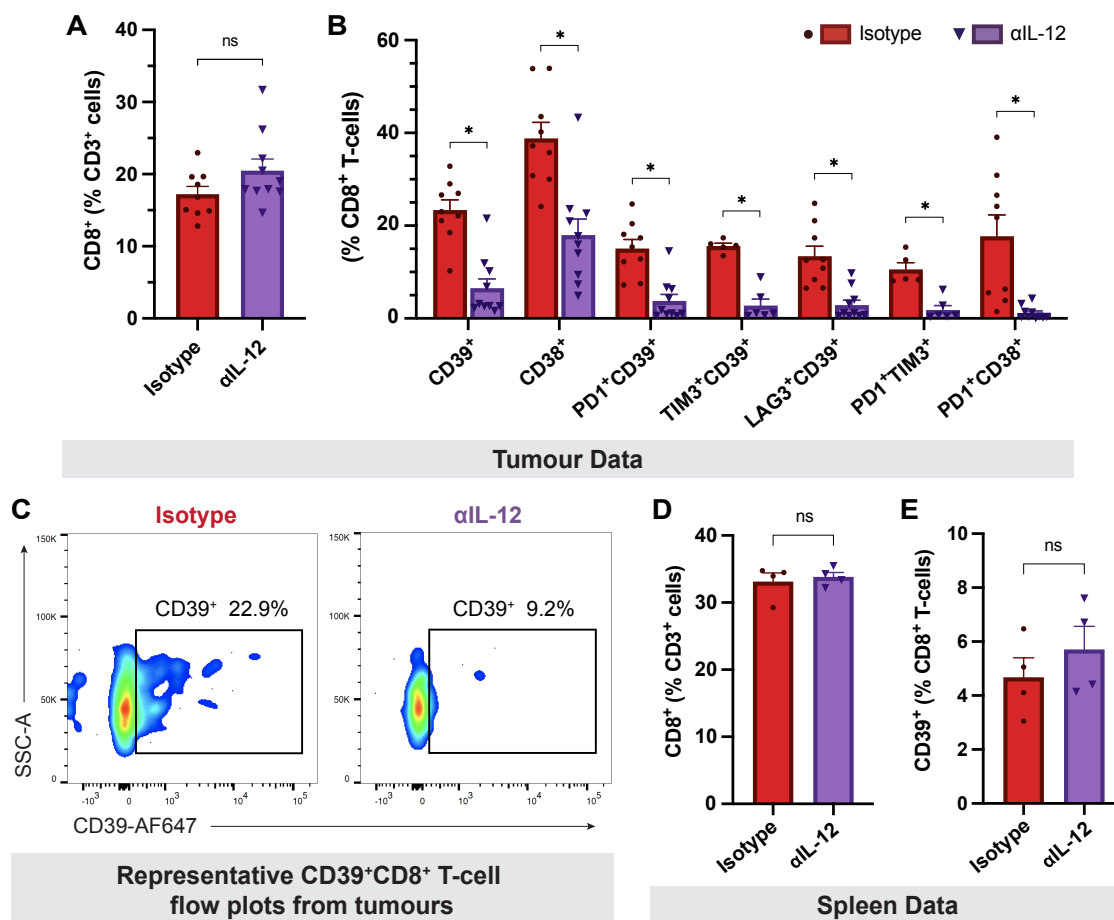


Figure 20. Frequency of CD39⁺CD8⁺ T-cells and other phenotypes from tumours and spleens of immunogenic neuro-2a tumour-bearing mice after α IL-12 treatment.

Mice were inoculated s.c. with 5×10^5 immunogenic neuro-2a cells. Isotype control (IgG2b, k) or α IL-12 treatment (0.5 mg via i.p. injections) began on day ~12. At endpoint, tumours and spleens were processed individually and stained for flow cytometric analysis of CD8⁺ T-cell populations. **A-C)** Data depicts results from tumours. Frequency of CD3⁺ TILs expressing CD8 (A). Frequency of CD8⁺ TILs expressing CD39, CD38, PD-1 & CD39, TIM-3 & CD39, LAG-3 & CD39, PD-1 & TIM-3, and PD-1 & CD38, from left to right, respectively (B). C) Representative dot plots with a gate depicting CD39⁺ cells, gated on CD8⁺ T-cells. **D-E)** Data depicts results from spleens. Frequency of CD3⁺ cells expressing CD8 (D) and frequency of CD8⁺ T-cells expressing CD39 (E). Data represent the mean \pm SEM of biological replicates. * $p \leq 0.05$, ns = not significant by multiple or single unpaired t-tests.

3.3.3 In vitro stimulation with IL-12 results in the greatest frequency of CD39⁺CD8⁺ T-cells expressing inhibitory receptors

Previously, we observed a correlation between IL-12 neutralization and decreased frequency of CD39⁺ and exhausted CD8⁺ TILs in immunogenic neuro-2a tumours (Figure 20). We considered whether CD8⁺ T-cells stimulated *in vitro* with IL-12 would induce inhibitory receptor expression on CD39⁺CD8⁺ T-cells. In addition, we investigated the effects of IL-27, or the combination of IL-12 and IL-27, on the frequency of exhausted CD39⁺CD8⁺ TILs. To this end, the stimulation assay described in section 3.2.2 (Figure 13) was conducted with additional stains for PD-1, LAG-3, and TIM-3.

Our data demonstrated that T-cell stimulation in the presence of IL-12, individually, induced the highest frequency of PD-1⁺CD39⁺CD8⁺ T-cells (Figure 21 a, d). Stimulation with both cytokines had a reduced effect compared to IL-12 alone. There was a moderately higher frequency of PD-1⁺ cells from the IL-27 stimulated group compared to the control conditions. These results suggest that IL-27 may attenuate the induction of PD-1 expression by IL-12 in this setting.

When analyzing the expression of LAG-3, we found the highest frequency of LAG-3⁺CD39⁺CD8⁺ T-cells when stimulated with IL-12 individually or in combination with IL-27 (Figure 21 b, e). Importantly, stimulation with IL-12 induced more LAG-3⁺ cells than stimulation with IL-27 or control conditions.

The analysis of TIM-3 showed that cells stimulated with IL-12 or control conditions had the highest frequency of TIM-3⁺ CD39⁺CD8⁺ T-cells (Figure 21 c, f). Stimulation with IL-27 resulted in less TIM-3⁺ cells than IL-12, while cells stimulated with both IL-12 and IL-27 demonstrated the lowest frequency of TIM-3⁺ cells (Figure 21 f).

The co-expression of multiple inhibitory receptors and CD39 has been associated with CD8⁺ T-cell exhaustion^{73,155,156}. Since this assay was conducted with isolated CD8⁺ T-cells, we were able to analyze the frequency of CD39⁺CD8⁺ T-cells that were triple positive (TP), meaning they were TIM-3⁺PD-1⁺LAG-3⁺. This was not possible when analyzing CD39⁺CD8⁺ TILs in mouse experiments, because the low abundance made the further analysis of multiple inhibitory receptors unreliable.

The results from the *in vitro* assay demonstrated the highest frequency of TP CD39⁺CD8⁺ T-cells when CD8⁺ T-cells were stimulated with IL-12 (Figure 22).

Stimulation with both cytokines had a reduced effect compared to IL-12 alone. There was no statistically significant difference between the frequency of TP cells from control and IL-27 stimulated groups. Similar to the PD-1 expression data (Figure 21 a, d), this data (Figure 22) suggests that IL-27 may attenuate the induction of inhibitory receptor expression by IL-12 in this setting. Collectively, these results demonstrate a correlation between IL-12 and inhibitory receptor expression on CD39⁺CD8⁺ T-cells, which is more distinct than that of IL-27.

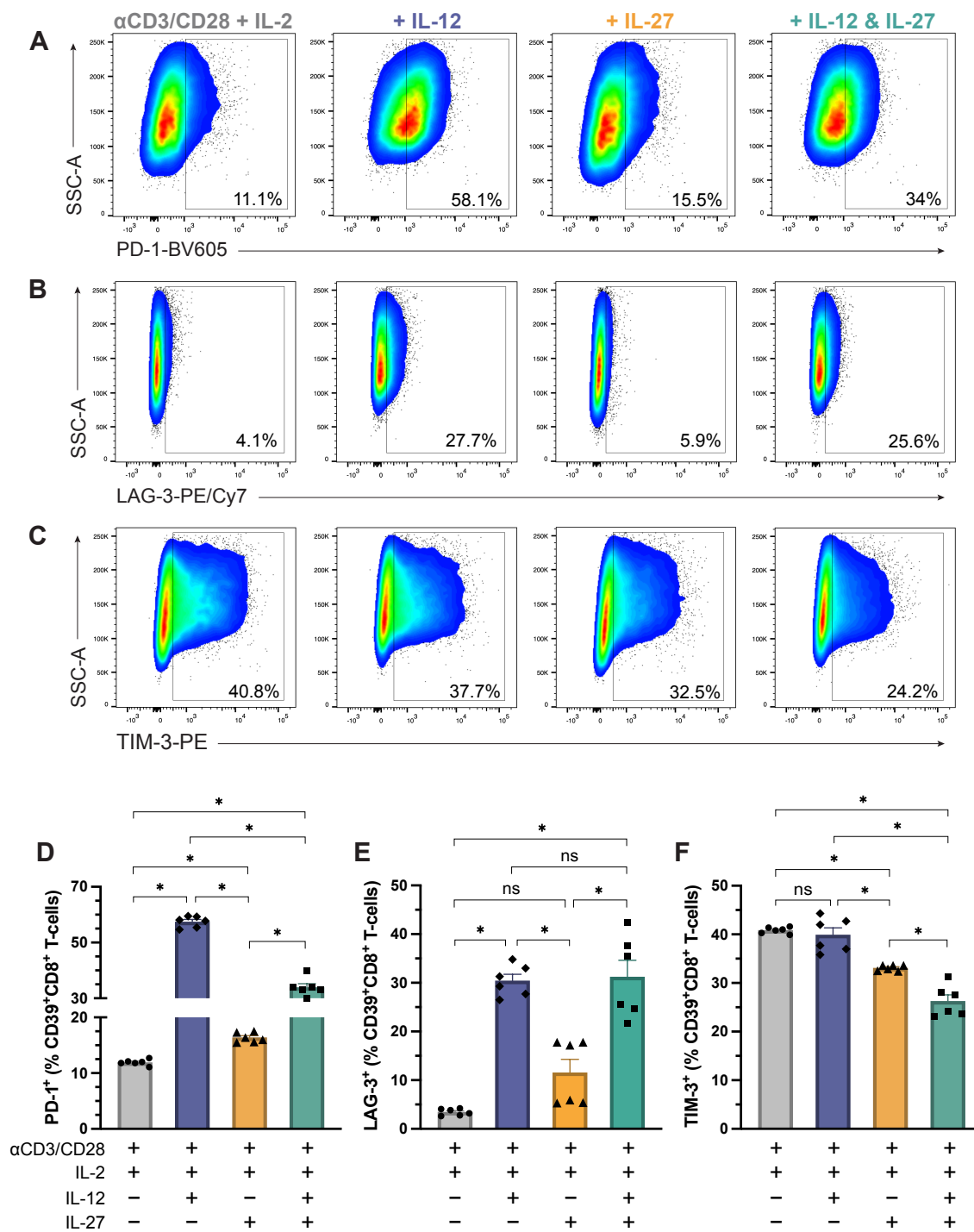


Figure 21. Inhibitory receptor expression on CD39⁺CD8⁺ T-cells from immunogenic neuro-2a primed mice after *in vitro* stimulation with IL-12 and/or IL-27.

Splenic CD8⁺ T-cells from immunogenic neuro-2a primed mice were stimulated with α CD3/CD28 Dynabeads and IL-2 \pm IL-12 and/or IL-27. After 48 hours, samples were stained for flow cytometric analysis of CD39, PD-1, LAG-3, and TIM-3 expression. **A-C)** Representative dot plots (left) and quantification (right) of PD-1⁺ (**A**), LAG-3⁺ (**B**), and TIM-3⁺ (**C**) CD39⁺CD8⁺ T-cells. Data is displayed as mean \pm SEM of technical replicates from two experiments (n = 6). * $p \leq 0.05$, ns = not significant by one-way ANOVA.

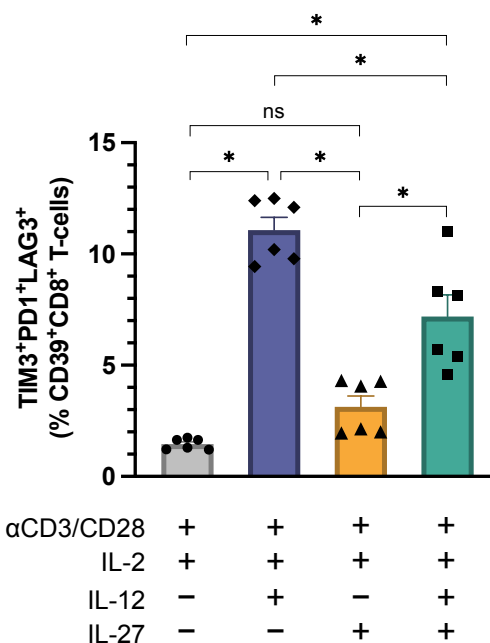


Figure 22. Frequency of TIM-3⁺PD-1⁺LAG-3⁺CD39⁺CD8⁺ T-cells from immunogenic neuro-2a primed mice after *in vitro* stimulation with IL-12 and/or IL-27.

Splenic CD8⁺ T-cells from immunogenic neuro-2a primed mice were stimulated with αCD3/CD28 Dynabeads and IL-2 ± IL-12 and/or IL-27. Samples were stained for flow cytometric analysis of CD39, PD-1, TIM-3, and LAG-3 expression after 48 hours. The graph depicts the quantification CD39⁺CD8⁺ T-cells co-expressing TIM-3, PD-1, and LAG-3. Data is displayed as mean ± SEM of technical replicates from two experiments (n = 6). * p ≤ 0.05, ns = not significant by one-way ANOVA.

3.4 The effector functionality of CD39^{+/−}CD8⁺ T-cells after stimulation with IL-12 and/or IL-27

Studies have shown that CD39 expression by CD8⁺ T-cells is associated with reduced IFN γ and TNF α production and limited cytotoxicity function of these cells^{73,74,98,99}. However, other studies demonstrate that CD39⁺CD8⁺ T-cells have more potent cytotoxic abilities than their CD39[−] counterparts, with high granzyme B and IFN γ production^{68,100–104}. Given the discrepancies, we sought to investigate the effector capability of CD39⁺CD8⁺ T-cells in the context of a stimulation assay. In doing so, we could compare the effector capability of CD39⁺ and CD39[−]CD8⁺ T-cells. Additionally, we could measure the effector capability of CD39⁺CD8⁺ T-cells after stimulation with IL-2, IL-12 and/or IL-27.

For this stimulation assay, a different methodology was used, in which bulk splenocytes from immunogenic neuro-2a vaccinated mice were stimulated with plate-bound α CD3 and CD28 Abs (Figure 23) rather than isolated CD8⁺ T-cells stimulated with α CD3/CD28 Dynabeads. This was due to time constraints, assay optimization circumstances, as well as animal and material availability. This adjustment, however, did provide the opportunity to corroborate the findings from the previous assay, in which we found IL-12 and IL-27 induced CD39 expression on CD8⁺ T-cells after *in vitro* stimulation (Figure 11, Figure 12, Figure 14, Figure 15). Moreover, repeating experiments under slightly different conditions and provides evidence of their reproducibility and increases the validity of previous findings^{157,158}.

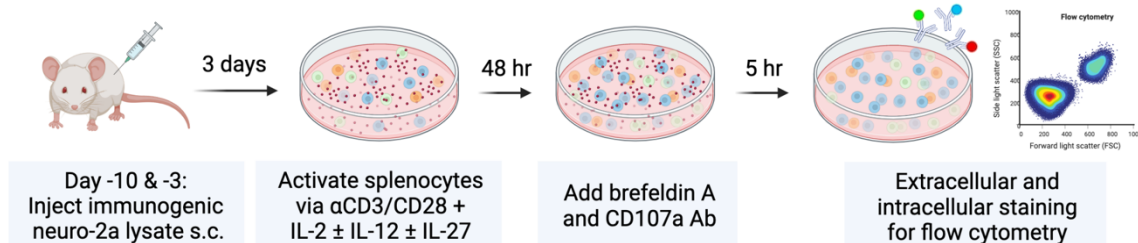


Figure 23. Simplified stimulation assay methodology with bulk splenocytes from neuro-2a-antigen-experienced mice for ICS.

Mice were injected s.c. with immunogenic neuro-2a lysate 10 and 3 days before beginning the assay. Bulk splenocytes for the control group were stimulated with plate-bound α CD3 and CD28 Abs and recombinant IL-2. Experimental groups were stimulated with additional recombinant cytokines, IL-12, IL-27, or both. After 48 hours, brefeldin A and α CD107a Ab were added and incubated for 5 hours. Samples were stained for extracellular and intracellular markers of interest for flow cytometric analysis.

Therefore, we assessed whether IL-12 and IL-27 affected CD39 expression on CD8⁺ T-cells using this assay (Figure 23) prior to addressing the effector capability of CD39⁺CD8⁺ T-cells. We found that the frequency of CD39⁺CD8⁺ T-cells was significantly higher when stimulated with IL-12 or IL-27 compared to the control group (Figure 24). In agreement with previous results (Figure 14 b-ii), the highest frequency of CD39⁺CD8⁺ T-cells was achieved when stimulated with both IL-12 and IL-27 (Figure 24). Next, we examined the MFI of CD39 on CD39⁺CD8⁺ T-cells to determine the level of CD39 expression. We found that stimulation with either IL-12 or IL-27 resulted in a significantly higher MFI than the control group, and the highest MFI was observed after being stimulated with both IL-12 and IL-27 (Figure 24). Together, results from the bulk splenocyte stimulation assay show that IL-12 and IL-27 induce CD39 expression on CD8⁺ T-cells, validating our previous findings (Figure 14 b-ii, Figure 15 b-ii).

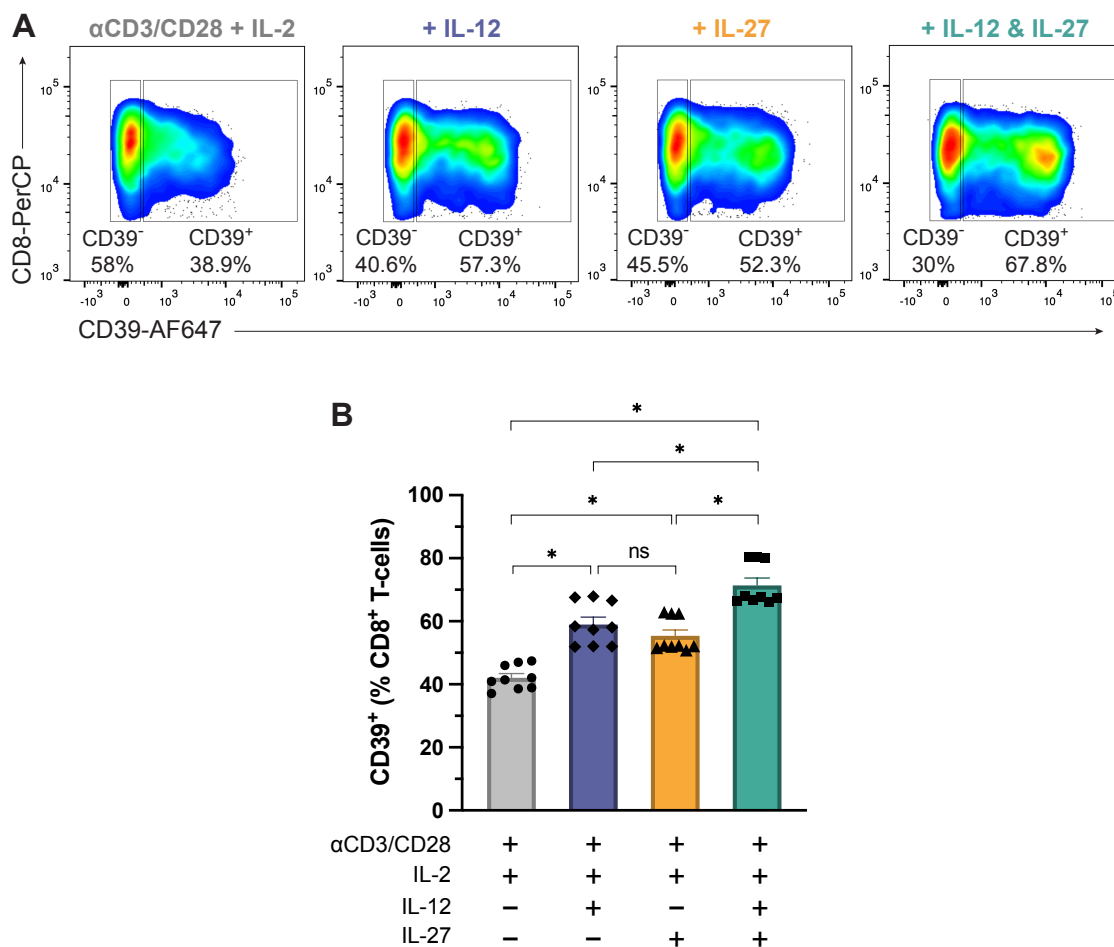


Figure 24. Frequency of CD39⁺CD8⁺ T-cells from immunogenic neuro-2a primed mice after *in vitro* stimulation in bulk splenocyte culture with IL-12 and/or IL-27.

Bulk splenocytes from immunogenic neuro-2a primed mice were stimulated with plate-bound αCD3 and αCD28 Abs and IL-2 ± IL-12 and/or IL-27. After 48 hours, samples were stained for flow cytometric analysis of CD39 expression. **A)** Representative dot plots with a gate depicting CD39⁺ cells, gated on CD8⁺CD3⁺ cells, corresponding to **B)** frequency of CD8⁺ T-cells expressing CD39. Data is displayed as mean ± SEM of technical replicates from three experiments (n = 9). * p ≤ 0.05, ns = not significant by one-way ANOVA.

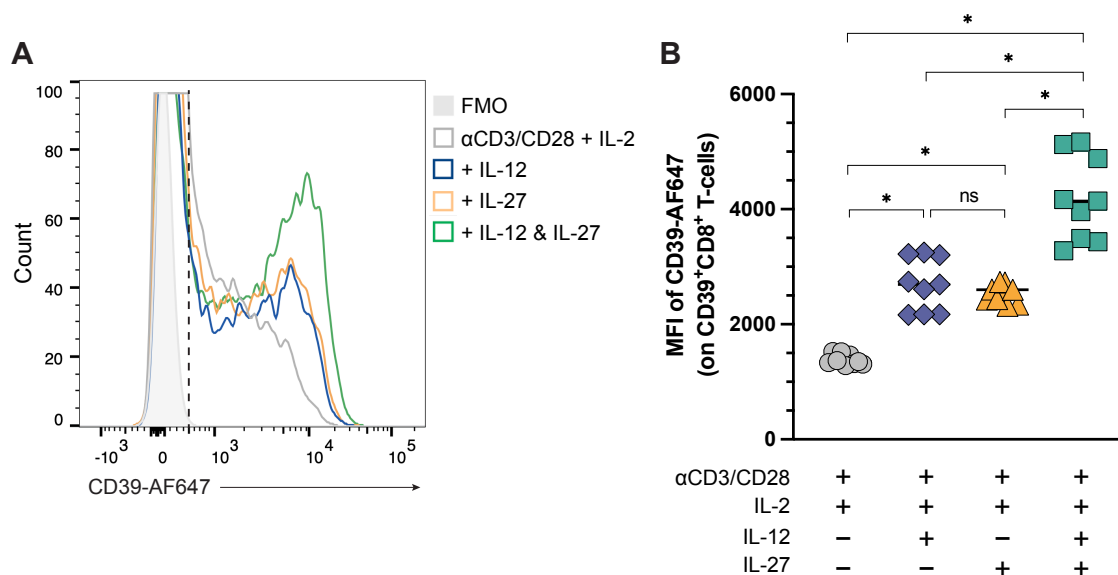


Figure 25. MFI of CD39 from CD39⁺CD8⁺ T-cells from immunogenic neuro-2a primed mice after *in vitro* stimulation in bulk splenocyte culture with IL-12 and/or IL-27.

Bulk splenocytes from immunogenic neuro-2a primed mice were stimulated with plate-bound α CD3 and α CD28 Abs and IL-2 \pm IL-12 and/or IL-27. After 48 hours, samples were stained for flow cytometric analysis of CD39 expression. **A)** Representative histograms of CD39 expression by CD8⁺ T-cells, in which the dotted line separates CD39⁻ (left) and CD39⁺ (right). **B)** Quantification of MFI of CD39-AF647 on CD39⁺CD8⁺ T-cells. Data are displayed as mean \pm SEM of technical replicates from three experiments (n = 9). * $p \leq 0.05$ by one-way ANOVA.

3.4.1 CD39 expression positively correlates with effector molecule production when stimulated with α CD3/CD28 and IL-2

With confirmation that IL-12 and IL-27 induce CD39 expression using this assay methodology, we could investigate the effector capability of CD39⁺CD8⁺ T-cells. To compare the effector function of CD39⁺ and CD39⁻CD8⁺ T-cells, we looked at those from the control group (α CD3/ α CD28 Abs and IL-2). Our data showed a higher frequency of CD39⁺CD8⁺ T-cells expressing CD107a, IFN γ , TNF α , and IL-2 than CD39⁻CD8⁺ T-cells (Figure 26 a-d, respectively).

Of note, the frequencies of IL-2 and TNF α were relatively low, measuring less than 5%. Since α CD3/ α CD28 Abs were used, this assay mimics the physiological reaction of CD8⁺ T-cells, indicating that a minor subpopulation of CD8⁺ T-cells can produce IL-2 and TNF α upon activation. Given the low frequency, the positive control, PMA and ionomycin stimulation data have been included for validation purposes. This activation method bypasses the TCR by raising the level of intracellular Ca²⁺ within T-cells^{159,160}. This data verifies that these CD8⁺ T-cells can produce TNF α and IL-2 under hyper-stimulated conditions (Figure 27 a-b). Notably, the higher frequency of CD39⁺CD8⁺ T-cells expressed CD107a and IFN γ (Figure 27 c-d) relative to CD39⁻CD8⁺ T-cells, supporting our previous findings (Figure 26 a-b).

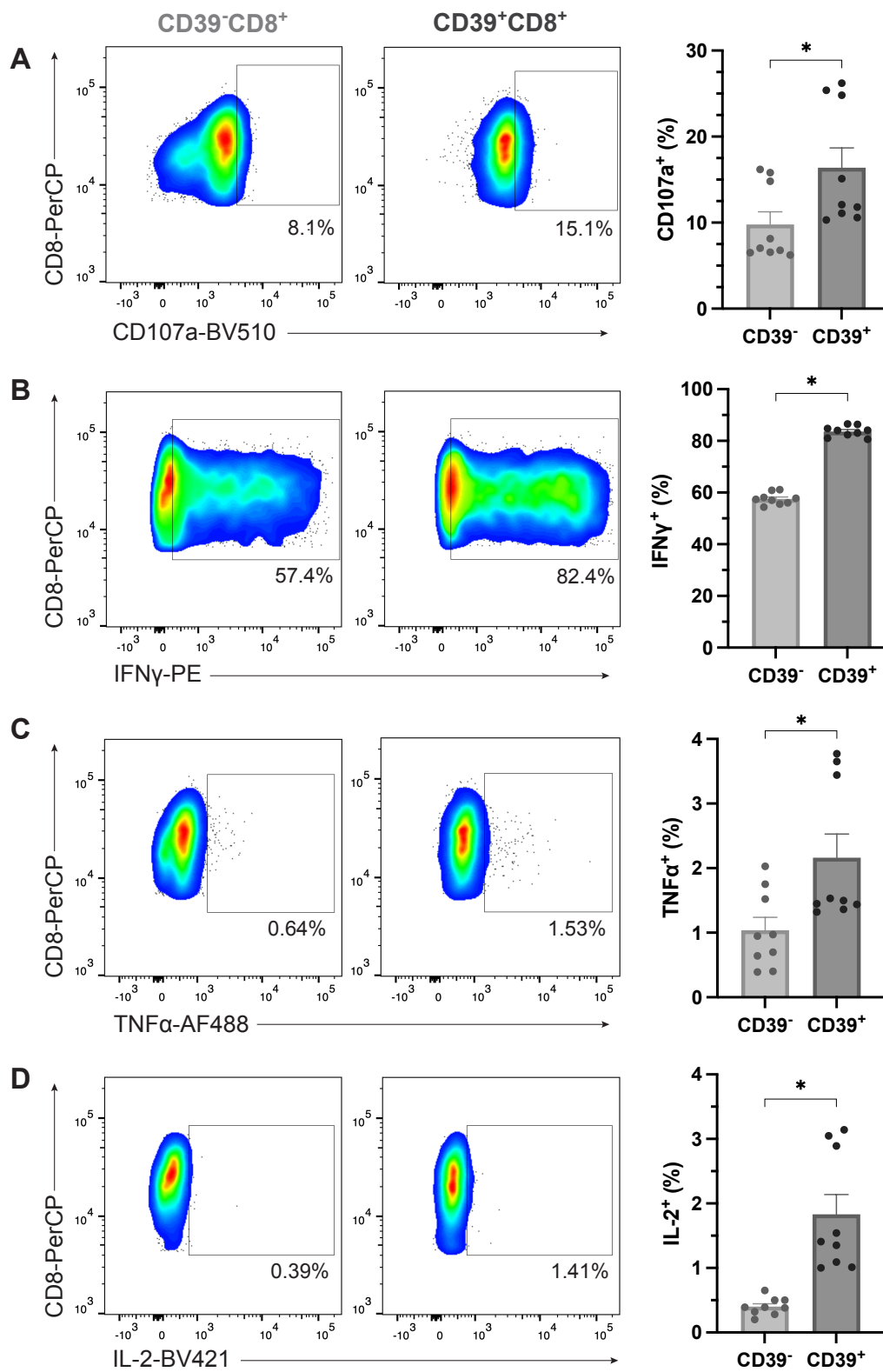


Figure 26. Effector molecule expression of CD39⁺ and CD39⁻CD8⁺ T-cells after *in vitro* stimulation with α CD3/CD28 and IL-2.

Bulk splenocytes from immunogenic neuro-2a primed mice were stimulated with plate-bound α CD3/ α CD28 Abs and IL-2. After 48 hours, BFA and α CD107a Ab were added, and 5 hours later samples were stained for flow cytometric analysis of CD39, IFN γ , TNF α and IL-2. **A-D)** Representative dot plots (left) and corresponding quantification (right) of CD107a⁺ (**A**), IFN γ ⁺ (**B**), TNF α ⁺ (**C**), and IL-2⁺ (**D**) CD39⁻ and CD39⁺CD8⁺ T-cells. Data is displayed as mean \pm SEM of technical replicates from three experiments (n = 9). * p \leq 0.05, ns = not significant by unpaired t-test.

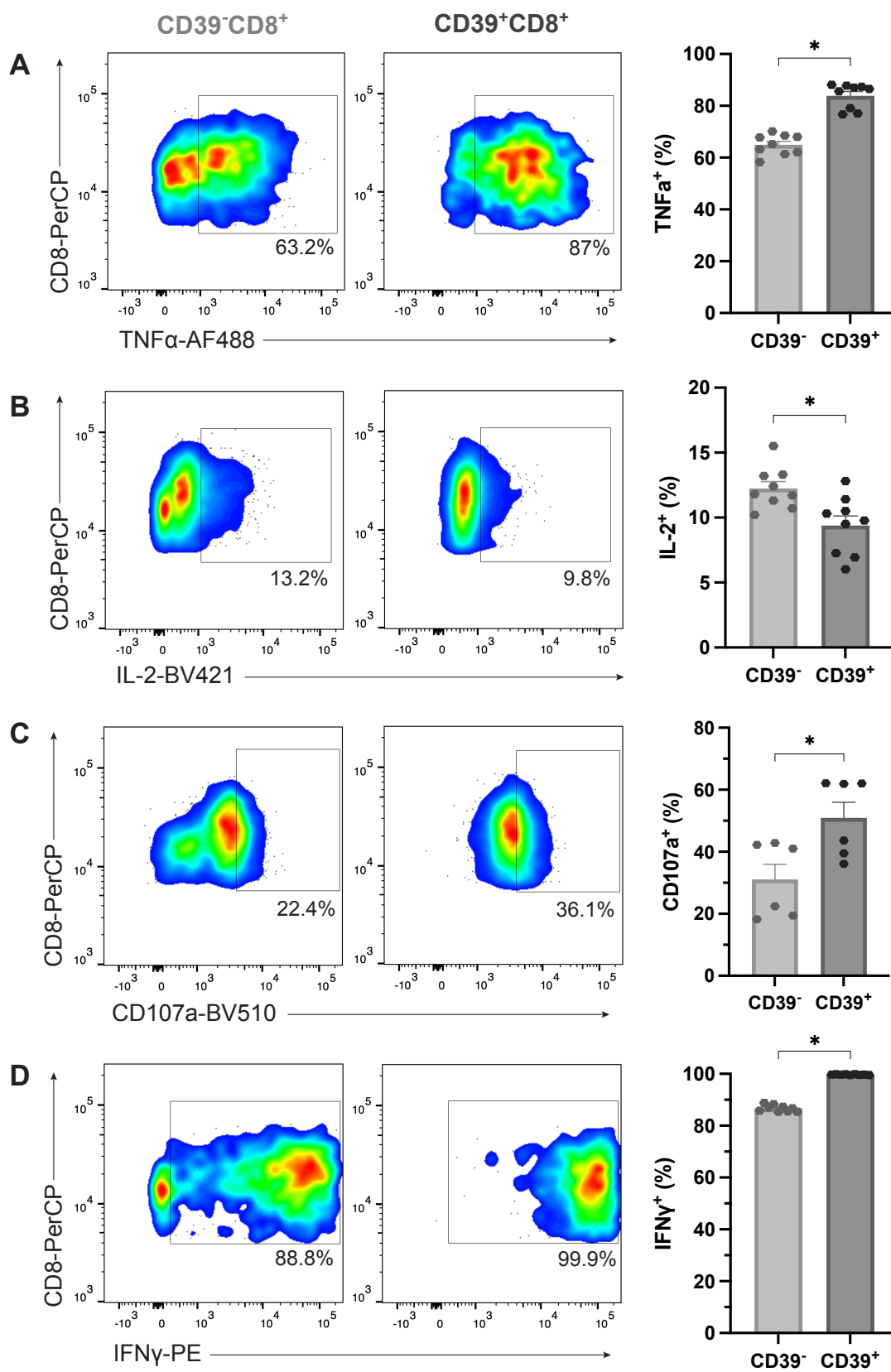


Figure 27. Effector molecule expression of CD39⁺ and CD39⁻CD8⁺ T-cells after *in vitro* stimulation with PMA, ionomycin, and IL-2.

Bulk splenocytes from immunogenic neuro-2a primed mice were stimulated with plate-bound α CD3 and α CD28 Abs and IL-2. After 48 hours, PMA, ionomycin, BFA and α CD107a Ab were added, and 5 hours later, samples were stained for flow cytometric analysis of CD39, IFN γ , TNF α and IL-2. **A-D**) Representative dot plots (left) and corresponding quantification (right) of CD107a⁺ (**A**), IFN γ ⁺ (**B**), TNF α ⁺ (**C**), and IL-2⁺ (**D**) CD39⁻ and CD39⁺CD8⁺ T-cells. Data is displayed as mean \pm SEM of technical replicates from two to three experiments (n = 6-9). * p \leq 0.05, ns = not significant by unpaired t-test.

In addition to the data above, the MFI of CD107a, IFN γ , TNF α , and IL-2 were analyzed. From samples stimulated with α CD3/ α CD28 Abs and recombinant IL-2, the MFI of IFN γ on IFN γ^+ CD39 $^{+/-}$ CD8 $^+$ T-cells are displayed (Figure 28). We found that T-cells expressing CD39 had a significantly higher MFI than CD39 $^-$ cells.

The MFI data for CD107a, TNF α , and IL-2 were not included as the distribution of cells on the flow plots was not bimodal (Figure 26 a, c, d). Altogether, these results show that CD39 $^+$ CD8 $^+$ T-cells can produce effector molecules when activated with PMA and ionomycin. Furthermore, when stimulated with α CD3 and α CD28 Abs, CD39 $^+$ CD8 $^+$ T-cells display increased anti-tumour potential as demonstrated by the significantly higher frequency of CD107a $^+$ and IFN γ^+ cells.

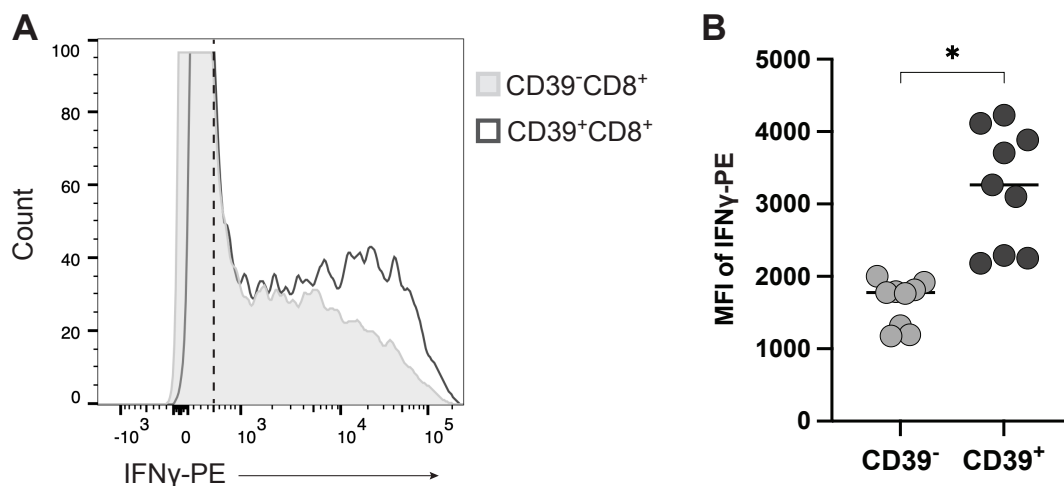


Figure 28. MFI of IFN γ from IFN γ ⁺ CD39⁺ and CD39⁻CD8⁺ T-cells after *in vitro* stimulation with α CD3/CD28 and IL-2.

A) Representative histogram of IFN γ expression, in which the dotted line separates IFN γ ⁻ (left) and IFN γ ⁺ (right) CD39⁻ and CD39⁺CD8⁺ T-cells. **B)** Quantification of MFI of IFN γ -PE from CD39⁻ and CD39⁺CD8⁺ T-cells. Data is displayed as mean \pm SEM of technical replicates from three experiments (n = 9). * p \leq 0.05 by unpaired t-test.

3.4.2 The presence of IL-12 and IL-27 differentially affects CD39⁺CD8⁺ T-cells effector molecule production

After establishing that more CD39⁺CD8⁺ T-cells expressed CD107a, IFN γ , TNF α and IL-2 than CD39⁻CD8⁺ T-cells via α CD3 and α CD28 Abs, we examined whether the effector capability of CD39⁺CD8⁺ T-cells would be different after stimulation with IL-12 and/or IL-27. We found that CD39⁺CD8⁺ T-cells stimulated with IL-27 had the greatest frequency of CD107a⁺ cells (Figure 29 a). Accordingly, T-cells stimulated in the presence of IL-12, individually or in combination with IL-27, had a significantly lower frequency of CD107a⁺ cells than IL-27 individually. The frequency of IFN γ ⁺ cells was highest when stimulated in the presence of IL-12 (Figure 29 b). Interestingly, we found CD39⁺CD8⁺ T-cells stimulated with IL-27 had the lowest frequency of IFN γ ⁺ cells. We found no difference in the expression of TNF α across conditions (Figure 29 c). Finally, the frequency of IL-2⁺ cells was significantly higher in cell cultures containing IL-27 (Figure 29 d). Taken together, these data indicate that the presence of IL-12 and IL-27 differentially affected the effector molecule production of CD39⁺CD8⁺ T-cells (Figure 29). More importantly, these results illustrate that extrinsic factors (i.e., the cytokine milieu) play an integral role in the functionality of CD39⁺CD8⁺ T-cells.

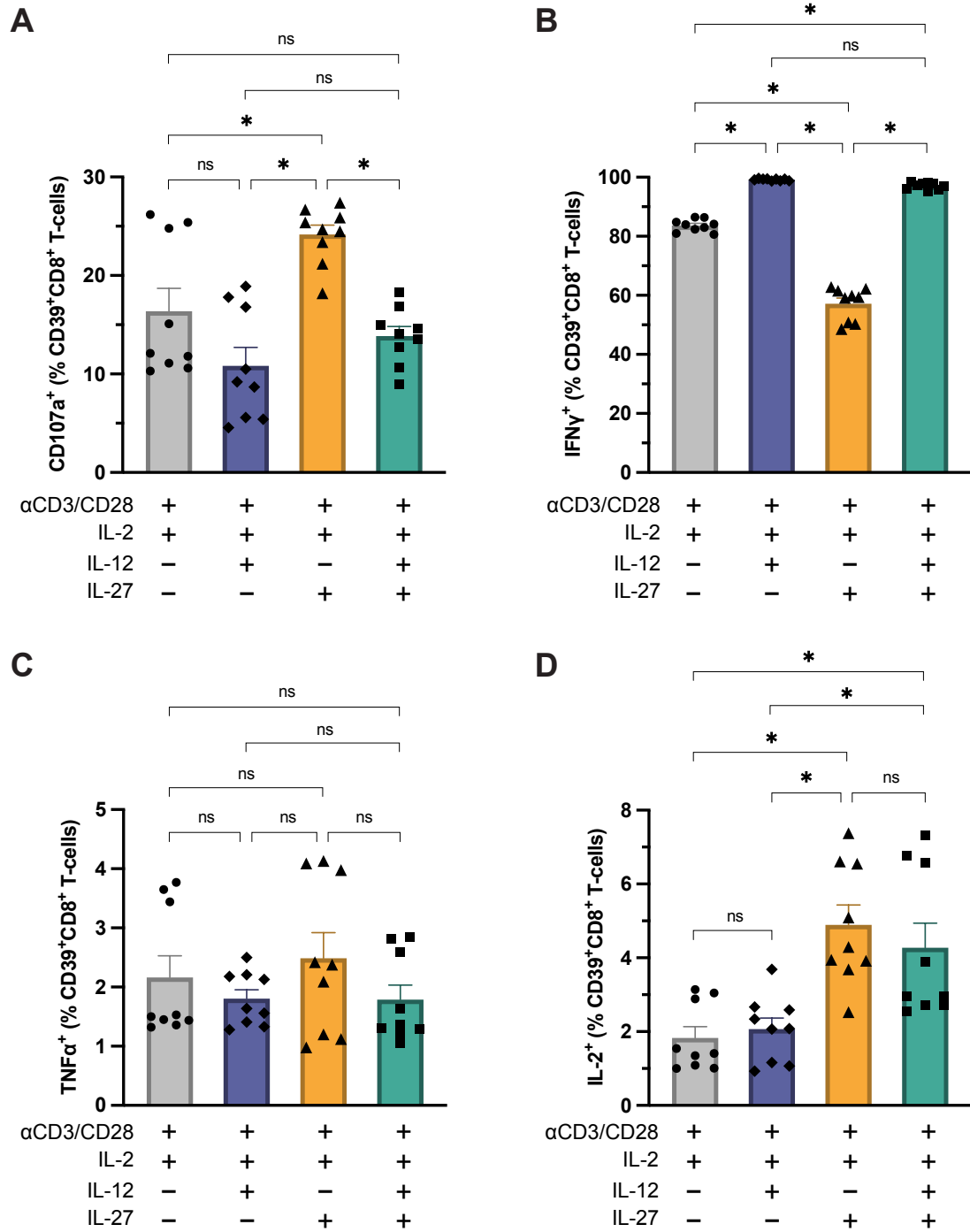


Figure 29. Effector molecule expression of CD39⁺CD8⁺ T-cells after *in vitro* stimulation with IL-12 and/or IL-27.

Bulk splenocytes from immunogenic neuro-2a primed mice were stimulated with plate-bound α CD3 and α CD28 Abs and IL-2 \pm IL-12 and/or IL-27. After 48 hours, BFA and CD107a were added, and 5 hours later, samples were stained for flow cytometric analysis of CD39, IFN γ , TNF α and IL-2. **A-D**) Representative dot plots (left) and corresponding quantification (right) of CD107a⁺ (**A**), IFN γ ⁺ (**B**), TNF α ⁺ (**C**), and IL-2⁺ (**D**) CD39⁺CD8⁺ T-cells. Data is displayed as mean \pm SEM of technical replicates from three experiments (n = 9). * p \leq 0.05, ns = not significant by one-way ANOVA.

Chapter 4 – Discussion

Tumour-specific CD8⁺ T-cells play a critical role in sustaining anti-tumour immunity. The function of these cells is modulated by the local molecular and cytokine milieu^{24,25}. Two such cytokines are IL-12 and IL-27, produced by activated APCs, and they have established roles in driving CD8⁺ T-cell differentiation and promoting effector function³⁸. Moreover, there is considerable evidence highlighting the role of IL-12, and more recently IL-27, in stimulating tumour-specific CD8⁺ T-cell-mediated anti-tumour immunity, directly and indirectly^{41–44,48–55,161}. Tumour-specific CD8⁺ T-cells within the TME often exhibit an exhausted phenotype, consistent with chronic antigen stimulation^{58,61,62,64,65}. Recent studies have demonstrated that tumour-specific CD8⁺ TILs can be primarily recognized by CD39 expression, as bystander CD8⁺ TILs do not express this enzyme^{67–72}. CD39 depletes pro-inflammatory ATP molecules and facilitates the generation of immunosuppressive adenosine^{76,77}. While there is correlation between CD39 expression and exhaustion, CD39 expression is not necessarily causative of the T-cell exhaustion. This is illustrated by studies showing CD39⁺CD8⁺ T-cells have anti-tumour potential (*in vitro*) or direct anti-tumour activity (*ex vivo* and *in vivo*)^{68,100–104}. Overall, there is a need to understand the factors contributing to CD39 expression on tumour-specific T-cells, and its subsequent effects on CD8⁺ T-cell function.

Since IL-12 and IL-27 contribute to tumour-specific CD8⁺ T-cell effector functions, these cytokines may also induce CD39 expression on these cells. Therefore, we hypothesized that IL-12 and IL-27 upregulate CD39 expression on CD8⁺ T-cells, and these cells would exhibit improved effector functions compared to CD39⁻CD8⁺ T-cells. In addition, we hypothesized that the function of CD39⁺CD8⁺ T-cells would be differentially affected by IL-12 and IL-27, because these cytokines signal through distinct pathways³⁸. IL-12 signalling activates STAT4, while IL-27 activates STAT1 and STAT3³⁸. These transcription factors can have shared or unique target genes. For example, STAT3 and STAT4 augment PD-1 expression¹⁶². Alternatively, STAT1 appears to limit PD-1 expression, as STAT1 deficient T-cells show increased PD-1 expression relative to STAT1⁺ T-cells^{163,164}. This highlights the differential effects of IL-12 and IL-27 on the phenotype of CD8⁺ T-cells, which may extend to the regulation of CD39.

Tumours with high CD8⁺ T-cell infiltration are considered ‘immunologically hot’, while those with low infiltration or exclusion are considered ‘immunologically cold’^{14,15}. As such, hot tumours are relatively more immunogenic and respond more favourably to ICIs. Our lab has engineered an immunogenic, syngeneic neuro-2a (neuroblastoma) cell line through CRISPR/Cas9 knockout of the *MLH1* gene. The MLH1 protein plays a crucial role in DNA MMR processing¹²⁶. Therefore, inducing MMR deficiency enables the accumulation of somatic mutations, increasing the likelihood of immune detection through neoantigen production^{117,125}. When comparing the characteristics of control and immunogenic neuro-2a tumours, we identified that reduced tumour burden was associated with a higher frequency of CD39⁺CD8⁺ TILs (Figure 7 and Figure 8 b). Further analysis confirmed that these cells exhibited effector or central memory phenotypes (Figure 9), indicative of anti-tumour potential^{146–148}. The correlation mentioned above supported the use of this model for the current study. A limitation of this experiment is the lack of IL-12 and IL-27 concentration measurements in the tumour and draining lymph nodes, which would have helped to provide a general understanding of their levels *in situ*.

We considered that IL-12 and IL-27 might play a role in CD39 expression because there is evidence that they contribute to tumour-specific CD8⁺ T-cell effector function³⁸. In exploring this theory, we stimulated CD8⁺ T-cells from naïve, or neuro-2a vaccinated mice in the presence of IL-12 and IL-27, individually or in combination. For these *in vitro* experiments, we focused on the ability of these cytokines to induce CD39 expression irrespective of antigen specificity in order to elucidate mechanisms of CD39 upregulation. IL-12 and IL-27 in combination produced an additive effect on CD39 upregulation when stimulating CD8⁺ T-cells from immunogenic or control neuro-2a vaccinated mice (Figure 14 and Figure 15). CD8⁺ T-cells from immunogenic neuro-2a vaccinated mice upregulated CD39 expression in the presence of IL-12 or IL-27 individually (Figures Figure 14 and Figure 15). This was not the case for CD8⁺ T-cells from control neuro-2a vaccinated mice, as IL-12 could not induce CD39 upregulation (Figure Figure 15). These results indicate an important role for neoantigens at the priming step in order for IL-12 to induce CD39 expression thereafter. As previously mentioned, the highest level of CD39 expression was found in samples stimulated with both IL-12 and IL-27 (Figure 14 b and Figure 15). These findings were corroborated by the results of a stimulation assay that used a slightly different

methodology (Figure 24 and Figure 25). All together, we have identified that IL-12 and IL-27 can induce the expression of CD39 on CD8⁺ T-cells, though stimulation with both cytokines produces an additive effect.

To investigate the relevance of this finding *in vivo*, we neutralized the biological activity of IL-12 in mice with established tumours. IL-12 was chosen since CD8⁺ T-cells from immunogenic neuro-2a antigen-experienced mice showed a higher frequency of CD39^{high}CD8⁺ T-cells when stimulated with IL-12 than IL-27 (Figure Figure 14 b-ii). After confirming that our α IL-12 Ab was effective (Figure 18 and Figure 19 d), we investigated the phenotype of CD8⁺ TILs. In immunogenic neuro-2a tumours, we observed less exhausted CD8⁺ TILs and more importantly, fewer CD39⁺CD8⁺ TILs with α IL-12 treatment (Figure 20 b, c). There was no difference in the frequency of CD39⁺CD8⁺ T-cells within the spleen, suggesting that IL-12 presence in the tumour is a critical factor. However, we did not look at the tumour-draining lymph nodes. Therefore, we cannot rule out that IL-12 neutralization does not affect CD8⁺ T-cells in secondary lymphoid organs, as intratumoural treatments with IL-12 have previously demonstrated^{165,166}. Nevertheless, our results indicate that IL-12 is functionally relevant to the induction of CD39⁺CD8⁺ TILs *in vivo*. Further experiments should be conducted done to assess the effect of neutralizing IL-27 activity *in vivo*.

Within the IL-12 neutralization experiment, we observed that treatment with α IL-12 did not affect volume of neuro-2a tumours (Figure 17). This was unexpected, as IL-12 has crucial functions in promoting and sustaining anti-tumour immunity^{165,167}. It is possible that this was a result of α IL-12 administration once tumours were already established, or that a therapy in combination with IL-12 neutralization would be necessary to observe an effect on tumour burden. Additional experiments should be conducted regarding the latter hypothesis, in order to investigate the importance of IL-12 and CD39⁺CD8⁺ T-cells in controlling immunogenic neuro-2a tumours.

As previously mentioned, IL-12 neutralization was associated with reduced frequency of exhausted CD8⁺ TILs in immunogenic neuro-2a tumours (Figure 20 b). As IL-12 and IL-27 contribute to the effector phenotype of CD8⁺ T-cells³⁸, we considered whether they play a role in inducing inhibitory receptor expression that contributes to the exhaustion phenotype. Using the *in vitro* CD8⁺ T-cell stimulation assay with IL-12 and/or

IL-27, we found distinct differences in the expression of PD-1, LAG-3 and TIM-3. The highest frequencies of PD-1⁺, LAG-3⁺, TIM-3⁺ and TP (TIM-3⁺PD-1⁺LAG-3⁺) CD39⁺CD8⁺ T-cells were found after stimulation with IL-12 (Figure 21 and Figure 22). Indeed, these results correlate with our *in vivo* data (Figure 20 b). Furthermore, relative to IL-12, we found that stimulation with IL-27 resulted in significantly fewer cells expressing inhibitory receptors (Figure 21 and Figure 22). Moreover, stimulation with both cytokines showed that IL-27 may hinder the induction of PD-1 and TIM-3 expression by IL-12, as the frequency of these cells were lower in the IL-12 and IL-27 stimulated group compared to IL-12 (Figure 21 d, f). This would also apply to the co-expression of PD-1, LAG-3 and TIM-3, as cells stimulated IL-12 and IL-27 had a lower frequency of TP CD39⁺CD8⁺ T-cells compared to IL-12 alone (Figure 22). Recent studies have highlighted that IL-27 can enhance the survival of tumour-specific CD8⁺ T-cells and contribute to CD8⁺ T-cell memory^{51,52,168}. Based on our results, it is possible that IL-27 acts to limit inhibitory receptor expression and, thereby, mitigate the suppressive signals that contribute to CD8⁺ T-cell exhaustion and dysfunction.

It is possible that the differential effects of IL-12 and IL-27 are attributed to differences in their downstream signalling pathways. In order to translate our findings to clinical applications, the mechanism by which IL-12 and IL-27 induce CD39 should be investigated. Many studies move to clinical trials, only to fail at early stages due to toxicities or adverse effects^{169,170}. Uncovering the mechanism would provide novel information to the field of immuno-oncology and immunotherapy that could be applied to regulate CD39 expression on CD8⁺ T-cells.

IL-27 has been shown to induce CD39 expression on CD4⁺ Tregs in a STAT1-dependent manner¹²⁷. While IL-12 in combination with IL-4 has been shown to induce CD39 expression on CD8⁺ Tregs¹²⁸, no mechanism has been investigated. Our future experiments will explore the mechanisms by which IL-12 and IL-27 induce CD39 expression on CD8⁺ T-cells, focusing on the transcription factors activated downstream of IL-12 and IL-27 that facilitate *ENTPDI* (gene encoding CD39) transcription. The literature shows transcription factors RUNX3 (runt-related transcription factor 3), STAT1 and STAT3 have established or putative binding sites at the promoter of *ENTPDI* and positively regulate CD39 expression^{127,171-173}. RUNX3 is induced downstream of IL-12

signalling, while STAT1 and STAT3 are induced by IL-27 signalling^{38,174}. Overall, further research is required to determine whether these three transcription factors are responsible for positively regulating CD39 expression downstream of IL-12 and IL-27 signalling.

The current literature contains conflicting evidence as to the anti-tumour potential of CD39⁺CD8⁺ T-cells^{68,73,74,98–104}; inspiring our own comparison between the effector function of CD39⁺ and CD39⁻CD8⁺ T-cells. After stimulation with α CD3/ α CD28 Abs and IL-2, we found higher levels of CD39⁺CD8⁺ T-cells expressed CD107a, IFN γ , TNF α , and IL-2 than their CD39⁻counterparts (Figure 26 a-d). Although the levels for TNF α , and IL-2 were less than 5%, hyperstimulation with PMA/ionomycin confirmed that these CD8⁺ T-cells are capable of producing TNF α and IL-2 (Figure 27 a, b). Previous studies have demonstrated CD8⁺ T-cell exhaustion is, in part, characterized by the progressive loss of effector function. The ability to produce IL-2 and TNF α is lost during the initial phases, while cells can still produce IFN γ and degranulate (marked by CD107a)⁶⁶. Additional analysis showed that CD39⁺CD8⁺ T-cells produced more IFN γ , on a per-cell basis than CD39⁻CD8⁺ T-cells (Figure 28). Overall, our data indicate that CD39⁺CD8⁺ T-cells are more capable of IFN γ production and cytotoxicity than their CD39⁻ counterparts. While CD39⁺CD8⁺ T-cells did display low-level characteristics of exhaustion, they were less than that of CD39⁻CD8⁺ T-cells (Figure 26 and Figure 28).

One limitation of this experiment is that it demonstrates the functional potential of CD39⁺CD8⁺ T-cells but does not directly establish the anti-tumour activity of these cells. To address this, *ex vivo* cytotoxicity assays will be used in future experiments, in which CD39⁺CD8⁺ TILs isolated from neuro-2a tumours would be co-cultured with neuro-2a cells to measure tumour cell death¹⁰². Additionally, adoptive cell transfer experiments of CD39⁺ or CD39⁻CD8⁺ TILs into immunodeficient and immunocompetent mice should be conducted, to determine whether CD39 expression affects CD8⁺ T-cell anti-tumour activity *in vivo*¹⁰⁴.

So far, our results show that CD39 expression is upregulated on CD8⁺ T-cells when stimulated with IL-12 and IL-27 (Figure 11, Figure 12, Figure 14 b and Figure 15), and these cytokines differentially affect the expression of inhibitory receptors PD-1, LAG-3 and TIM-3 (Figure 21 and Figure 22). Moreover, higher frequencies of CD39⁺CD8⁺ T-

cells produced IFN γ and expressed CD107a compared to CD39⁻ cells (Figure 26, Figure 27 and Figure 28). Taken together, we considered that IL-12 and IL-27 might have distinct effects on the cytokine production (IFN γ , TNF α and IL-2) and cytotoxic capacity (CD107a) of CD39⁺CD8⁺ T-cells.

Relative to samples stimulated (α CD3/ α CD28 Abs and IL-2) with IL-12, we found that CD39⁺CD8⁺ T-cells stimulated with IL-27 had the greatest frequency of CD107a⁺ cells (Figure 29 a). When analyzing inhibitory receptor expression, stimulation with IL-27 resulted in the lowest TP CD39⁺CD8⁺ T-cells (Figure 22). Coupled with the increased frequency of CD107a⁺ cells, it appears that cells stimulated with IL-27 are less exhausted than those stimulated with IL-12⁶². However, the frequency of IFN γ ⁺ cells was significantly higher when stimulated in the presence of IL-12 (Figure 29 b). Surprisingly, CD39⁺CD8⁺ T-cells stimulated with IL-27 had the lowest frequency of IFN γ ⁺ cells; though greater than 50% of CD39⁺CD8⁺ T-cells produced IFN γ , indicating that IL-27 did not completely abrogate their ability. These results were in contrast to others that show IL-27 induces IFN γ production by CD8⁺ T-cells⁴⁸⁻⁵². Notably, our CD39⁺CD8⁺ T-cells stimulated with both IL-12, and IL-27 showed the same frequency of IFN γ ⁺ cells as those stimulated with IL-12 individually (Figure 29 b). Similarly, one study showed that while IL-27 and TCR stimulation alone induced minimal IFN γ ⁺CD8⁺ T-cells, IL-27 synergized with IL-12 to produce high levels of IFN γ ⁵³.

We found the frequency of IL-2⁺ cells was significantly higher in cell cultures containing IL-27 (Figure 29 c, d). There is evidence that autocrine IL-2 signalling promotes the expansion potential of tumour-specific CD8⁺ T-cells, which was associated with improved anti-tumour immunity¹⁷⁵. This data coupled with the results from our assay (Figure 29 a, b, d), indicate that IL-27 may contribute to the expansion and anti-tumour activity of CD39⁺CD8⁺ T-cells. Further investigation is warranted to support this claim; however, the notion is also supported by studies showing IL-27 can enhance the survival and self-renewal of tumour-specific CD8⁺ T-cells^{51,52,168}. As previously described, additional experiments are required to assess the effects of neutralizing IL-27 activity *in vivo*. Our results from the *in vitro* experiments emphasize the importance of this investigation.

In our study, it is important to recognize that while IL-12 induced the highest expression of PD-1⁺, LAG-3⁺, TIM-3⁺, and TP CD39⁺CD8⁺ T-cells (Figure 21 and Figure 22), these cells are functional upon *in vitro* stimulation (Figure 29). This data highlights that, although CD39⁺CD8⁺ T-cells may exhibit an exhausted phenotype based on inhibitory receptor expression, they have functional potential. Regardless of the differential effects of IL-12 and IL-27 on the effector functionality of CD39⁺CD8⁺ T-cells, our results illustrate that extrinsic factors (i.e., the cytokine milieu) play an integral role in the anti-tumour activity of CD39⁺CD8⁺ T-cells.

An important limitation to consider is that our *in vivo* experiments utilized a subcutaneous neuroblastoma tumour model. With the neuro-2a cells engrafted under the skin (in the right flank), tumours could be easily monitored and measured using calipers. Even so, the subcutaneous model does not allow the establishment of an organ-specific TME, as neuroblastomas most commonly develop in the adrenal glands¹¹⁹. The use of an orthotopic model, in which the neuro-2a cells are injected into the tissue of origin (adrenal gland), would overcome this limitation. However, the operation of such a model is technically challenging due to the small size of adrenal glands and fragility of kidneys in mice¹⁷⁶.

In general, tumour-specific CD8⁺ TILs are essential for sustaining anti-tumour immunity and cancer remission^{56,57}. The knowledge of basic T-cell biology has enabled the development of immunotherapies for cancer treatment^{59,177}. However, their effectiveness remains limited in treating most patients with solid tumours^{16,61,110}. Identifying and further understanding the mechanisms underlying tumour-specific CD8⁺ T-cell development, phenotype, and function are key to improving response to immunotherapies.

References

1. Dvorak, H. F., Weaver, V. M., Tlsty, T. D. & Bergers, G. Tumor Microenvironment and Progression. *J. Surg. Oncol.* **103**, 468–474 (2011).
2. Schiavoni, G., Gabriele, L. & Mattei, F. The Tumor Microenvironment: A Pitch for Multiple Players. *Front. Oncol.* **3**, 90 (2013).
3. Hanahan, D. & Weinberg, R. A. Hallmarks of Cancer: The Next Generation. *Cell* **144**, 646–674 (2011).
4. Schreiber, R. D., Old, L. J. & Smyth, M. J. Cancer Immunoediting: Integrating Immunity's Roles in Cancer Suppression and Promotion. *Science* **331**, 1565–1570 (2011).
5. Zitvogel, L., Tesniere, A. & Kroemer, G. Cancer despite immunosurveillance: immunoselection and immunosubversion. *Nat. Rev. Immunol.* **6**, 715–727 (2006).
6. Mittal, D., Gubin, M. M., Schreiber, R. D. & Smyth, M. J. New insights into cancer immunoediting and its three component phases — elimination, equilibrium and escape. *Curr. Opin. Immunol.* **27**, 16–25 (2014).
7. Koebel, C. M. *et al.* Adaptive immunity maintains occult cancer in an equilibrium state. *Nature* **450**, 903–907 (2007).
8. Loeser, S. *et al.* Spontaneous tumor rejection by cbl-b-deficient CD8⁺ T cells. *J. Exp. Med.* **204**, 879–891 (2007).
9. Eyles, J. *et al.* Tumor cells disseminate early, but immunosurveillance limits metastatic outgrowth, in a mouse model of melanoma. *J. Clin. Invest.* **120**, 2030–2039 (2010).

10. Clemente, C. G. *et al.* Prognostic value of tumor infiltrating lymphocytes in the vertical growth phase of primary cutaneous melanoma. *Cancer* **77**, 1303–1310 (1996).
11. Naito, Y. *et al.* CD8⁺ T cells infiltrated within cancer cell nests as a prognostic factor in human colorectal cancer. *Cancer Res.* **58**, 3491–3494 (1998).
12. Sharma, P. *et al.* CD8 tumor-infiltrating lymphocytes are predictive of survival in muscle-invasive urothelial carcinoma. *Proc. Natl. Acad. Sci.* **104**, 3967–3972 (2007).
13. Oshi, M. *et al.* CD8 T Cell Score as a Prognostic Biomarker for Triple Negative Breast Cancer. *Int. J. Mol. Sci.* **21**, 6968 (2020).
14. Galon, J. & Bruni, D. Approaches to treat immune hot, altered and cold tumours with combination immunotherapies. *Nat. Rev. Drug Discov.* **18**, 197–218 (2019).
15. Ren, X. *et al.* Immunological Classification of Tumor Types and Advances in Precision Combination Immunotherapy. *Front. Immunol.* **13**, 790113 (2022).
16. Maleki Vareki, S. High and low mutational burden tumors versus immunologically hot and cold tumors and response to immune checkpoint inhibitors. *J. Immunother. Cancer* **6**, 157 (2018).
17. Li, F. *et al.* The association between CD8⁺ tumor-infiltrating lymphocytes and the clinical outcome of cancer immunotherapy: A systematic review and meta-analysis. *eClinicalMedicine* **41**, 101134 (2021).
18. Wherry, E. J. & Masopust, D. Chapter 5 - Adaptive Immunity: Neutralizing, Eliminating, and Remembering for the Next Time. in *Viral Pathogenesis 3rd Edition* 57–69 (Academic Press, 2016).

19. Raskov, H., Orhan, A., Christensen, J. P. & Gögenur, I. Cytotoxic CD8⁺ T cells in cancer and cancer immunotherapy. *Br. J. Cancer* **124**, 359–367 (2021).
20. Hanahan, D. & Weinberg, R. A. The Hallmarks of Cancer. *Cell* **100**, 57–70 (2000).
21. Coulie, P. G., Van den Eynde, B. J., van der Bruggen, P. & Boon, T. Tumour antigens recognized by T lymphocytes: at the core of cancer immunotherapy. *Nat. Rev. Cancer* **14**, 135–146 (2014).
22. Lee, C.-H., R, Y., K, J. & Ta, C. Update on Tumor Neoantigens and Their Utility: Why It Is Good to Be Different. *Trends Immunol.* **39**, (2018).
23. McDonnell, A. M., Robinson, B. W. S. & Currie, A. J. Tumor antigen cross-presentation and the dendritic cell: where it all begins? *Clin. Dev. Immunol.* **2010**, 539519 (2010).
24. Curtsinger, J. M. & Mescher, M. F. Inflammatory cytokines as a third signal for T cell activation. *Curr. Opin. Immunol.* **22**, 333–340 (2010).
25. Mescher, M. F. *et al.* Signals required for programming effector and memory development by CD8⁺ T cells. *Immunol. Rev.* **211**, 81–92 (2006).
26. Borst, J., Ahrends, T., Bąbała, N., Melief, C. J. M. & Kastenmüller, W. CD4⁺ T cell help in cancer immunology and immunotherapy. *Nat. Rev. Immunol.* **18**, 635–647 (2018).
27. Bennett, S. R. M., Carbone, F. R., Karamalis, F., Miller, J. F. A. P. & Heath, W. R. Induction of a CD8⁺ Cytotoxic T Lymphocyte Response by Cross-priming Requires Cognate CD4⁺ T Cell Help. *J. Exp. Med.* **186**, 65–70 (1997).
28. Bennett, S. R. M. *et al.* Help for cytotoxic-T-cell responses is mediated by CD40 signalling. *Nature* **393**, 478–480 (1998).

29. Schoenberger, S. P., Toes, R. E. M., van der Voort, E. I. H., Offringa, R. & Melief, C. J. M. T-cell help for cytotoxic T lymphocytes is mediated by CD40–CD40L interactions. *Nature* **393**, 480–483 (1998).
30. Lai, Y.-P., Lin, C.-C., Liao, W.-J., Tang, C.-Y. & Chen, S.-C. CD4⁺ T cell-derived IL-2 signals during early priming advances primary CD8⁺ T cell responses. *PLoS One* **4**, e7766 (2009).
31. Liu, Y.-T. & Sun, Z.-J. Turning cold tumors into hot tumors by improving T-cell infiltration. *Theranostics* **11**, 5365–5386 (2021).
32. D'Souza, W. N. & Lefrançois, L. Frontline: An in-depth evaluation of the production of IL-2 by antigen-specific CD8 T cells in vivo. *Eur. J. Immunol.* **34**, 2977–2985 (2004).
33. Malek, T. R. The biology of interleukin-2. *Annu. Rev. Immunol.* **26**, 453–479 (2008).
34. Murphy, K. & Weaver, C. T-cell mediated cytotoxicity. in *Janeway's Immunobiology 9th Edition* 387–392 (Garland Science, 2016).
35. Basu, R. *et al.* Cytotoxic T Cells Use Mechanical Force to Potentiate Target Cell Killing. *Cell* **165**, 100–110 (2016).
36. Aktas, E., Kucuksezer, U. C., Bilgic, S., Erten, G. & Deniz, G. Relationship between CD107a expression and cytotoxic activity. *Cell. Immunol.* **254**, 149–154 (2009).
37. Betts, M. R. & Koup, R. A. Detection of T-Cell Degranulation: CD107a and b. in *Methods in Cell Biology* vol. 75 497–512 (Academic Press, 2004).
38. Xu, M. *et al.* Regulation of Antitumor Immune Responses by the IL-12 Family Cytokines, IL-12, IL-23, and IL-27. *Clin. Dev. Immunol.* **2010**, 1–9 (2010).

39. Bacon, C. M. *et al.* Interleukin 12 induces tyrosine phosphorylation and activation of STAT4 in human lymphocytes. *Proc. Natl. Acad. Sci. U. S. A.* **92**, 7307–7311 (1995).
40. Hibbert, L., Pflanz, S., De Waal Malefyt, R. & Kastelein, R. A. IL-27 and IFN- α signal via Stat1 and Stat3 and induce T-Bet and IL-12Rbeta2 in naive T cells. *J. Interferon Cytokine Res.* **23**, 513–522 (2003).
41. Rubinstein, M. P. *et al.* Interleukin-12 enhances the function and anti-tumor activity in murine and human CD8⁺ T cells. *Cancer Immunol. Immunother. CII* **64**, 539–549 (2015).
42. Alspach, E., Lussier, D. M. & Schreiber, R. D. Interferon γ and Its Important Roles in Promoting and Inhibiting Spontaneous and Therapeutic Cancer Immunity. *Cold Spring Harb. Perspect. Biol.* **11**, a028480 (2019).
43. Ma, X. *et al.* The interleukin 12 p40 gene promoter is primed by interferon gamma in monocytic cells. *J. Exp. Med.* **183**, 147–157 (1996).
44. Zhao, J., Zhao, J. & Perlman, S. Differential effects of IL-12 on Tregs and non-Treg T cells: roles of IFN- γ , IL-2 and IL-2R. *PLoS One* **7**, e46241 (2012).
45. Grohmann, U. *et al.* A tumor-associated and self antigen peptide presented by dendritic cells may induce T cell anergy in vivo, but IL-12 can prevent or revert the anergic state. *J. Immunol.* **158**, 3593–3602 (1997).
46. Leonard, J. P. *et al.* Effects of Single-Dose Interleukin-12 Exposure on Interleukin-12–Associated Toxicity and Interferon- γ Production. *Blood* **90**, 2541–2548 (1997).
47. Jones, D. S. *et al.* Cell surface–tethered IL-12 repolarizes the tumor immune microenvironment to enhance the efficacy of adoptive T cell therapy. *Sci. Adv.* **8**, eabi8075 (2022).

48. Chiyo, M. *et al.* Expression of IL-27 in murine carcinoma cells produces antitumor effects and induces protective immunity in inoculated host animals. *Int. J. Cancer* **115**, 437–442 (2005).
49. Hisada, M. *et al.* Potent antitumor activity of interleukin-27. *Cancer Res.* **64**, 1152–1156 (2004).
50. Salcedo, R. *et al.* Immunologic and Therapeutic Synergy of IL-27 and IL-2: Enhancement of T Cell Sensitization, Tumor-Specific CTL Reactivity and Complete Regression of Disseminated Neuroblastoma Metastases in the Liver and Bone Marrow. *J. Immunol. Baltim. Md 1950* **182**, 4328–4338 (2009).
51. Schneider, R., Yaneva, T., Beauseigle, D., El-Khoury, L. & Arbour, N. IL-27 increases the proliferation and effector functions of human naïve CD8⁺ T lymphocytes and promotes their development into Tc1 cells. *Eur. J. Immunol.* **41**, 47–59 (2010).
52. Ding, M. *et al.* IL-27 improves adoptive CD8⁺ T cells' antitumor activity via enhancing cell survival and memory T cell differentiation. *Cancer Sci.* **113**, 2258–2271 (2022).
53. Morishima, N. *et al.* Augmentation of effector CD8⁺ T cell generation with enhanced granzyme B expression by IL-27. *J. Immunol. Baltim. Md 1950* **175**, 1686–1693 (2005).
54. Shinozaki, Y. *et al.* Tumor-specific cytotoxic T cell generation and dendritic cell function are differentially regulated by interleukin 27 during development of anti-tumor immunity. *Int. J. Cancer* **124**, 1372–1378 (2009).

55. Yoshimoto, T. *et al.* Antiproliferative activity of IL-27 on melanoma. *J. Immunol. Baltim. Md 1950* **180**, 6527–6535 (2008).
56. Rao, S., Gharib, K. & Han, A. Cancer Immunosurveillance by T Cells. *Int. Rev. Cell Mol. Biol.* **342**, 149–173 (2019).
57. Paul, M. S. & Ohashi, P. S. The Roles of CD8⁺ T Cell Subsets in Antitumor Immunity. *Trends Cell Biol.* **30**, 695–704 (2020).
58. Jiang, W. *et al.* Exhausted CD8⁺ T Cells in the Tumor Immune Microenvironment: New Pathways to Therapy. *Front. Immunol.* **11**, 622509 (2021).
59. Jiang, X. *et al.* Adoptive CD8⁺ T cell therapy against cancer: Challenges and opportunities. *Cancer Lett.* **462**, 23–32 (2019).
60. Durgeau, A., Virk, Y., Corgnac, S. & Mami-Chouaib, F. Recent Advances in Targeting CD8 T-Cell Immunity for More Effective Cancer Immunotherapy. *Front. Immunol.* **9**, 14 (2018).
61. Morotti, M. *et al.* Promises and challenges of adoptive T-cell therapies for solid tumours. *Br. J. Cancer* **124**, 1759–1776 (2021).
62. Wherry, E. J. T cell exhaustion. *Nat. Immunol.* **12**, 492–499 (2011).
63. Zajac, A. J. *et al.* Viral Immune Evasion Due to Persistence of Activated T Cells Without Effector Function. *J. Exp. Med.* **188**, 2205–2213 (1998).
64. Crespo, J., Sun, H., Welling, T. H., Tian, Z. & Zou, W. T cell anergy, exhaustion, senescence and stemness in the tumor microenvironment. *Curr. Opin. Immunol.* **25**, 214–221 (2013).
65. Wherry, E. J. & Kurachi, M. Molecular and cellular insights into T cell exhaustion. *Nat. Rev. Immunol.* **15**, 486–499 (2015).

66. Wherry, E. J., Blattman, J. N., Murali-Krishna, K., van der Most, R. & Ahmed, R. Viral Persistence Alters CD8 T-Cell Immunodominance and Tissue Distribution and Results in Distinct Stages of Functional Impairment. *J. Virol.* **77**, 4911–4927 (2003).
67. Simoni, Y. *et al.* Bystander CD8 + T cells are abundant and phenotypically distinct in human tumour infiltrates. *Nature* **557**, 575–579 (2018).
68. Duhon, T. *et al.* Co-expression of CD39 and CD103 identifies tumor-reactive CD8 T cells in human solid tumors. *Nat. Commun.* **9**, 2724 (2018).
69. Goncharov, M. M. *et al.* Pinpointing the tumor-specific T cells via TCR clusters. *eLife* **11**, e77274 (2022).
70. Eiva, M. A., Omran, D. K., Chacon, J. A. & Powell Jr., D. J. Systematic analysis of CD39, CD103, CD137, and PD-1 as biomarkers for naturally occurring tumor antigen-specific TILs. *Eur. J. Immunol.* **52**, 96–108 (2022).
71. Fehlings, M. *et al.* Checkpoint blockade immunotherapy reshapes the high-dimensional phenotypic heterogeneity of murine intratumoural neoantigen-specific CD8+ T cells. *Nat. Commun.* **8**, 562 (2017).
72. Gubin, M. M. *et al.* Checkpoint blockade cancer immunotherapy targets tumour-specific mutant antigens. *Nature* **515**, 577–581 (2014).
73. Gupta, P. K. *et al.* CD39 Expression Identifies Terminally Exhausted CD8+ T Cells. *PLOS Pathog.* **11**, e1005177 (2015).
74. Canale, F. P. *et al.* CD39 Expression Defines Cell Exhaustion in Tumor-Infiltrating CD8+ T Cells. *Cancer Res.* **78**, 115–128 (2018).
75. Junger, W. G. Immune cell regulation by autocrine purinergic signalling. *Nat. Rev. Immunol.* **11**, 201–212 (2011).

76. Zimmermann, H. Extracellular metabolism of ATP and other nucleotides. *Naunyn-Schmiedeberg's Arch. Pharmacol.* **362**, 299–309 (2000).
77. Robson, S. C., Sévigny, J. & Zimmermann, H. The E-NTPDase family of ectonucleotidases: Structure function relationships and pathophysiological significance. *Purinergic Signal.* **2**, 409–430 (2006).
78. Deaglio, S. *et al.* Adenosine generation catalyzed by CD39 and CD73 expressed on regulatory T cells mediates immune suppression. *J. Exp. Med.* **204**, 1257–1265 (2007).
79. Pellegatti, P. *et al.* Increased level of extracellular ATP at tumor sites: in vivo imaging with plasma membrane luciferase. *PLoS One* **3**, e2599 (2008).
80. Yip, L. *et al.* Autocrine regulation of T-cell activation by ATP release and P2X7 receptors. *FASEB J.* **23**, 1685–1693 (2009).
81. Corriden, R., Insel, P. A. & Junger, W. G. A novel method using fluorescence microscopy for real-time assessment of ATP release from individual cells. *Am. J. Physiol. Cell Physiol.* **293**, C1420-1425 (2007).
82. Schenk, U. *et al.* Purinergic control of T cell activation by ATP released through pannexin-1 hemichannels. *Sci. Signal.* **1**, ra6 (2008).
83. Loomis, W. H., Namiki, S., Ostrom, R. S., Insel, P. A. & Junger, W. G. Hypertonic stress increases T cell interleukin-2 expression through a mechanism that involves ATP release, P2 receptor, and p38 MAPK activation. *J. Biol. Chem.* **278**, 4590–4596 (2003).
84. Ravichandran, K. S. Find-me and eat-me signals in apoptotic cell clearance: progress and conundrums. *J. Exp. Med.* **207**, 1807–1817 (2010).

85. Aswad, F. & Dennert, G. P2X7 receptor expression levels determine lethal effects of a purine based danger signal in T lymphocytes. *Cell. Immunol.* **243**, 58–65 (2006).
86. Di Virgilio, F. ATP as a death factor. *BioFactors Oxf. Engl.* **8**, 301–303 (1998).
87. Di Virgilio, F., Sarti, A. C. & Coutinho-Silva, R. Purinergic signaling, DAMPs, and inflammation. *Am. J. Physiol.-Cell Physiol.* **318**, C832–C835 (2020).
88. Muller-Haegle, S., Muller, L. & Whiteside, T. L. Immunoregulatory activity of adenosine and its role in human cancer progression. *Expert Rev. Clin. Immunol.* **10**, 897–914 (2014).
89. Liu, H. & Xia, Y. Beneficial and detrimental role of adenosine signaling in diseases and therapy. *J. Appl. Physiol.* **119**, 1173–1182 (2015).
90. Yu, M. *et al.* CD73 on cancer-associated fibroblasts enhanced by the A2B-mediated feedforward circuit enforces an immune checkpoint. *Nat. Commun.* **11**, 515 (2020).
91. Huang, S., Apasov, S., Koshiba, M. & Sitkovsky, M. Role of A2a extracellular adenosine receptor-mediated signaling in adenosine-mediated inhibition of T-cell activation and expansion. *Blood* **90**, 1600–1610 (1997).
92. Koshiba, M., Kojima, H., Huang, S., Apasov, S. & Sitkovsky, M. V. Memory of extracellular adenosine A2A purinergic receptor-mediated signaling in murine T cells. *J. Biol. Chem.* **272**, 25881–25889 (1997).
93. Mirabet, M. *et al.* Expression of A2B adenosine receptors in human lymphocytes: their role in T cell activation. *J. Cell Sci.* **112**, 491–502 (1999).
94. Raskovalova, T. *et al.* Inhibition of cytokine production and cytotoxic activity of human antimelanoma specific CD8⁺ and CD4⁺ T lymphocytes by adenosine-protein kinase A type I signaling. *Cancer Res.* **67**, 5949–5956 (2007).

95. Linnemann, C. *et al.* Adenosine regulates CD8 T-cell priming by inhibition of membrane-proximal T-cell receptor signalling. *Immunology* **128**, e728–e737 (2009).
96. Conway, E. J. & Cooke, R. The deaminases of adenosine and adenylic acid in blood and tissues. *Biochem. J.* **33**, 479–492 (1939).
97. Franco, R. *et al.* Cell surface adenosine deaminase: Much more than an ectoenzyme. *Prog. Neurobiol.* **52**, 283–294 (1997).
98. Lee, Y., Park, J., Park, S.-H. & Shin, E.-C. CD39+CD8+ T cells exhibit a distinct phenotype among tumor-infiltrating tumor-antigen-specific CD8+ T cells. *J. Immunol.* **202**, 195.2 (2019).
99. Qi, Y. *et al.* Tumor-infiltrating CD39+CD8+ T cells determine poor prognosis and immune evasion in clear cell renal cell carcinoma patients. *Cancer Immunol. Immunother.* **69**, 1565–1576 (2020).
100. Zhu, W. *et al.* CD8+CD39+ T Cells Mediate Anti-Tumor Cytotoxicity in Bladder Cancer. *OncoTargets Ther.* **14**, 2149–2161 (2021).
101. Liu, T. *et al.* High-affinity neoantigens correlate with better prognosis and trigger potent antihepatocellular carcinoma (HCC) activity by activating CD39+CD8+ T cells. *Gut* **70**, 1965–1977 (2021).
102. Zou, F. *et al.* The CD39+ HBV surface protein-targeted CAR-T and personalized tumor-reactive CD8+ T cells exhibit potent anti-HCC activity. *Mol. Ther.* **29**, 1794–1807 (2021).
103. Miller, B. C. *et al.* Subsets of exhausted CD8+ T cells differentially mediate tumor control and respond to checkpoint blockade. *Nat. Immunol.* **20**, 326–336 (2019).

104. Tallón de Lara, P. *et al.* CD39+PD-1+CD8+ T cells mediate metastatic dormancy in breast cancer. *Nat. Commun.* **12**, 769 (2021).
105. Gameiro, S. F. *et al.* Treatment-naïve HPV+ head and neck cancers display a T-cell-inflamed phenotype distinct from their HPV- counterparts that has implications for immunotherapy. *Oncoimmunology* **7**, e1498439 (2018).
106. Laumont, C. M. *et al.* Single-cell Profiles and Prognostic Impact of Tumor-Infiltrating Lymphocytes Coexpressing CD39, CD103, and PD-1 in Ovarian Cancer. *Clin. Cancer Res.* **27**, 4089–4100 (2021).
107. Yeong, J. *et al.* Intratumoral CD39+CD8+ T Cells Predict Response to Programmed Cell Death Protein-1 or Programmed Death Ligand-1 Blockade in Patients With NSCLC. *J. Thorac. Oncol. Off. Publ. Int. Assoc. Study Lung Cancer* **16**, 1349–1358 (2021).
108. Attrill, G. H. *et al.* Higher proportions of CD39+ tumor-resident cytotoxic T cells predict recurrence-free survival in patients with stage III melanoma treated with adjuvant immunotherapy. *J. Immunother. Cancer* **10**, e004771 (2022).
109. Sade-Feldman, M. *et al.* Defining T Cell States Associated with Response to Checkpoint Immunotherapy in Melanoma. *Cell* **175**, 998-1013.e20 (2018).
110. Robert, C. A decade of immune-checkpoint inhibitors in cancer therapy. *Nat. Commun.* **11**, 3801 (2020).
111. Chan, D. V. *et al.* Differential CTLA-4 expression in human CD4+ versus CD8+ T cells is associated with increased NFAT1 and inhibition of CD4+ proliferation. *Genes Immun.* **15**, 25–32 (2014).

112. Hegel, J. K., Knieke, K., Kolar, P., Reiner, S. L. & Brunner-Weinzierl, M. C. CD152 (CTLA-4) regulates effector functions of CD8⁺ T lymphocytes by repressing Eomesodermin. *Eur. J. Immunol.* **39**, 883–893 (2009).
113. Pedicord, V. A., Montalvo, W., Leiner, I. M. & Allison, J. P. Single dose of anti-CTLA-4 enhances CD8⁺ T-cell memory formation, function, and maintenance. *Proc. Natl. Acad. Sci. U. S. A.* **108**, 266–271 (2011).
114. Rodig, N. *et al.* Endothelial expression of PD-L1 and PD-L2 down-regulates CD8⁺ T cell activation and cytotoxicity. *Eur. J. Immunol.* **33**, 3117–3126 (2003).
115. Chemnitz, J. M., Parry, R. V., Nichols, K. E., June, C. H. & Riley, J. L. SHP-1 and SHP-2 Associate with Immunoreceptor Tyrosine-Based Switch Motif of Programmed Death 1 upon Primary Human T Cell Stimulation, but Only Receptor Ligation Prevents T Cell Activation. *J. Immunol.* **173**, 945–954 (2004).
116. Patsoukis, N. *et al.* PD-1 alters T-cell metabolic reprogramming by inhibiting glycolysis and promoting lipolysis and fatty acid oxidation. *Nat. Commun.* **6**, 6692 (2015).
117. Kloor, M. & von Knebel Doeberitz, M. The Immune Biology of Microsatellite-Unstable Cancer. *Trends Cancer* **2**, 121–133 (2016).
118. Cheung, N.-K. V. & Dyer, M. A. Neuroblastoma: developmental biology, cancer genomics and immunotherapy. *Nat. Rev. Cancer* **13**, 397–411 (2013).
119. Louis, C. U. & Shohet, J. M. Neuroblastoma: molecular pathogenesis and therapy. *Annu. Rev. Med.* **66**, 49–63 (2015).
120. Statistics Canada, Ellison, L. F., Xie, L. & Sung, L. Trends in paediatric cancer survival in Canada, 1992 to 2017. *Health Rep.* **32**, 3–15 (2021).

121. Pugh, T. J. *et al.* The genetic landscape of high-risk neuroblastoma. *Nat. Genet.* **45**, 279–284 (2013).
122. Brodeur, G. M. & Bagatell, R. Mechanisms of neuroblastoma regression. *Nat. Rev. Clin. Oncol.* **11**, 704–713 (2014).
123. Hwang, W. L. *et al.* Clinical Impact of Tumor Mutational Burden in Neuroblastoma. *J. Natl. Cancer Inst.* **111**, 695–699 (2019).
124. Li, G.-M. Mechanisms and functions of DNA mismatch repair. *Cell Res.* **18**, 85–98 (2008).
125. Willis, J. A., Reyes-Uribe, L., Chang, K., Lipkin, S. M. & Vilar, E. Immune Activation in Mismatch Repair Deficient Carcinogenesis: More Than Just Mutational Rate. *Clin. Cancer Res. Off. J. Am. Assoc. Cancer Res.* **26**, 11–17 (2020).
126. Ellison, A. R. Human MutL homolog (MLH1) function in DNA mismatch repair: a prospective screen for missense mutations in the ATPase domain. *Nucleic Acids Res.* **32**, 5321–5338 (2004).
127. Park, Y.-J. *et al.* IL-27 confers a protumorigenic activity of regulatory T cells via CD39. *Proc. Natl. Acad. Sci.* **116**, 3106–3111 (2019).
128. Noble, A., Mehta, H., Lovell, A., Papaioannou, E. & Fairbanks, L. IL-12 and IL-4 activate a CD39-dependent intrinsic peripheral tolerance mechanism in CD8⁺ T cells. *Eur. J. Immunol.* **46**, 1438–1448 (2016).
129. El-Hajjar, M. *et al.* Inducing mismatch repair deficiency sensitizes immune-cold neuroblastoma to anti-CTLA4 and generates broad anti-tumor immune memory. *Mol. Ther.* **31**, (2022).

130. Nebot-Bral, L. *et al.* Overcoming resistance to α PD-1 of MMR-deficient tumors with high tumor-induced neutrophils levels by combination of α CTLA-4 and α PD-1 blockers. *J. Immunother. Cancer* **10**, e005059 (2022).
131. Ruffell, B. *et al.* Macrophage IL-10 blocks CD8⁺ T cell-dependent responses to chemotherapy by suppressing IL-12 expression in intratumoral dendritic cells. *Cancer Cell* **26**, 623–637 (2014).
132. de Mingo Pulido, Á. *et al.* TIM-3 regulates CD103⁺ dendritic cell function and response to chemotherapy in breast cancer. *Cancer Cell* **33**, 60-74.e6 (2018).
133. Everts, B. *et al.* Migratory CD103⁺ dendritic cells suppress helminth-driven type 2 immunity through constitutive expression of IL-12. *J. Exp. Med.* **213**, 35–51 (2016).
134. Dong, L. *et al.* Surface-bound bovine serum albumin carrier protein as present in recombinant cytokine preparations amplifies T helper 17 cell polarization. *Sci. Rep.* **6**, 36598 (2016).
135. Batten, M. *et al.* IL-27 supports germinal center function by enhancing IL-21 production and the function of T follicular helper cells. *J. Exp. Med.* **207**, 2895–2906 (2010).
136. Scharping, N. E. *et al.* Mitochondrial stress induced by continuous stimulation under hypoxia rapidly drives T cell exhaustion. *Nat. Immunol.* **22**, 205–215 (2021).
137. Fantuzzi, G., Reed, D. A. & Dinarello, C. A. IL-12–induced IFN- γ is dependent on caspase-1 processing of the IL-18 precursor. *J. Clin. Invest.* **104**, 761–767 (1999).
138. Curtis, M. M., Way, S. S. & Wilson, C. B. IL-23 promotes the production of IL-17 by antigen-specific CD8 T cells in the absence of IL-12 and type-I interferons. *J. Immunol. Baltim. Md 1950* **183**, 381–387 (2009).

139. Nowak-Terpiłowska, A., Śledziński, P. & Zeyland, J. Impact of cell harvesting methods on detection of cell surface proteins and apoptotic markers. *Braz. J. Med. Biol. Res.* **54**, e10197 (2021).
140. Braun, M. *et al.* IL12-mediated sensitizing of T-cell receptor-dependent and -independent tumor cell killing. *Oncoimmunology* **5**, e1188245 (2016).
141. Oehen, S. & Brduscha-Riem, K. Differentiation of Naive CTL to Effector and Memory CTL: Correlation of Effector Function with Phenotype and Cell Division. *J. Immunol.* **161**, 5338–5346 (1998).
142. Opata, M. M. & Stephens, R. Early Decision: Effector and Effector Memory T Cell Differentiation in Chronic Infection. *Curr. Immunol. Rev.* **9**, 190–206 (2013).
143. Baaten, B. J. G., Tinoco, R., Chen, A. T. & Bradley, L. M. Regulation of Antigen-Experienced T Cells: Lessons from the Quintessential Memory Marker CD44. *Front. Immunol.* **3**, 23 (2012).
144. Strauss, G. *et al.* CD95 co-stimulation blocks activation of naive T cells by inhibiting T cell receptor signaling. *J. Exp. Med.* **206**, 1379–1393 (2009).
145. Yang, S., Liu, F., Wang, Q. J., Rosenberg, S. A. & Morgan, R. A. The Shedding of CD62L (L-Selectin) Regulates the Acquisition of Lytic Activity in Human Tumor Reactive T Lymphocytes. *PLoS ONE* **6**, e22560 (2011).
146. Kansas, G. S., Wood, G. S. & Tedder, T. F. Expression, distribution, and biochemistry of human CD39. Role in activation-associated homotypic adhesion of lymphocytes. *J. Immunol.* **146**, 2235–2244 (1991).
147. Gouttefangeas, C. *et al.* The CD39 molecule defines distinct cytotoxic subsets within alloactivated human CD8-positive cells. *Eur. J. Immunol.* **22**, 2681–2685 (1992).

148. Bono, M. R., Fernández, D., Flores-Santibáñez, F., Roseblatt, M. & Sauma, D. CD73 and CD39 ectonucleotidases in T cell differentiation: Beyond immunosuppression. *FEBS Lett.* **589**, 3454–3460 (2015).
149. Wu, A. *et al.* In vivo vaccination with tumor cell lysate plus CpG oligodeoxynucleotides eradicates murine glioblastoma. *J. Immunother. Hagerstown Md* 1997 **30**, 789–797 (2007).
150. Salewski, I. *et al.* In vivo vaccination with cell line-derived whole tumor lysates: neoantigen quality, not quantity matters. *J. Transl. Med.* **18**, 402 (2020).
151. Wilkinson, V. L. *et al.* Characterization of anti-mouse IL-12 monoclonal antibodies and measurement of mouse IL-12 by ELISA. *J. Immunol. Methods* **189**, 15–24 (1996).
152. Sheng, S. Y. *et al.* The Characteristics of Naive-like T Cells in Tumor-infiltrating Lymphocytes From Human Lung Cancer. *J. Immunother.* **40**, 1–10 (2017).
153. Principe, N. *et al.* Tumor Infiltrating Effector Memory Antigen-Specific CD8⁺ T Cells Predict Response to Immune Checkpoint Therapy. *Front. Immunol.* **11**, 584423 (2020).
154. Balança, C.-C. *et al.* Dual Relief of T-lymphocyte Proliferation and Effector Function Underlies Response to PD-1 Blockade in Epithelial Malignancies. *Cancer Immunol. Res.* **8**, 869–882 (2020).
155. Baitsch, L. *et al.* Exhaustion of tumor-specific CD8⁺ T cells in metastases from melanoma patients. *J. Clin. Invest.* **121**, 2350–2360 (2011).

156. Thommen, D. S. *et al.* A transcriptionally and functionally distinct PD-1+ CD8+ T cell pool with predictive potential in non-small cell lung cancer treated with PD-1 blockade. *Nat. Med.* **24**, 994–1004 (2018).
157. Vaux, D. L., Fidler, F. & Cumming, G. Replicates and repeats—what is the difference and is it significant? *EMBO Rep.* **13**, 291–296 (2012).
158. Molnar, C. & Gair, J. Chapter 1.2 The Process of Science. in *Concepts of Biology – 1st Canadian Edition* (BCcampus, 2015).
159. Ai, W., Li, H., Song, N., Li, L. & Chen, H. Optimal Method to Stimulate Cytokine Production and Its Use in Immunotoxicity Assessment. *Int. J. Environ. Res. Public Health* **10**, 3834–3842 (2013).
160. Hou, H. *et al.* Establishment of the Reference Intervals of Lymphocyte Function in Healthy Adults Based on IFN- γ Secretion Assay upon Phorbol-12-Myristate-13-Acetate/Ionomycin Stimulation. *Front. Immunol.* **9**, 172 (2018).
161. Siddiqui, F. *et al.* Anti-angiogenic effects of interleukin-12 delivered by a novel hyperthermia induced gene construct. *Int. J. Hyperthermia* **22**, 587–606 (2006).
162. Austin, J. W., Lu, P., Majumder, P., Ahmed, R. & Boss, J. M. STAT3, STAT4, NFATc1, and CTCF regulate PD-1 through multiple novel regulatory regions in murine T cells. *J. Immunol. Baltim. Md 1950* **192**, 4876–4886 (2014).
163. Friedrich, J. *et al.* STAT1 deficiency supports PD-1/PD-L1 signaling resulting in dysfunctional TNF α mediated immune responses in a model of NSCLC. *Oncotarget* **9**, 37157–37172 (2018).

164. Ryan, N. *et al.* STAT1 inhibits T cell exhaustion and myeloid derived suppressor cell accumulation to promote anti-tumor immune responses in head and neck squamous cell carcinoma. *Int. J. Cancer* **146**, 1717–1729 (2020).
165. Kilinc, M. O. *et al.* Reversing Tumor Immune Suppression with Intratumoral IL-12: Activation of Tumor-Associated T Effector/Memory Cells, Induction of T Suppressor Apoptosis, and Infiltration of CD8⁺ T Effectors. *J. Immunol.* **177**, 6962–6973 (2006).
166. Kilinc, M. O., Gu, T., Harden, J. L., Virtuoso, L. P. & Egilmez, N. K. Central Role of Tumor-Associated CD8⁺ T Effector/Memory Cells in Restoring Systemic Antitumor Immunity. *J. Immunol.* **182**, 4217–4225 (2009).
167. Habiba, U. e *et al.* The multifaceted role of IL-12 in cancer. *Adv. Cancer Biol. - Metastasis* **5**, 100053 (2022).
168. Liu, Z. *et al.* IL-27 enhances the survival of tumor antigen-specific CD8⁺ T cells and programs them into IL-10-producing, memory precursor-like effector cells. *Eur. J. Immunol.* **43**, 468–479 (2013).
169. Hwang, T. J. *et al.* Failure of Investigational Drugs in Late-Stage Clinical Development and Publication of Trial Results. *JAMA Intern. Med.* **176**, 1826–1833 (2016).
170. Fogel, D. B. Factors associated with clinical trials that fail and opportunities for improving the likelihood of success: A review. *Contemp. Clin. Trials Commun.* **11**, 156–164 (2018).
171. Cao, W. *et al.* Ecto-NTPDase CD39 is a negative checkpoint that inhibits follicular helper cell generation. *J. Clin. Invest.* **130**, 3422–3436 (2020).

172. Mascanfroni, I. D. *et al.* IL-27 acts on DCs to suppress the T cell response and autoimmunity by inducing expression of the immunoregulatory molecule CD39. *Nat. Immunol.* **14**, 1054–1063 (2013).
173. Chalmin, F. *et al.* Stat3 and Gfi-1 Transcription Factors Control Th17 Cell Immunosuppressive Activity via the Regulation of Ectonucleotidase Expression. *Immunity* **36**, 362–373 (2012).
174. Zhuang, Y., Huang, Z., Nishida, J., Zhang, L. & Huang, H. Signaling Pathways That Lead to the Silencing of the Interleukin-4-Producing Potential in Th1 Cells. *J. Interferon Cytokine Res.* **29**, 399–406 (2009).
175. Redeker, A. *et al.* The Quantity of Autocrine IL-2 Governs the Expansion Potential of CD8⁺ T Cells. *J. Immunol.* **195**, 4792–4801 (2015).
176. Han, R. *et al.* Different tumorigenicity and distinct metastasis and gene signature between orthotopic and subcutaneous neuroblastoma xenografted mice. *Aging* **14**, 1932–1940 (2022).
177. Baumeister, S. H., Freeman, G. J., Dranoff, G. & Sharpe, A. H. Coinhibitory Pathways in Immunotherapy for Cancer. *Annu. Rev. Immunol.* **34**, 539–573 (2016).

Curriculum Vitae

PERSONAL INFORMATION

Name: Lara Gerhardt
Position title: M.Sc. Student

EDUCATION

Dates	Program	Institution and Discipline
2020-09 – present	M.Sc.	Western University, London ON. Discipline: Pathology and Laboratory Medicine Thesis Title: The role of IL-12 and IL-27 in modulating CD39 expression on CD8 ⁺ T-cells and their effector function. Thesis Advisor: Saman Maleki, PhD
2016-09 – 2020-04	B.Sc.	Queen's University, Kingston ON Discipline: Biochemistry

DISTINCTIONS & AWARDS

Dates	Category	Title & Description
2022-04	Award	Dr. M. Daria Haust Award for the Best Basic Science Presentation , Western University Pathology and Laboratory Medicine Research Day 2022 <i>This award recognizes a graduate student's excellence in research design and performance as well as the presentation of the research topic.</i>
2021-04	Award	Dr. Frederick Winnett Luney Graduate Award , Western University <i>Awarded annually to a graduate student(s) in the MSc/MClSc and PhD programs of Pathology and Laboratory Medicine, based on academic achievement and research merit.</i>
2020-04	Distinction	Cum laude , Queen's University <i>GPA of 3.71/4.3</i>

PROFESSIONAL ACTIVITIES: ADMINISTRATIVE & COMMITTEE MEMBERSHIPS

[selected = selected following application and consideration by the governing body]

Dates	University Committee Membership & Description
2021-09 – 2022-08	<p>Vice President of Multimedia, Western Pathology Association, Western University, London, ON. <i>[selected]</i></p> <p><i>Create promotional graphics for social, academic, and other events hosted by the WPA in coordination with executive members.</i></p>
2021-05 – 2022-05	<p>Steering Committee Member, Translational Immuno-Oncology Research Group, Western University, London, ON. <i>[selected]</i></p> <p><i>Organize and executing meetings and events including journal clubs, workshops and the Annual Immuno-Oncology Symposium.</i></p>
2019-09 – 2020-04	<p>Head of Marketing, Biochemistry Department Student Council, Queen’s University, Kingston, ON. <i>[selected]</i></p> <p><i>Create a marketing plan and help Marketing team members develop graphics for clothing merchandise. Work with executive members to integrate all ideas and information into marketing deliverables.</i></p>
2017-09 – 2019-04	<p>Marketing Team Member, Biochemistry Department Student Council, Queen’s University, Kingston, ON. <i>[selected]</i></p> <p><i>Create graphics for advertising social and academic events. Collaboratively plan and advertise events such as career conferences, seminars, and resume workshops.</i></p>

PUBLICATIONS

Peer-Reviewed Articles

2. El-Hajjar M, **Gerhardt L**, Krishnamoorthy M, Figueredo R, Zheng X, Koropatnick J, Maleki Vareki S. Inducing mismatch repair deficiency sensitizes immune-cold neuroblastoma to anti-CTLA4 and generates broad anti-tumor immune memory. *Molecular Therapy* (in press: MOLECULAR-THERAPY-D-22-00693)

Role: *Co-author (contributions: study design, animal work, flow cytometry, data analysis, writing and reviewing)*

1. Krishnamoorthy M, **Gerhardt L**, Maleki Vareki S. Immunosuppressive Effects of Myeloid-Derived Suppressor Cells in Cancer and Immunotherapy. *Cells*. (2021) doi: 10.3390/cells10051170. PMID: 34065010.

Role: Co-first author (contributions: conceptualization, writing, reviewing and editing)

ABSTRACTS

Platform Presentations

3. **Gerhardt L**, Maleki Vareki S. Turning immunologically cold tumours hot: translational and clinical research in the Maleki lab. Presented at the Translational Immuno-Oncology Research Group Retreat. London, ON, Canada. November 2022.
2. **Gerhardt L**, Figueredo R, Maleki Vareki S. Investigating IL-12 family cytokine involvement in modulating CD39 expression by CD8⁺ T-cells using an immunogenic neuroblastoma model. Presented at Pathology and Laboratory Medicine Research Day. Virtual Meeting. March 2022.
· *Received the Dr. M. Daria Haust Award for the Best Basic Science Presentation*
1. **Gerhardt L**, Figueredo R, Maleki Vareki S. Investigating the role of IL-12 family cytokines in promoting CD39 expression on CD8⁺ T-cells. Presented at the 3rd Annual Immuno-Oncology Symposium. Virtual Meeting. February 2022.

Poster Presentations

6. **Gerhardt L**, Figueredo R, Maleki Vareki S. IL-12 and IL-27 upregulate CD39 expression on CD8⁺ T-cells and differentially affect CD39⁺CD8⁺ T-cell effector function. Presented at the Society for Immunotherapy of Cancer Annual Meeting 2022. Boston, MA, USA. November 2022.
5. Suchý M, Figueredo R, **Gerhardt L**, Maleki S, Lee TY, Kovacs M. GMP-Level Production of Radiometallated Immune Checkpoint Inhibitor Nivolumab: Why and How? Presented at The Fourth International Symposium on Technetium and Other Radiometals in Chemistry and Medicine. Bressanone BZ, Italy. September 2022. [Poster only]
4. **Gerhardt L**, Figueredo R, Maleki Vareki S. The role of IL-12 & IL-27 inducing CD39 expression on CD8⁺ T-cells in cancer. Presented at Oncology Research and Education Day. London, ON, Canada. June 2022.
3. El-Hajjar M, **Gerhardt L**, Krishnamoorthy M, Figueredo R, Zheng X, Koropatnick J, Maleki Vareki S. Inducing mismatch repair deficiency in neuroblastoma activates antitumor immunity and sensitizes tumors to anti-CTLA4

therapy. Presented virtually at Society for Immunotherapy of Cancer Annual Meeting 2021. Washington, DC, USA. November 2021.

2. **Gerhardt L**, Figueredo R, Maleki Vareki S. The role of IL-12 family cytokines in CD39 induction on tumor-specific T-cells. Presented at Oncology Research & Education Day. Virtual Meeting. June 2021.
1. **Gerhardt L**, El-Hajjar M, Figueredo R, Maleki Vareki S. Mechanism of CD39 induction on tumor-specific T-cells and its role in anti-tumor immunity. Presented at Pathology and Laboratory Medicine Research Day. Virtual Meeting. April 2021.

PROFESSIONAL DEVELOPMENT

Dates	Category	Description
2022-01 – 2022-04	Teaching	Teaching Assistant , One Health 4100, Western University <i>Graded essays and reports, and provided constructive, individualized feedback to students.</i>
2021-04	Teaching	TA eLearning Series , Centre for Teaching and Learning, Western University <i>Completed seven modules designed to equip participants with strategies for being an effective teaching assistant in blended and online classrooms.</i>
2021-01 – present	Education	Translational Immuno-Oncology Research Group Journal Club , Centre for Translational Cancer Research, Western University and London Regional Cancer Program <i>Weekly presentations of cancer immunology, immunotherapy and immuno-imaging research articles.</i>
2020-11	Education	Primer on Tumor Immunology and Cancer Immunotherapy , Society for Immunotherapy of Cancer Pre-Conference Program 2020 <i>Educational program designed to provide a foundation for understanding core immunology principles as they relate to basic and clinical research in immunotherapy of cancer.</i>
2020-09 – present	Education	Experimental Oncology Journal Club , London Regional Cancer Program and Western University <i>Weekly presentations of cancer biology, immunology, and virology research articles.</i>

2019-09 – Research **Undergraduate Research Project**, Queen’s University,
2020-04 Queen’s Cancer Research Institute

***Discipline:** Biochemistry, Cancer Biology & Genetics*

***Thesis Title:** Investigating the mechanisms of microRNA-29b in malignant melanoma*

***Thesis Advisor:** Andrew Craig, PhD*

COMMUNITY OUTREACH

Dates	Title & Description
2021-02 – 2021-04	<p>Editor for Let’s Talk Cancer Biochemistry and Immunology Blogs, Canadian Cancer Society’s London Research Information and Outreach Team, London, ON</p> <p><i>Revise, edit and authenticate lay articles for communicating the progress in cancer research to the general London, ON community.</i></p>
2017-09 – 2020-03	<p>Adult Mental Health Unit Volunteer, Kingston General Hospital, Kingston, ON</p> <p><i>Provide intellectual and social stimulation for patients in need, as well as conduct structured and unstructured therapeutic, recreational activities for patients.</i></p>